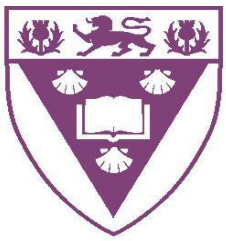

RHODES UNIVERSITY

Grahamstown • 6140 • South Africa

GOLD MINERALIZATION IN A HIGH GRADE METAMORPHIC TERRANE IN THE HANDENI DISTRICT, EASTERN TANZANIA

GODFREY STEPHEN BITESIGIRWE

A thesis submitted in partial fulfillment of the requirements for the degree of

MASTER OF SCIENCE

(Exploration Geology)

Rhodes University

P.O. Box 94

Grahamstown 6140

South Africa

November 2013

ABSTRACT

Most orogenic type gold deposits are formed under low greenschist facies to mid amphibolite facies metamorphic conditions and deposition is either structurally or lithologically controlled. A few known gold deposits found in high grade metamorphic terranes include those in the Yilgarn craton in Australia, Renco in Zimbabwe, Hemlo in Canada and the recently discovered Handeni deposit in Tanzania.

Within Tanzania, gold deposits are mainly hosted in Archaean low grade metamorphic rocks commonly known as the Lake Victoria greenstone belt. The greenstone belts of Tanzania are of Nyanzian age (> 2.5Ga) and are located to the south and east of Lake Victoria on the Tanzania craton. The Tanzania Craton is surrounded by Usagaran 1.9 Ga rocks (the east African orogenic belt (EAO) better known as the Mozambique belt) to the east and the Ubendian belt to the south and west. Published reports show that the eastern part of the Tanzania Craton is dominated by the fragments of Archaean rocks.

Metamorphism along East Africa and the Tanzania Craton is due to several geological events. These geological events include the intrusion of granites in the Archaean Tanzania Craton (3 Ga), subduction of ocean plate resulted to the formation of Usagaran belt (1.9 Ga), opening and closure of Mozambique Ocean, which resulted in the formation of the Mozambique belt between 700 – 800 Ma and the Pan African orogeny at 640 – 620 Ma, which is associated with the formation of Gondwana. It is believed that fragments from the Archaean Tanzania craton were re - metamorphosed during these events.

The Handeni project (the focus of this thesis) is located in the northern portion of the eastern part of the Usagaran belt (1.9 Ga) comprising the eastern part of Archaean Tanzania Craton. The area is characterized by Proterozic rocks of basaltic composition. The documented 2.7 Ga rocks at the Kilindi Handeni Superterrane at the northern part of the Usagaran belt correlate well with 2.7 Ga of Nyanzian rocks of Archaean Tanzania craton. The Handeni project area is geologically dominated by metamorphosed and deformed units of quartzofeldspathic gneisses, migmatitic gneiss, garnet silicified rock, garnetiferous amphibolite, garnetiferous granulite, graphitic schist and hornblende pyroxenite. Intensive deformation features that were developed include folds (sheath folds, micro and macro scales), faults, shears and regional thrusts.

This thesis focuses on identifying the protolith of the rocks, alteration minerals, and metamorphic assemblages in the project area in order to understand the timing of gold

mineralization. Geological investigation of core, ore petrology and mineralogy, mineral composition by using JEOL microprobe analysis and XRF analysis of bulk rocks were utilized. All the analytical work was done at the Geology laboratory, Rhodes University.

Petrographic analysis shows that the rocks sampled in the study area are characterized by alteration minerals such as calcite, dolomite and sericite. Sulphide minerals including chalcopyrite, pyrrhotite, pyrite, pentlandite and gersdorffite were identified. Gold mineralization is associated with disseminated sulphides in association with trace amounts of base metals. Four rock types were proposed as host rocks for the mineralization, namely garnet silicified rock with superimposed quartz veins, garnetiferous amphibolite, garnetiferous granulite and hornblende pyroxenite.

Fold troughs, filled fractures associated with episodes of folding, quartz veins and shear zones are suggested as gold precipitation sites. The presence of high grade metamorphic rocks containing gold, intermediate to low grade assemblages with sulphides and associated hydrothermal alteration as well as a complex deformation history suggests that the Handeni mineralization took place over an extended time period stretching from a ductile to a brittle environment.

ACKNOWLEDGEMENTS

My sincere thanks goes to Dr. Reyno Scheepers Group president of IPP Resources and President and C.E.O of Handeni Gold Incorporated for funding my studies. His technical support and advice are highly appreciated. I would also like to thank his wife Mrs. Claire Scheepers for supporting my studies.

My special gratitude to the management of IPP Resources specifically Dr. A. R. Mengi, the executive chairman of the IPP group of companies, for facilitating my study at Rhodes University.

Special thanks to Professor Yong Yao, for his guidance throughout the study and supervising this thesis. Dr. Peter Horvath, Prof. Goonie Marsh, Dr. Harilaos Tsikos and Dr. Steve Prevec are thanked for their technical support for the whole year. Mrs. Ashley Goddard the Exploration Geology Administrator is acknowledged for her support during attendance of module courses and Mr. John Hepple for all the laboratory work. Thanks to Dr. Gelu Constin for the technical support in the use of Jeol JXA 8230 Superprobe, instrument sponsored by NRF/NEP grant 40113 (UID 74464).

Special thanks to Dr. Marian Munteanu; his guidance, corrections and advice are highly appreciated. Thanks to all my friends for their great moral support and advice, to mention a few, Bernard McDonald, Benjamin Clavery Safi, Sisonke Mawonga, Thomas Kegan, Tsholofelo Malatji, Luckmore Salimo, Demand Gwatinetsa and Ali Assane.

I am grateful to my family: Mellania, Abella, McSteve and MacSteve as well as my lovely mother Khadija Manyema for their sacrifice and patience during my absence for one year, as my responsibilities of father and elder of the family were diminished during this year.

Last but not least I thank the Almighty God for keeping me healthy and energetic from the start until the end of this journey.

DECLARATION

I, ***GODFREY STEPHEN BITESIGIRWE*** declare this thesis is my own and original work except where the specific acknowledgement is made to the work of others. It is submitted in partial fulfillment of the Degree of Master of Science in Geology Exploration at the University of Rhodes. It has not been submitted before for any degree or examination in any other University or tertiary institution.

Date:  Signed: 24 March, 2014.

DEDICATION

This dissertation is dedicated to Dr. Reyno Scheepers, Group President of IPP Resources, and C.E.O. of HG Ltd. for the scholarship and all the financial support throughout my study life.

Also to my late father Mr. Stephen Abdon Bitesigirwe for his good effort on providing me a basic education during his life.

TABLE OF CONTENTS

LIST OF FIGURES

LIST OF TABLES

CHAPTER 1 INTRODUCTION

1.1 BACKGROUND

Gold exploration has been conducted worldwide in Neoarchean Superterranes for some decades and is becoming depleted for world class deposits. There is a need to look for new prospective geological terranes as many greenstone belts worldwide are approaching maturity in terms of exploration (Kabete *et al,* 2012a). This paves a way for exploration and mining in medium to high grade metamorphic terranes.

There are very few gold deposits that have been discovered and mined in mid to high metamorphic grades, however some of the better known include, Western Australia at Yilgarn block, Big Bell, and Fraser's mine, Zimbabwe at Gladstone – Renco mine, Canada at Lupin, and Hemlo, India at Kolar goldfield (Barnicoat *et al,* 1991; Frost *et al,* 2002) and the recently discovered Kilindi-Handeni Superterrane in Tanzania (Groves *et al,* 2010).

Tanzania, as part of the East African countries, is the fourth largest gold producer in Africa after South Africa, Ghana and Mali with its reported gold production at around 40 tonnes annual export in 2011 (Ministry of Energy and Minerals - MEM, 2012). Tanzania's gold production comes mainly from three major open-pit mines, namely Golden Pride, Geita and North Mara mines and one major underground mine known as Bulyanhulu. All these gold mines are hosted in Archaean granite - greenstone belts.

This thesis investigates existing gold mineralization in the Proterozoic rocks of Handeni district as possibly being associated with Archaean rocks in age and the probability that this mineralization could be as a result of tectonic events occasioned by the metamorphism and deformations that occurred historically within the region. An important aspect of the discussion around the mineralization in the Handeni area is the role and importance of Lake Victoria Goldfield (LVG) in Archaean greenstones as potential protoliths to the Proterozoic Handeni Lithologies. This would postulate that the Archaean rocks in LVG were present as fragments in the Usagaran belt and that these lithologies were metamorphosed with other Proterozoic rocks in the belt.

Limited research has been conducted on the Kilindi Handeni Superterrane (KHS) and much less is known about the nature and genesis of gold mineralization in Handeni district when

compared to information available on the LVG Archean deposits. Recent work by Kabete (2008) at the University of Western Australia found that the Proterozoic rocks of Handeni – Kilindi region were Archaean in age and belonged to the same Nyanzian system hosting the gold deposit of the LVG. The research suggested that the KHS was part of Archaean granite - greenstone terrane which was fragmented and metamorphosed by later Proterozoic orogenic and tectonic events (Kabete *et al*, 2012b).

This thesis consists of data derived from: i) whole rock geochemistry and protolith recognition ii) mineralogy and petrology and iii) identification and characterization of alteration assemblages. These three sets of data will be used to describe geological and geochemical characteristics of the mineralization styles in Handeni district. These contributions help to understand the nature of gold mineralization in Handeni district.

1.2 PROBLEM IDENTIFICATION

The eastern part of Tanzania, where the easternmost border of the Tanzania Craton is located, is believed to be overprinted by later Proterozoic tectonic events. The area hosts several gold deposits and occurrences. The genetic characteristics of these deposits that control the gold mineralization style have not been well investigated or properly understood. This situation hinders the discovery of new similar gold deposits in the region. In such a case, two research questions arise:

- Does gold mineralization in the Handeni district occur during low-grade metamorphism?
- Is gold mineralization in the Handeni district overprinted and/or mobilized or remobilized by a high-grade metamorphic event?

To address these questions, appropriate data for the geological and geochemical characterizations of Handeni gold deposits in eastern Tanzania were used in this thesis.

1.3 STUDY AREA

Handeni Gold Inc. (HNDI) owns four large prospecting licenses located south of the town of Handeni in eastern Tanzania (Fig. 1). Within these four licenses known gold occurrences are at Kwandege, Masala, Njembe and Magambazi. There are also numerous other smaller showings. Handeni Gold Inc. commenced drilling on two selected targets namely the Kwandege and Magambazi East projects in 2010. The Magambazi East project is adjacent to

the East African Metals (formerly CANACO Resources Inc.) deposit with a reported reserve of 0.72 Moz at 1.48g/t. These two projects (Magambazi East and Kwandege) are located in the Handeni and the Kilindi districts contiguous to each other and form the integral part of this thesis as the Handeni project. The Handeni project is located on the eastern part of Tanzania approximately 170 km northwest of Dar es Salaam and about 45 km southwest of Handeni town (Fig. 1).

Figure 1. Location of the study area of the HNDI gold prospects at Handeni project (Howard, 2011).

1.4 RESEARCH HYPOTHESIS

- Association between lithology, structure and metamorphism can assist in the identification of potential mineralization sites in the Kilindi-Handeni district.
- Mineralization of an area within the wider district may be controlled by lithology and structure.
- Geophysical and remote sensing datasets may be used to determine geospatial features related to gold mineralization in the district and also update geological maps.

1.5 RESEARCH OBJECTIVES

The main objective of this research is to utilize geochemical analysis, petrographic and airborne geophysical datasets to understand the processes responsible for gold mineralization in the Handeni project area. To address these objectives properly, the following sub objectives have been formulated:

- To identify the protoliths of the Proterozoic Handeni lithologies.
- To identify alteration and metamorphic assemblages in Handeni lithologies.
- To understand controls on or nature of gold mineralization in the Proterozoic rocks of Handeni district.

CHAPTER 2 GOLD IN ARCHAEAN GREENSTONE BELTS

2.1 INTRODUCTION

This chapter reviews gold deposits in the Archaean greenstone terranes associated with mid to high grade metamorphism and their worldwide gold distribution and geological settings.

2.2 EXAMPLES OF GOLD DEPOSITS IN ARCHAEAN GREENSTONE BELTS

Archaean greenstone belts are zones of metamorphosed rocks characterized by mafic to ultramafic rocks of igneous origin, commonly basalts with associated sedimentary rocks interleaved. They exhibit a low grade metamorphic facies, which occur within the Archaean and Proterozoic cratons, commonly between the granite and the gneissic units. These greenstone belts are common sources of gold deposits associated with hydrothermal fluids, banded iron formations, schist and silicified gneisses with veining (Borg, 1992).

There are a few countries in the world where gold deposits have been discovered in mid to high grade metamorphic terranes. These include gold deposits such as Griffins Find deposit in granulite facies and Big Bell deposit in Yilgarn Craton of Western Australia (amphibolite to granulite facies) with a production of about 2 Moz of gold and total endowment of about 4 Moz (Phillips *et al*, 2009). Others include the Lupin deposit in Canada, Gladstone Renco mine with about 1 Moz of gold endowment in Zimbabwe and the Kolar goldfield in India (Barnicoat *et al,* 1991), the Lucky Draw deposit and Challenger in Australia and Hemlo deposit in Ontario Canada containing approximately25 Moz of gold (Frost *et al,* 2002 & Phillips *et al*, 2009).

Limited published research exists regarding gold deposits occurring in high grade metamorphic terranes based on their economic significance (Groves *et al,* 1998). Existing research suggests that the pre metamorphic protoliths for Archaean greenstone belts are the predominantly volcano-plutonic terranes of oceanic back arc basalt and felsic to mafic rocks that were affected by tectonic events resulting in metamorphism and deformation of existing geologies.

These terranes were formed during tectonic processes involving accretion and collision of orogenies and resulted in complex regions (metamorphic belts) forming as new continental crust. Groves *et al.* (2003) suggested that gold bearing deposits can be generated and/or modified during each active tectonic phase (magmatic arcs and fore arcs, deformation and metamorphism and or uplifting and erosion) associated with orogenic development.

According to Barnicoat *et al (*1991) the formation of gold deposits at high metamorphic grades is related to the presence of gold mineralization in the Archaean rocks of middle amphibolite to lower granulite facies. The higher grade metamorphism caused by the effect of tectonic events results from the metamorphism and deformation of the country rocks (Archaean rocks in this case). The abundance of gold mineralization associated with sulphides is a result of the mobilization and remobilization of the sulphides minerals within the system after melting of the host rocks (Frost *et al*, 2002).

Phillips *et al* (2009) suggests some of the main characteristics related to gold deposits in the high grade metamorphic terranes, in relationship with the Archaean, referred to as the Big Bell or Hemlo type:

- In high strain, more ductile structures than those typical for the greenschist facies
- Found near granite – greenstone margins
- Minor to negligible carbonate alteration
- Lack of quartz veins
- Higher metamorphic grade is reflected in alteration assemblages
- Partial melting has occurred in some deposits
- Desulphidation, decarbonation and retrogression have all been important in dictating the present nature of these deposits
- Foliation – parallel veins and replacement deposits
- Veins with coarse grained granoblastic quartz
- Mineral assemblages; Microcline-muscovite-andalusite, garnet-pyroxene-biotite – or amphibolite-biotite-calcite alteration in ore zones.

2.3 MINERALOGY AND CHEMISTRY OF GOLD DEPOSIT

Frost *et al* (2002) recommended that metamorphism and deformation result in mobilization and remobilization (internally and externally) of sulphide ore bodies. The mobilization process associated with hydrothermal and melting processes of sulphide ore bodies possibly result in high abundances of Ag, As, Bi, Hg, Se, Sb, Sn, Tl and/or Te, elements with melting points below 1000 ^{o}C. Melting minerals in the ore could be concentrated as melt or a result of crystallization of residual phases. Gold melts at temperatures higher than 1000 ^{o}C but the element is commonly associated with low melting point chalcophile elements in polymetallic melts as a result of phase relationships. The low melting point chalcophile elements (LMCE) are Zn, Ga, As, Se, Ag, In, Sb, Te, Hg, Tl, Pb, Bi and Cd (Table 1).

Table 1. Elements with low melting points associated with metamorphosed ore deposits (Frost et al, 2002).

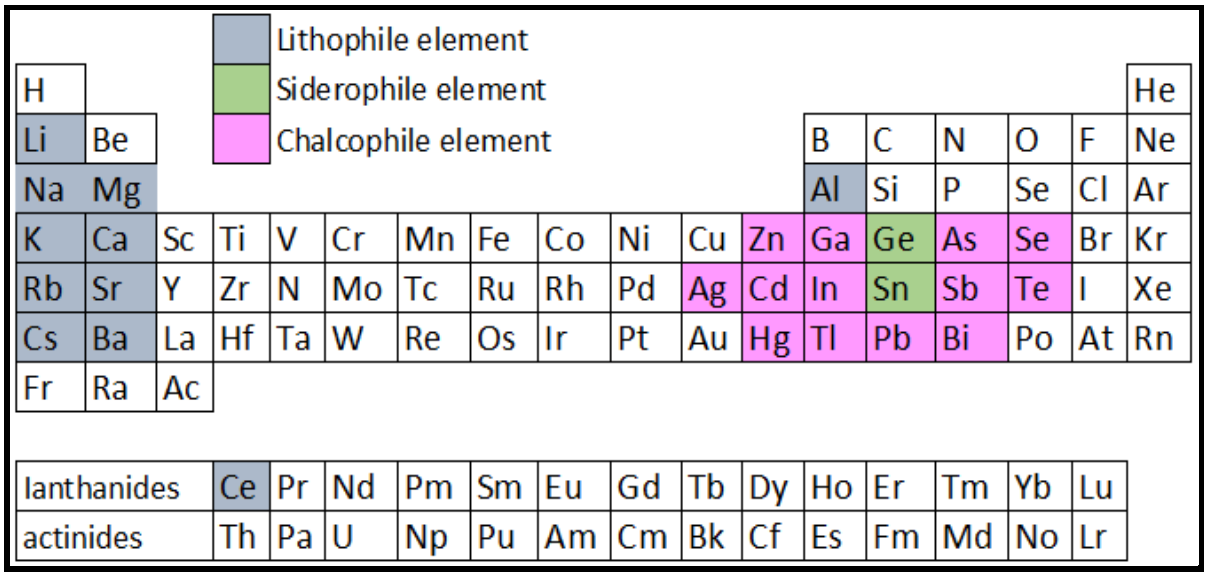

According to Frost *et al (*2002), a limited number of disseminated gold deposits which have been formed under high grade metamorphic terranes have the assemblage that positively show that they could have melted at peak temperatures such as Lucky Draw deposit in Australia, the Renco deposit in Zimbabwe and Hemlo deposit in Ontario Canada, where the gold was emplaced into amphibolite grade shear zones that cut the granulite grade gneisses about 600 ^{o} C as opposed to the 1000 ^{o}C which has been mentioned above.

Phillips *et al* (2009) suggests that based on the correlation between the metamorphic grade of the surrounding rocks and the alteration assemblages associated with some of the deposits (Marvel Loch, Bullfinch, Yilgarn Star, Bounty, Great Victoria, Corinthian and Hopes Hill in the Southern Cross greenstone belt of Western Australia) it is possible that gold was formed before peak metamorphism, these can be evidenced from Lac Lilois gold deposit in the Ashuanipi complex of northeastern Canada where the T-P was 775 ^{o}C at 7 – 7.5 Kbar. Table 2 summarized the major gold deposits in high grade metamorphic terrane.

Table 2. Gold deposits in high grade metamorphic terranes (Phillips et al, 2009).

Deposit	Griffins Find	Big Bell	Renco	Hemlo	Challenger
Country	Australia	Australia	Zimbabwe	Canada	Australia
Craton	Yilgarn	Yilgarn	Zimbabwe	Superior	Cawler
Endowment (Moz-Au)	<0.1	4	-1	25	2
Metamorphic grade	Granulite	Upper Amphibolite	Granulite	Upper Amphibolite	Granulite
K-alteration present at peak m/m	Possibly	Yes	Yes	Probably	Yes
Partial melting					
Silicate wallrock assemblage	Yes(dikes)	Yes(dikes)	Yes	Yes	Yes
Ore sulphide assemblage	Likely	Likely	Likely	Demostrated	Demostrated
Retrogression	Yes(dikes)	Yes(dikes)	Yes	Yes	Yes
			Significant	Significant	Partial
Quartz veining: mineralized	Yes	Yes	Yes	Yes	Yes
Reference	Qiu et al (1997)	Qiu et al (1997)	Phillips and de Nooy (1988)	Tomkins et al (2004b)	Tomkins and Mavrogenes (2002)

2.4 GOLD DEPOSITS IN METAMORPHIC BELTS

Metamorphic belts are the complex regions where accretion or collision has added to, or thickened, continental crust. Small to large scale gold deposits can be formed at all stages of orogenic evolution, so that evolving metamorphic belts contain diverse gold deposit types that may be juxtaposed or overprinted on each other (Phillips *et al*, 2009; Goldfarb *et al*, 2005 & Groves *et al*, 2003).

Bohmke *et al* (1986) suggested that the granulites hosting the gold mineralization in Renco are; garnetiferous granulite, felsic granulite, charnokite and enderbite granulite, mafic granulite and laminated recrystallized quartz granulite associated reefs. Gold deposition was related to igneous metamorphic events accompanied by the introduction of more sulphur whereas accompanying deformation caused folding of the reef horizons and minor redistribution of the native metals and silica where-by wide zones were developed in the hinges of folds. Gold is controlled by reef structures, commonly found in the syncline fold troughs and occasionally in the anticline fold crests. Gold mineralization is associated with copper, bismuth and iron which is remarkable as the related hydrothermal assemblage survived during the high grade metamorphism. Sulphides related to gold mineralization are pyrrhotite, pyrite and chalcopyrite.

The greatest challenge to exploring gold deposits in mid to high grade metamorphic terranes is to understand the origin of the gold deposit type as overprinted or remobilized during the major compressional orogeny that shaped the final geometry of the hosting metamorphic belts (Groves *et al*, 2003, Phillips *et al*, 2009 & Grove, 2010).

Spear (1993) and Winter (2001) summarized the metamorphic facies of the igneous rocks and their protoliths as can be related to Archaean rocks:

a) Greenschist facies (low grade about < 500 ^{o} C) containing the assemblage: Amphibole (Actinolite) + Chlorite + Epidote $\pm$ Quartz $\pm$ Plagioclase (Albite). The equilibrium mineral assemblage and their protolith of various rocks are:

- Basalt ==> chlorite-actinolite-albite $\pm$ epidote
- Ultramafic ==> chlorite-serpentine $\pm$ talc $\pm$ tremolite $\pm$ diopside $\pm$ brucite
- Pelites ==> quartz – albite – k-feldspar – chlorite – muscovite – garnet – pyrophyllite – graphite
- Calc-silicate ==> calcite $\pm$ dolomite $\pm$ quartz $\pm$ micas $\pm$ scapolite $\pm$ wollastonite

b) Amphibolite facies between 500 ^{o}C and 700 ^{o}C: Hornblende + Quartz + Plagioclase $\pm$ Garnet $\pm$ Epidote, and its equilibrium mineral assemblages of various protolith rock types consists of:

- Basalt-ortho-amphibolite==> hornblende/actinolite $\pm$ biotite $\pm$ quartz $\pm$ chlorite.
- High Magnesia Basalts==> anthophyllite (Mg rich amphibole) + biotite + quartz +chlorite
- Ultramafic rocks ==> tremolite, asbestiform, talc, pyroxene, wollastonite-prograde metamorphic olivine (rarely)
- Sedimentary para-amphibolite==> hornblende/actinolite $\pm$ albite $\pm$ quartz $\pm$ garnet $\pm$ (calcite $\pm$ wollastonite)

c) Granulite facies about >700 ^{o}C: Garnet + Pyroxene + Plagioclase + Quartz $\pm$ Hornblende. In the case of a protolith, the rock is made up of gabbro. The following minerals resulted by granulite metamorphism: pyroxene-plagioclase-garnet and rarely biotite-hornblende-quartz. Below is the typical transition of amphibolite and biotite into granulite facies as shown:

- Amphibole ==> pyroxene + water
- Biotite ==> Orthopyroxene + garnet + K-feldspar + water (Bowen, 1989).

In Tanzania, gold mineralization is mainly found in three geological settings associating with Archaean rocks. These are: i) the lake Victoria Gold Field (LVG) about < 2.85 Ga greenschist amphibolite facies, ii) the central Tanzania region composed of granitoid and migmatitc gneissic terranes and the Dodoma Basement and Dodoma Schists Superterranes underlain by

< 2.85 Ga greenschist amphibolite facies and schist belts, iii) the Proterozoic Tanzania regions, of Ubendian and Usagaran Belts (Kabete *et al*, 2012b) refer to Figure 2.

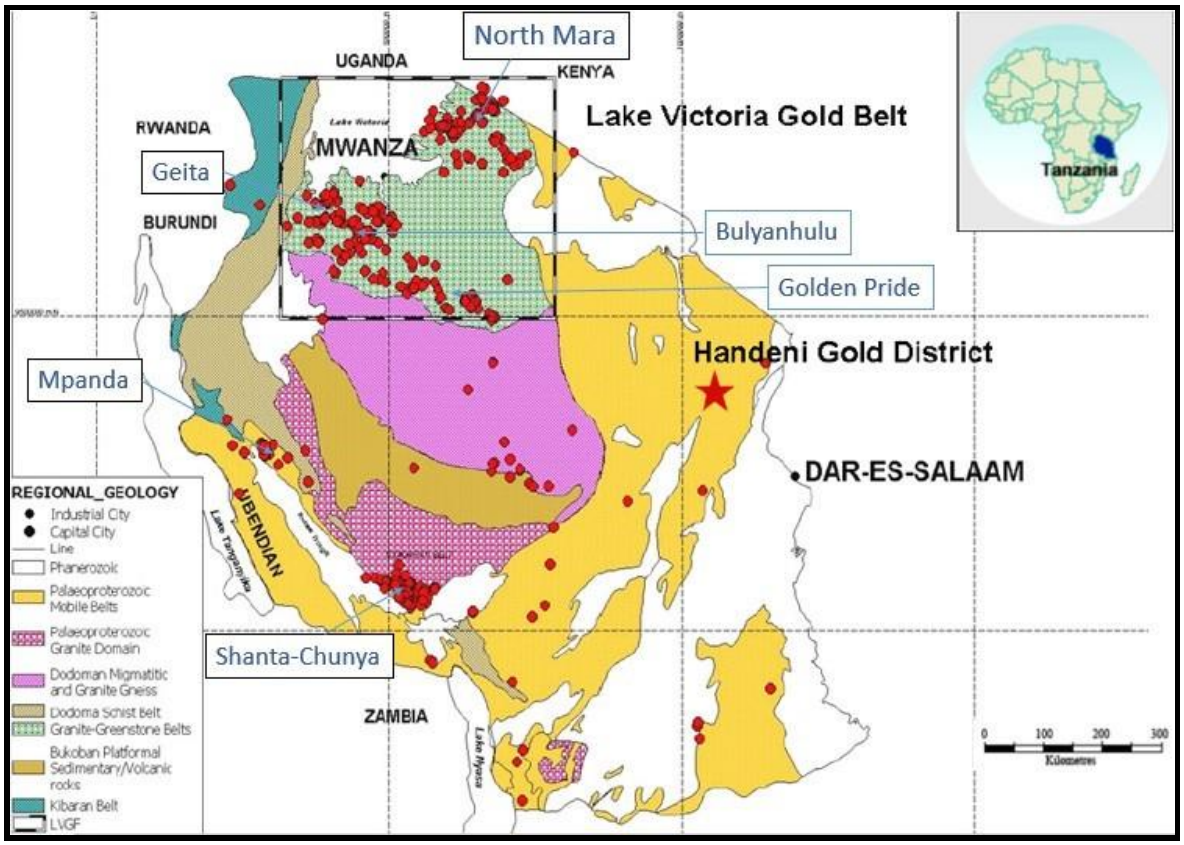

Figure 2. Gold occurrences and active mines (red dots) in Tanzania (Howard, 2011).

Gold mineralization in the Ubendian belt (Proterozoic age) (south western Tanzania) was discovered in the early 1920s known as Lupa goldfield (Fig. 2). Modern exploration activities in this area have led to the discovery of a 1.48 Moz mine operated by Shanta Gold Mine Ltd (www.shantagold.com). This contributed to more exploration activities in areas characterized by Proterozoic rocks in the country.

Groves (2010) proposed that the rocks of the Usagaran belt are related to the reworking of rocks from the eastern Tanzania Craton (Archaean rocks). Gold in KHS (Usagaran belt of Proterozoic age) was discovered in late 2003 by artisanal miners in the Handeni district. This was followed by influx of medium and large exploration companies that acquired several prospecting licenses over prospective parts of this terrane. To date 0.72 Moz at 1.48 g/t resources has been published by East African Metals Ltd, one of the exploration companies holding prospecting licenses in the terrane (Archibald, 2012).

CHAPTER 3 REGIONAL GEOLOGICAL SETTING

3.1 INTRODUCTION

This chapter explains in brief the tectonic setting with regard to the evolution of the geology of Tanzania, the evolution of the East Africa Orogeny in relation to Gondwana, the Tanzania Craton, Mozambique belt and Usagaran System. Also, presents the general review of the Tanzania geology, the general stratigraphic sequence in terms of age of formations, the structural features and the metamorphism with regard to gold mineralization. The genesis of gold deposit in relation to tectonic setting in low to high grade metamorphic terranes will also be discussed.

3.2 GEOTECTONIC EVOLUTION

3.2.1 East Africa Geotectonic Evolution

The geotectonic evolution of the Proterozoic supercontinents of the East Africa region reflects the tectonic setting of the Neoproterozoic African Orogeny (Pan African) as related to arc assembly and continental collision as the implication of Gondwana breakup (Stern, 1994; Sommer *et al*, 2005). The Pan African (Neoproterozoic) event encompass protracted orogenic cycles from 950 to 450 Ma, that can be used to characterize the structural differentiation of Africa into cratons and mobile belts as coined by Kennedy (1964) in Stern (1994) and Kroner *et al* (2004) during the latest Precambrian and earliest Paleozoic.

Stern (1994) uses the Wilson cycle to suggest the formation of EAO as; i) formed from the fossil fragments of Neoproterozoic characterized by ophiolites, granulites and structures which represent the opening and closing of an oceanic basin that lay between the older crust blocks of East and West Gondwanaland and ii) formed during a protracted period of juvenile crust formation in intra oceanic arcs culminating in continental collision evidenced by the abundance of ophiolites and juvenile arc assemblages (Fig. 3).

Stern (1994) associated the African plate with rifting, which separates the Nubian plate to the west from the Somalian plate to the east. This reflects the fact that the EAO started by rifting of a continent about 870 Ma, which led to the development of a passive margin and perhaps two aulacogen – like structures, one of which evolved into a narrow ocean basin. The west part of the EAO is well preserved despite having been deformed and metamorphosed whereas the eastern part is poorly developed, most likely due to poor exposure or intensive deformation and

metamorphism. As proposed by Stern (1994) it may be due to the fact that the eastern margin of EAO developed later as an Andean type convergent margin.

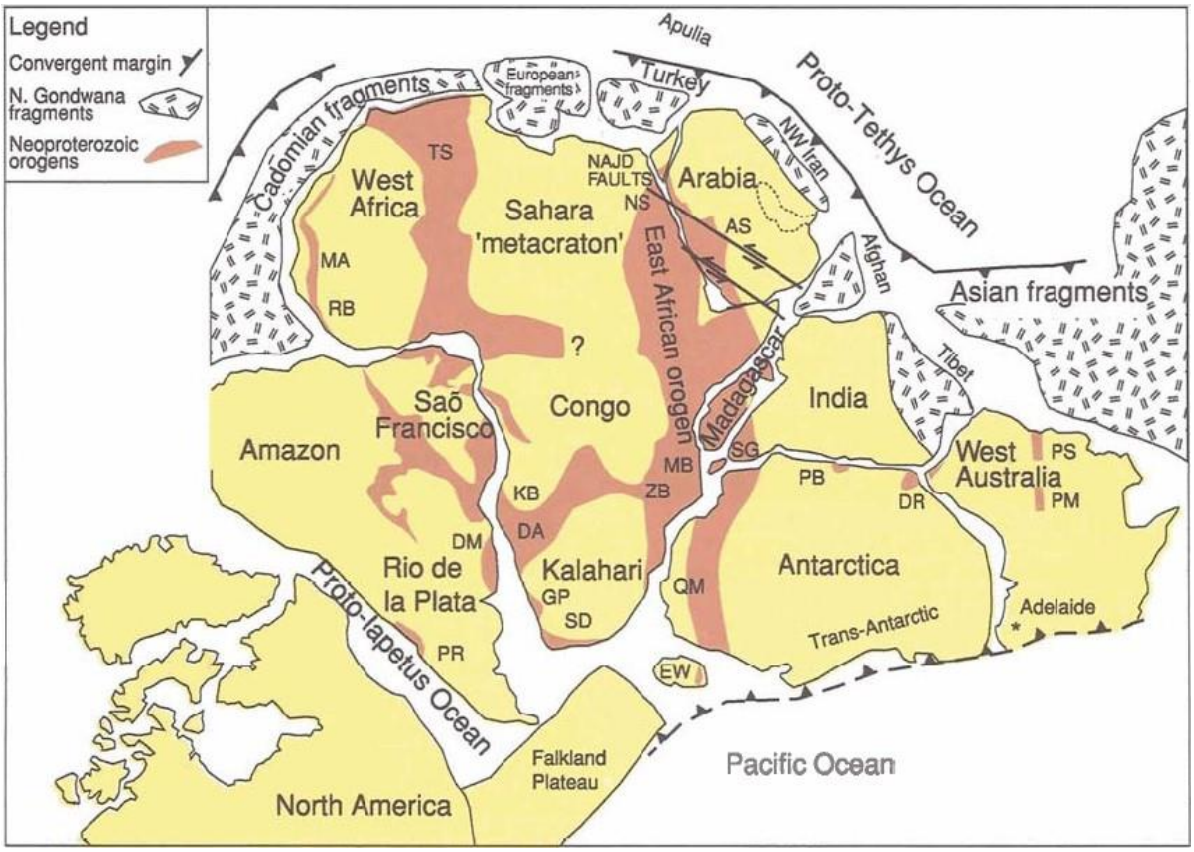

Figure 3. Map of Gondwana at the end of Neoproterozoic time (~540 Ma) showing the general arrangement of Pan – African belts including the EAO (Kroner et al, 2004).

3.2.2 Tanzania Craton

The Tanzania Craton is among the seven major cratonic nuclei forming the foundation of Africa between 3.8 to 2.5 Ga before the forming of continental crust. Others are the Zimbabwe, Congo, Man Shield, Reguibat Shield, Kaapavaal and East Sahara or Nile cratons. Previously there were three large cratons namely West Africa, Central Africa which were include Congo and Tanzania craton and the Southern Africa craton which were include the Zimbabwe and Kaapvaal cratons. These cratons were merged during the Neoarchean and Paleoproterozoic (Dirks *et al*, 2002 and Brick, 2011).

The Tanzania Craton forms the highest part of the East Africa plateau (Archaean in age) surrounded by rocks of different ages, most commonly Proterozoic. The craton itself mainly consists of rocks of Archaean ages including the Dodoma rocks at the central part as the oldest, Nyanzian greenstone at the south and east of Lake Victoria and Kavirondian north western part

as well as other Archaean metasediments (Dawson, 2008). To the east it borders with the Usagaran belt and Mozambique belt, south the Ubendian belt, and west the Karagwe Ankolean and Bukoban (Fig. 4). The Tanzania Craton consists of mafic to ultramafic rocks, high grade TTG type orthogneiss, quartzite and phyllite of the > 2.9 Ga Dodoma Terrane in the central part as well as migmatized and gneisses rocks. South of Lake Victoria the craton consists of 2.6-2.8 Ga old tectonised greenstone belts including the bimodal volcanics of the Nyanzian Group overlain by the volcanics and clastic sediments, which are generally intruded by large volumes of granite. There are also widespread kimberlite intrusions similar to other cratons. The syntectonic emplacement of granites took place between 2.7 and 2.5 Ga (Dirks *et al* 2002, Thomson *et al*, 2012 and Dawson 2008).

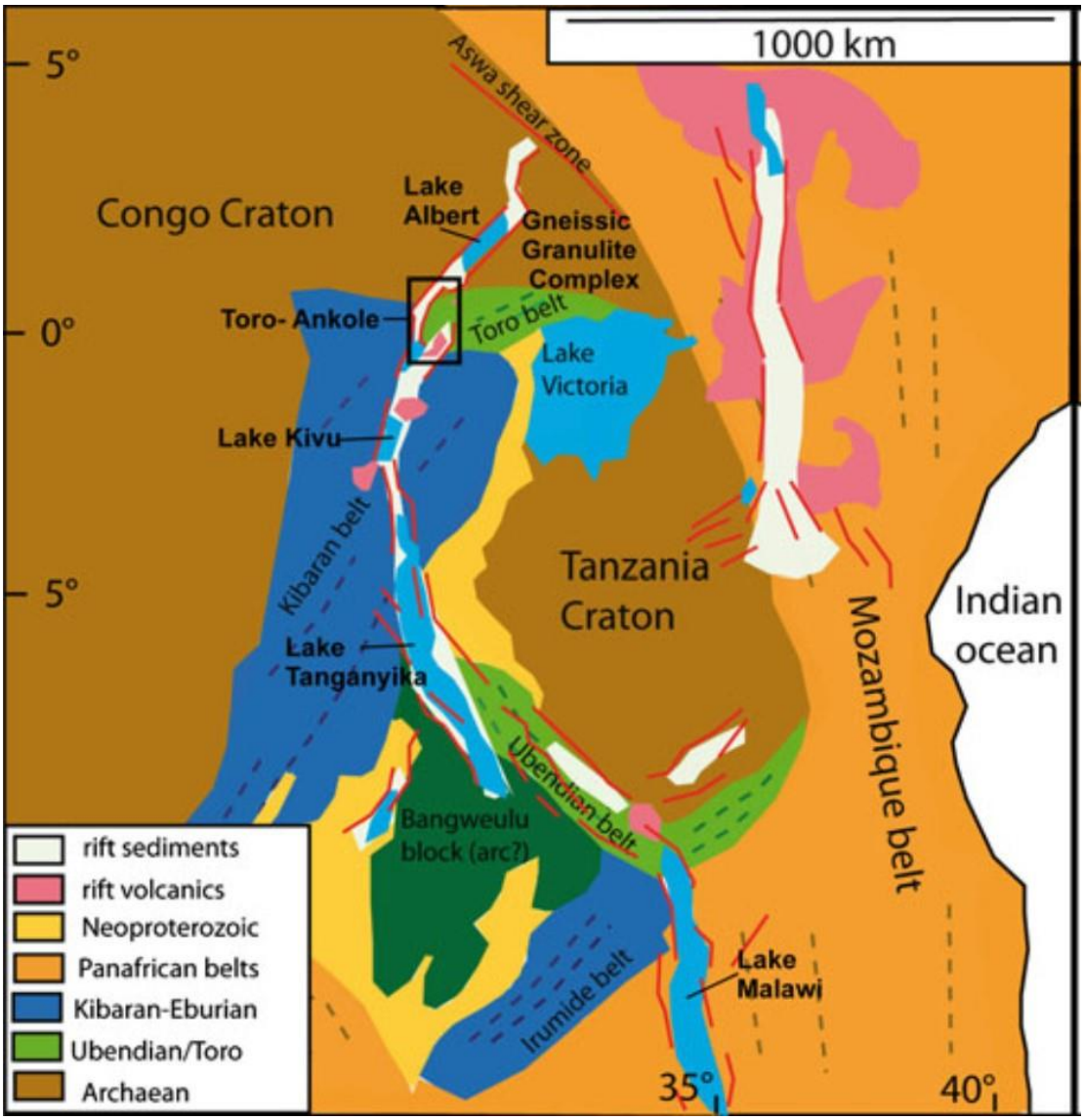

Figure 4. The geological overview of East Africa showing Congo –Tanzania Craton (Link et al 2010).

3.2.3 The Mozambique Belt

During the Pan African orogeny and the breakup of the Gondwana super continent, a suture formed between the Somalian and the African plates, the so called Mozambique Belt (MB) (Fig. 5). The emplacement of the MB was between 700 and 800 Ma ago. It contains some components created during the opening and closing of the Mozambique Ocean and subsequent continent – continent collision which resulted in the Gondwana breakup and its assembly. Moller *et al* (1998) documented that the MB mostly comprises upper amphibolite grade gneisses, rare rocks from eastern Tanzania craton (reworked) and the rocks from the Usagaran belt. The rocks from the Usagaran belt and the eastern Tanzania Craton were emplaced between 2.9 to 2.6 Ga (Reddy *et al* 2003). Grantham *et al* (2003), Moller *et al* (1998) and Yoshida *et al* (2002) suggested that the protolith of these rocks are related to magmatic under - plating and a period of residence in the mid to lower crust and subsequent cooling between 640 and 620 Ma ago.

The eastern part of the MB is also characterized by high grade arc derived rocks of various ages including from 841 to 632 Ma. The western portion of the MB contains sedimentary rocks, although, both parts contain metasediments of Neoproterozoic age. The difference in age indicates two different basins with regards to the origin of the rocks, the eastern basin rocks being thrust over those of the western basin during the closure of the Mozambique Ocean in between 585 and 550 Ma (Moller *et al*, 1998).

Kroner *et al* (2004) documented that the MB of East Africa at the southern part of EAO, contains polydeformed high-grade metamorphic assemblages, exposing middle to lower crustal levels, whose original environment of formation and structural evolution are more difficult to reconstruct. The MB in Tanzania is bordered with the Usagaran belt and the Tanzania craton to the east and with the Phanerozoic sedimentary basin (recent covers) to the west, Malisa *et al* (1990) suggested that the polydeformed high grade metamorphic rocks of the MB in Tanzania is characterized by major horizontal displacement as a result of thrusting and repetition of the stratigraphic sequence.

Fritz *et al* (2009) documented three mobile belts that were involved successively in the Archaean Tanzania Craton with eastward accretion; Usagaran belt (Western Palaeoproterozoic) with peak metamorphism (partly granulite facies) around 2 - 1.8 Ga, the Central Neoproterozoic Mozambique belt (CMB) peak metamorphism between 650 Ma to 580 Ma and the Galana Belt exposed in southern Kenya with peak metamorphism around 550 Ma.

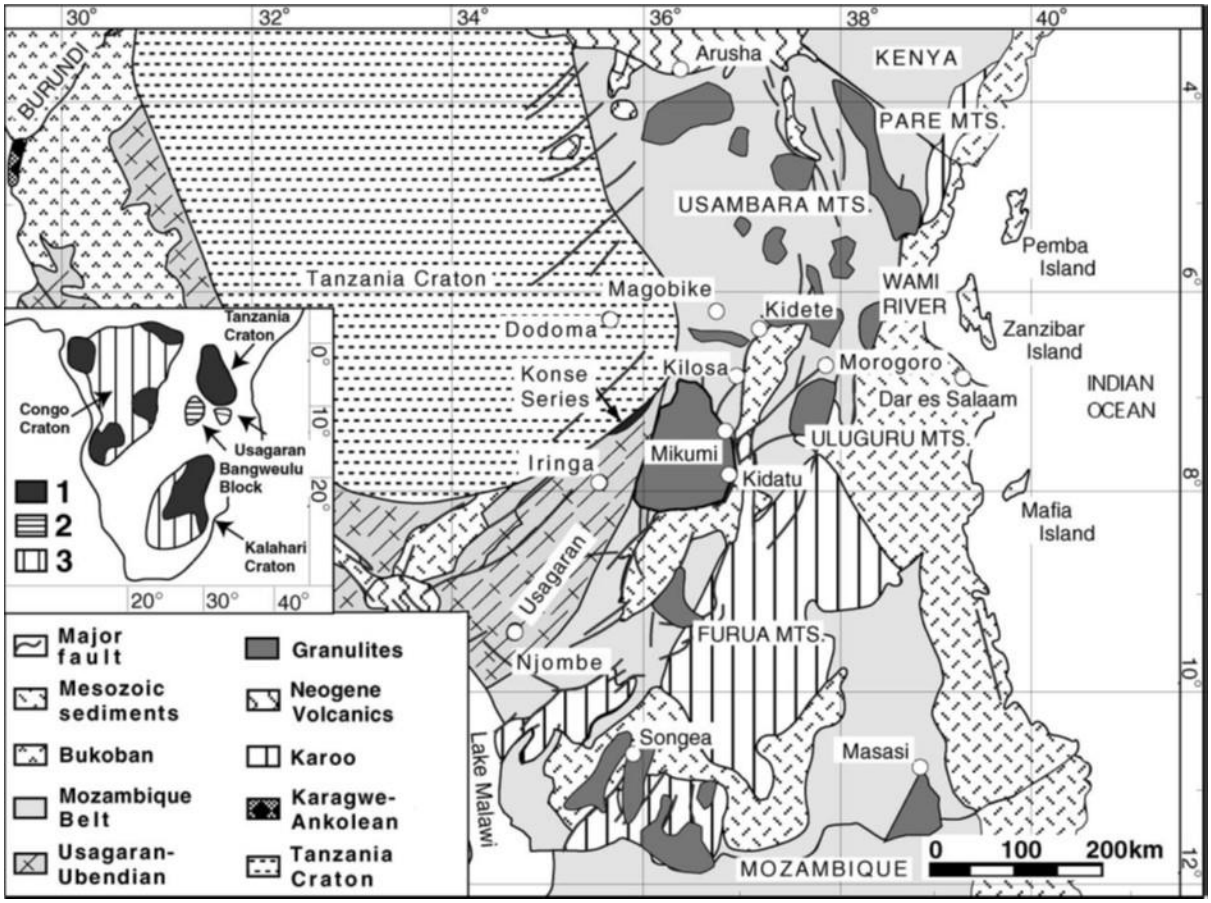

Figure 5. Simplified geological sketch map of the MB in the central part of the supercontinent Gondwana, the inset shows the main cratonic areas, within the southern part of the African continent: 1. Archaean; 2. including possible Archaean; 3. Bangweulu block (Sommer et al 2005).

3.2.4 Usagaran Orogeny (Belt/System)

The Usagaran belt is the north – south stretching orogeny of Proterozoic age (2 Ga) evidenced from eclogite dating (Moller *et al*, 1995). It is formed during the subduction of the lithosphere about 2 Ga ago. It is bordered by the Tanzania Craton to the west and MB to the east as well as southwards by the Ubendian belt (Fig. 6). It consists of high grade metamorphic units from amphibolite to granulites complexes (Malisa *et al*, 1990).

The Usagaran belt was formed during the subduction of a stretched or rifted continental margin in associated with the EAO and MB with subsequent sinistral slanting convergence (Reddy *et al*, 2003; 2004). Fritz *et al* (2005) argued that the Usagaran belt was formed during an Island arc regime and is associated with the strike slip tectonics. The Usagaran belt comprises rocks of granulite to amphibolite facies which are believed to originate from the sedimentary and

volcanic formations considered to have been deposited in the Palaeoproterozoic and subsequently metamorphosed from low to high grade (Reddy *et al*, 2004).

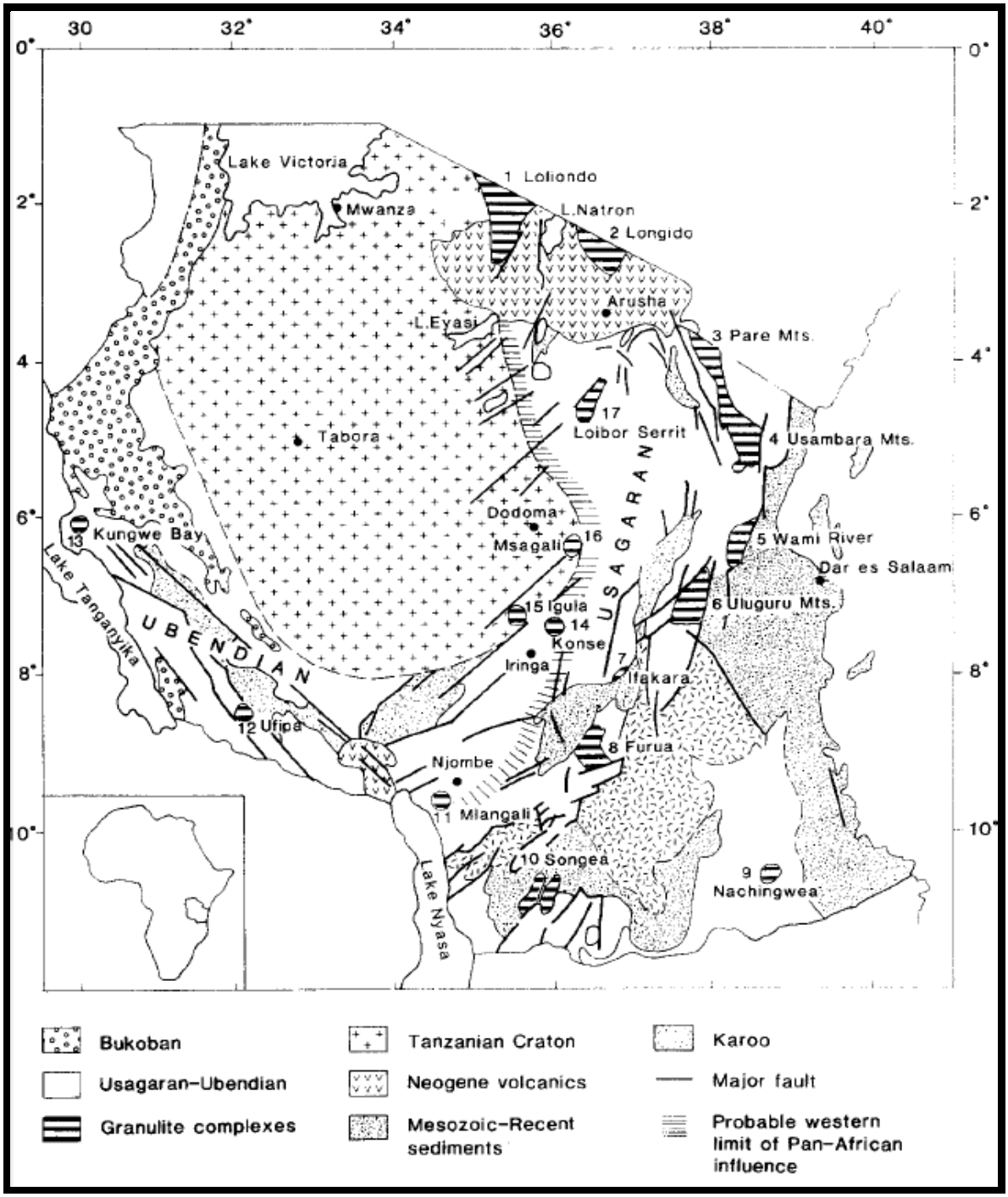

Figure 6. Outline of the Tanzania geology with location of Usagaran belt and major occurrences of granulite facies, which are represented with the number 1 to 17 with their local names (Malisa et al, 1990).

3.2.5 Tectonics Related to Gold Formation

Goldfarb *et al* (2005) and Groves *et al (*2003) suggested that gold deposition within a high grade metamorphic terrane occurred during compressional to transpressional regimes and throughout much of the upper crust, in deformed accretionary belts adjacent to continental margins. These metamorphic grades resulted from the orogenic development during continental collisions which involves thermal and stress anomalies. Also, gold deposits can be generated and/or modified during each evolutionary stage of orogenic development.

Orogenic gold type deposits occur over a large crustal depth range from deep-seated low salinity H_2O-CO_2±CH_4±N_2 ore fluids and with Au transported as thio-complexes. Tectonic deformational events resulted in structural features such as fractures, shears, folds and faults which led to the flow of fluids (magmatic or hydrothermal fluids). Formation of veins are related to the magmatism and metamorphism during silicification or intrusion of the silica rich rocks, in orogenic gold types veining is coeval with structures (shears) (Grovel *et al,* 2000).

Metamorphic processes have been implicated in many of the world's major gold deposits from low to high grade metamorphic terranes. Most of the orogenic gold deposits formed in metamorphic terrane of different ages: they are geometrically related from single veins to vein arrays, as stratabound replacement and as disseminated deposits. Most of them are structurally controlled hosted in mafic to ultramafic rocks sequences metamorphosed to greenschist and amphibolitic and even granulite facies (Groves *et al,* 2003; Phillips *et al,* 2009).

Gold can occur as free gold or in association with other elements. This implies that gold formed in a high temperature environment. Colvine *et al* (1988) suggested that if gold is related to hydrothermal fluid in a metamorphic terrane, it originated from a higher grade metamorphic terrane called the granulitisation zone. Two chemical aspects are important for gold precipitations, either by decreasing the solubility of gold or a decrease in the total dissolved sulphur. Thus if gold is transported in H_2O-CO_2±CH_4±N_2 fluids, the precipitation would be by reduced sulphur complexes as a results of decomposition from low salinity, H_2O-CO_2±CH_4±N_2 fluids (Groves *et al,* 2000, Colvine *et al,* 1988, and Fyfe *et al,* 1978).

Figure 7 summarises the orogenic gold type deposits develop in diverse environments such as the fore arc region of a convergent continental margin over a wide range of crustal depths. Deposits may also develop in deformed back-arc sedimentary sequences seaward of the craton

margin. Reduced intrusion-related gold deposits form inland of accreted terranes along shelf sequences of a craton margin, (Groves *et al*, 1998; 2000; 2003 & Goldfarb *et al*, 2005).

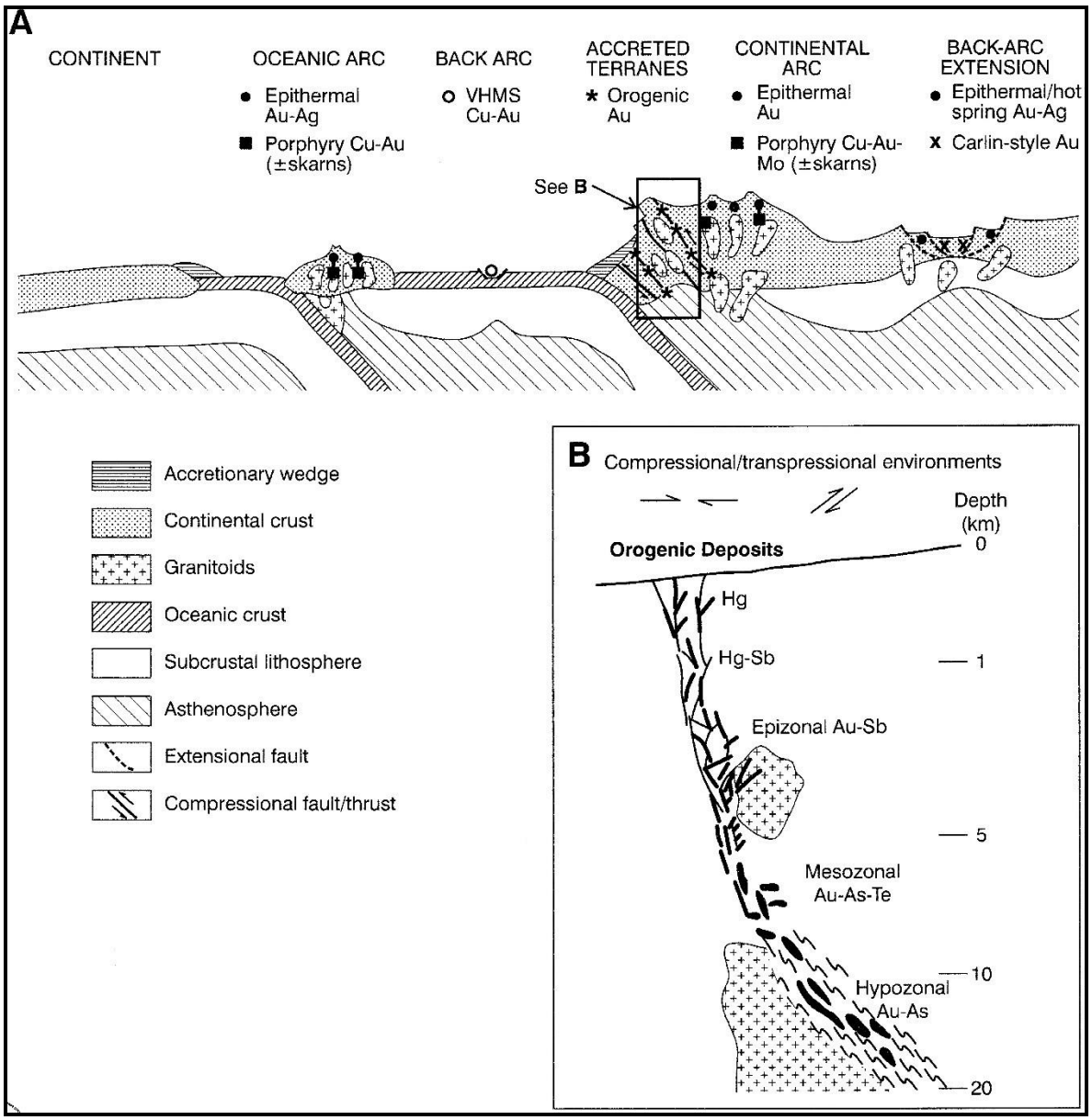

Figure 7. Schematic diagram showing the tectonic settings of orogenic lode gold deposit types. A) Plate tectonic environments of formation of orogenic lode–gold deposits and other largely syn-volcanic or syn-intrusive gold-rich deposit styles B) Depth profile of orogenic lode–gold deposit (Groves et al, 1998; 2000; 2003; Goldfarb et al, 2005).

3.3 GEOLOGY OF TANZANIA

The geology of Tanzania represents the geological framework of the African continent; its present appearance is a result of a series of events that start from the evolution of Archaean shields "Dodoma shields" to its modification through metamorphic reworking and accretion of other continental rocks, which later on covered by the sediments derived from continent (Quenelle *et al*, 1956; Harpum, 1970 & Semkiwa *et al*, 2005). Its landscape is influenced by pre-rift magmatism followed by active rifting both in the eastern and western sides of the country. It consists of rocks from the Archaean age, Proterozoic rocks from Ubendian and Usagaran and the Phanerozoic sedimentary rocks from the Bukoban and the Karoo series.

The Tanzania Craton covers most of the central and one third of the western part of the country, it is roughly bounded by the EARS and the Proterozoic Usagaran and Ubendian belts. The Archaean rock hosts the kimberlitic pipes and one of the biggest kimberlite in Africa where host the diamond deposits "Mwadui" (Fig. 8), also the major source of the lode gold deposits "greenstone belts – Nyanzian system" (Semkiwa *et al*, 2005).

The Archaean basement terrain is bounded by the series of the **Proterozoic** mobile belts, the Usagaran belt to the east and the Ubendian belt to the west. The Proterozoic rocks from the Usagaran System host most of the colorful gemstones including ruby and tanzanite, and newly discovered gold deposits. Recent work by Kabete (2008) in Groves (2010) interprets that the portion of the Usagaran belt which may contain Archaean crustal rocks which underwent high grade metamorphism may contain gold as well. The Ubendian belt is an example of the economic potential for base metals and gold deposits as exemplified by the Lupa gold field in Chunya area (Semkiwa *et al*, 2005).

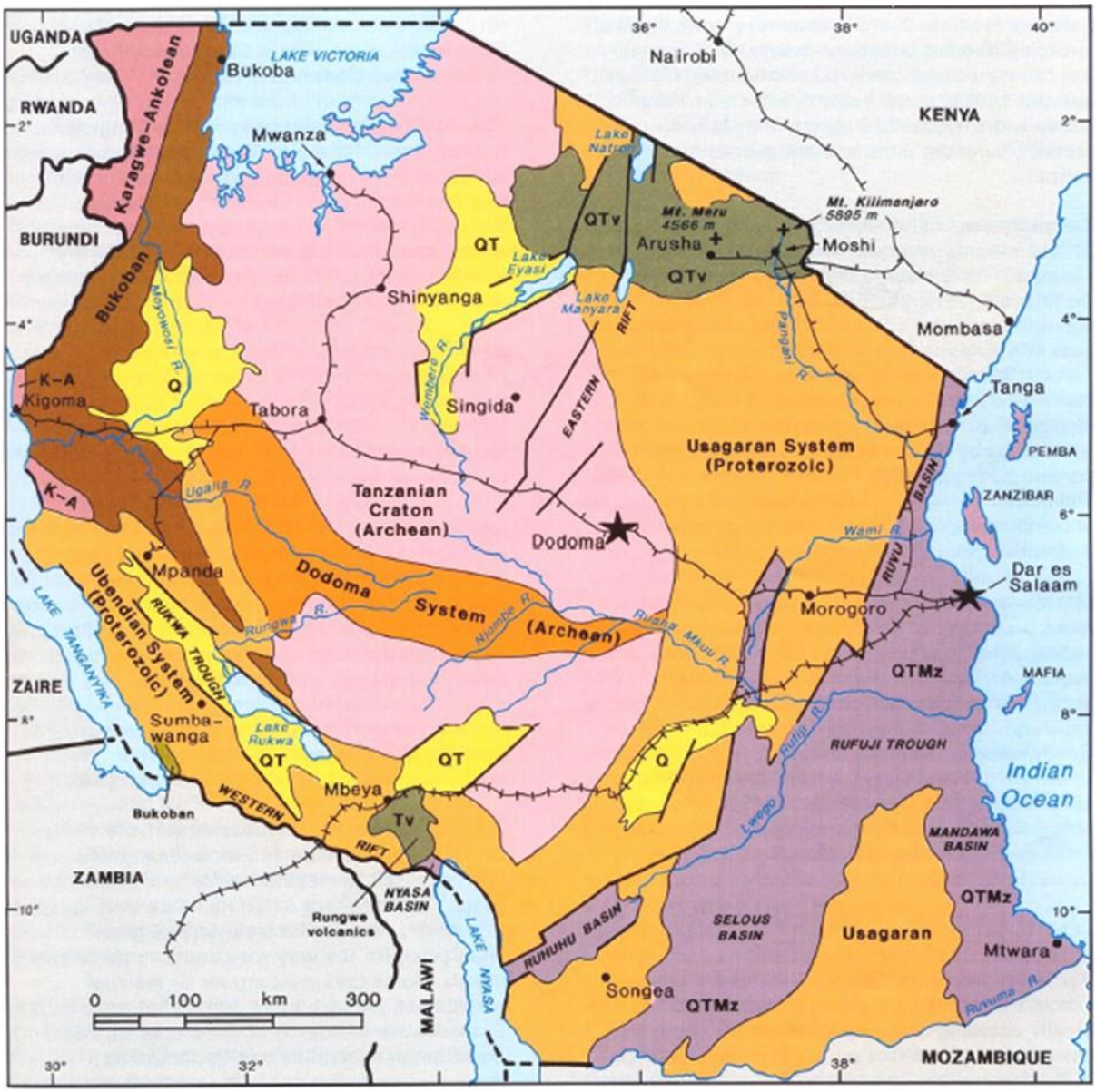

Figure 8. Generalized geology of Tanzania (Semkiwa et al, 2005).

According to Semkiwa *et al* (2005), **Phanerozoic** rocks are represented by a series of sedimentary units of Paleozoic to Mesozoic age, which is followed by a pre – rift period of kimberlitic and related alkali mantle – derived intrusive and extrusive activity that presaged active rifting. Rocks related to this event intrude up to Upper Mesozoic and Lower Cenozoic sedimentary formations which include the Karoo formation, which are rich in coal and uranium deposits. A period of rift-related intrusive and extrusive activity followed, concentrated in the Arusha area – to the northeast and Mbeya area – to the southwest, which is responsible for mountain-sized volcanoes such as Mt. Meru and Mt. Kilimanjaro. Harris (1981) documented that placer gold; diamond and colored gemstone deposits found across the country resulting

from a wide variety of recent and largely semi to unconsolidated wind, water, and weathering-derived recent formations.

3.3.1 Stratigraphy

The lithological structural provinces in Tanzania cover from the Archaean, Proterozoic to Phanerozoic eons including the Paleozoic, Mesozoic and Cenozoic era (Quenelle *et al*, 1956; Harpum, 1970; Harris, 1981). Stratigraphic sequence of the geology of Tanzania is represented in Figure 9.

Archaean rocks older than 2.5 Ga form the oldest unit. It consists of granite – greenstone belts in which linear belts of greenstones (volcano-sedimentary) sequences, are found within a larger region of predominantly granitic rocks (Harpum, 1970). The Archaean consists of the Dodoman System, Nyanzian System, Buganda Toro system (the granite gneiss system which is not well documented in Tanzania) and the Kavirondian system (Quenelle *et al*, 1956). Rammlmair *et al* (1990) suggesting four generations of the granitoid in relation to Archaean rocks of Tanzania. It ranges from the Nyanzian basement granites, granitic gneisses and migmatites (G3) to synorogenic granites, granodiorites (G4 and G5) and post orogenic alkali granites and syenites (G6).

Dodoman System is the oldest basement. Its rocks have the age of about 3 Ga older than the greenstone 2.7 Ga and its surrounding granites, forms an east - southeast trending of the lowermost Archaean rocks in the country. It consists mainly of rocks originated from the sedimentary sequence, mafic volcanics and ultra – mafic intrusive. Also, they contain rocks from low to high grade metamorphic facies (Quenelle *et al*, 1956 and Thomas *et al*, 2012).

The Nyanzian System aged at 2.7 Ga. It consists of a series of typical volcano – sedimentary sequences or greenstone belts within a much larger area of granite – gneiss complexes. It evolved complex volcanics from mafic to felsic sub aerial volcanic rocks derived from volcaniclastic rocks. The iron formations and associated intrusive of a variety of intermediate to felsic compositions are present as well. All of these comprises the greenstone belts of Nyanzian System (Harpum, 1970). Harris (1981) divided the Nyanzian into two series, the upper and lower series. The lower series consists of; primary basalt, andesite, dacite pillow lava, banded iron formation (BIF), recrystallized chert, shale, and conglomerate. The upper series consists of felsic lava assemblages, tuffs, ferruginous cherts, BIF and meta-pelites. The greenstones are generally metamorphosed to greenschists facies and are folded with abundant

structures developed. It is of major economic importance due to its gold deposits from small to large scale mining and the diamondiferous kimberlite.

Kavirondian System is the youngest system in the Archaean of Tanzania. It is located in the northern part of the country. It consists mainly of conglomerates, coarse arkosic, feldspathic grits and quartzites along with minor granitic and volcanic rocks. It is unconformably with the Nyanzian System (Harpum, 1970)

Proterozoic rocks of Tanzania are divided into two systems, the Usagaran belt and Ubendian belt aged between 2 Ga and 1.8 Ga. The Usagaran belt covers the eastern part of Tanzania, characterized by rocks of high grade metamorphism of both sedimentary and igneous origin. Sommer *et al* (2005) documented that, Usagaran belt consists of deformed and metamorphosed rocks characterized by post Usagaran granitoids and minor supracrustal successions at its northern part. At its southern part, it consists of weakly deformed and nearly unmetamorphosed rocks. These rocks include the rhyolite, dacitic and andesitic volcanic rocks, which overlie the older Usagaran basement. Moller *et al* (1995) documented that the Usagaran belt characterized with amphibolitized eclogites intercalated with other layers of pelites (metapelites and semipelites) and occasionally carbonate.

According to Harpum (1970); Stern (1994) and Moller *et al* (2000), the metamorphic assemblages of the Usagaran belt resulted from the Pan African tectonothermal event that affected the MB resulted to the amphibolite granulite facies related to granitisation and migmatisation origin. Part of the Usagaran belt contains the same rocks as the Nyanzian System, which overprinted by high grade metamorphic events caused by tectonic activities. This raises the economic importance of the system; apart from rich in colored gemstone but also it contains gold deposits (Groves, 2010; Kabete *et al*, 2012; Reddy *et al*, 2003; 2004, Kroner *et al*, 2004).

The Ubendian belt located to the south west of the country, is characterized by the rocks of lower Proterozoic to Archaean mobile belt that bound the Archaean Craton. Harris (1981) suggests that the Ubendian belt contains variety of high-grade metamorphic rocks of both sedimentary and igneous origin as the Usagaran belt, whereas gneisses; minor mafic and ultramafic intrusive are the dominant lithology. The lithologies are folded and trending northwest to southwest. Its economic importance are colored gemstone deposits, gold and base metals.

Karagwe-Ankolean System dated 1.3 to 1.4 Ga years extends west of Lake Victoria, and is found along the northwest boundary of Tanzania with Burundi, Rwanda, and Uganda. It is younger than the other two system in Proterozoic, consisting mainly of argillaceous and arenaceous formations. Harpum (1970) suggests that the sedimentary features of the Karagwe-Ankolean rocks replicate shallow-water deposition. Low-grade metamorphism has transformed many of these units to sericite schists and quartzites. Its economic importance comes from the intrusion of granites which host the tin and tungsten mineralization.

Phanerozoic rocks of Tanzania consist of Bukoban System, Karoo System and Mesozoic Kimberlite Pipes. The Bukoban System is the recent cover overlying the Nyanzian System rocks at the northwestern part of Tanzania bordering the Uganda, Kenya and Burundi (Figure 10) (Semkiwa *et al*, 2005). The system comprises with the following rocks, sandstones, quartzites, shales, red beds, dolomitic limestone and chert along with the amygdaloidal basalts, and gabbroic to doleritic sills and dykes. The economic importance of the Bukoban System is the association of mafic rocks containing copper deposits (Harris, 1981).

The Karoo System covers nearly the eastern coast of Tanzania, the southwest to northeast flanks and overlies the Usagaran to the immediate eastern part whereas there is no Karoo, which covers to the western side; though Harpum (1970) reported that there are series of dolerite dyke swarms concentrated on the Iramba Plateau and the Crater Highlands, both shoulders of the Eyasi graben and in the Musoma area. Harris (1981) suggested that the Karoo system comprises of continental sediments ranging from Late Permian to Jurassic in age, these include coarse sandstones, shales and siltstones, structurally the Karoo lies unconformably upon the Precambrian basement. Economic importance of the Karoo system is the coal formation and the secondary uranium deposits.

Mesozoic rocks, kimberlite pipes, Harpum (1970) documented six provinces of kimberlites in western Tanzania. These are the Shinyanga - Mwadui, Mabuki, Speke Gulf, Lake Eyasi and Iramba Plateau kimberlite provinces; several carbonatite intrusive complexes have been recognized and mapped. Cenozoic is the youngest unit characterized by sedimentary and extrusive volcanics. It includes the marine and continental sedimentary rocks of the coastal plain and inland basins as well as Miocene to modern alkali and sub alkalic extrusive related to rifting.

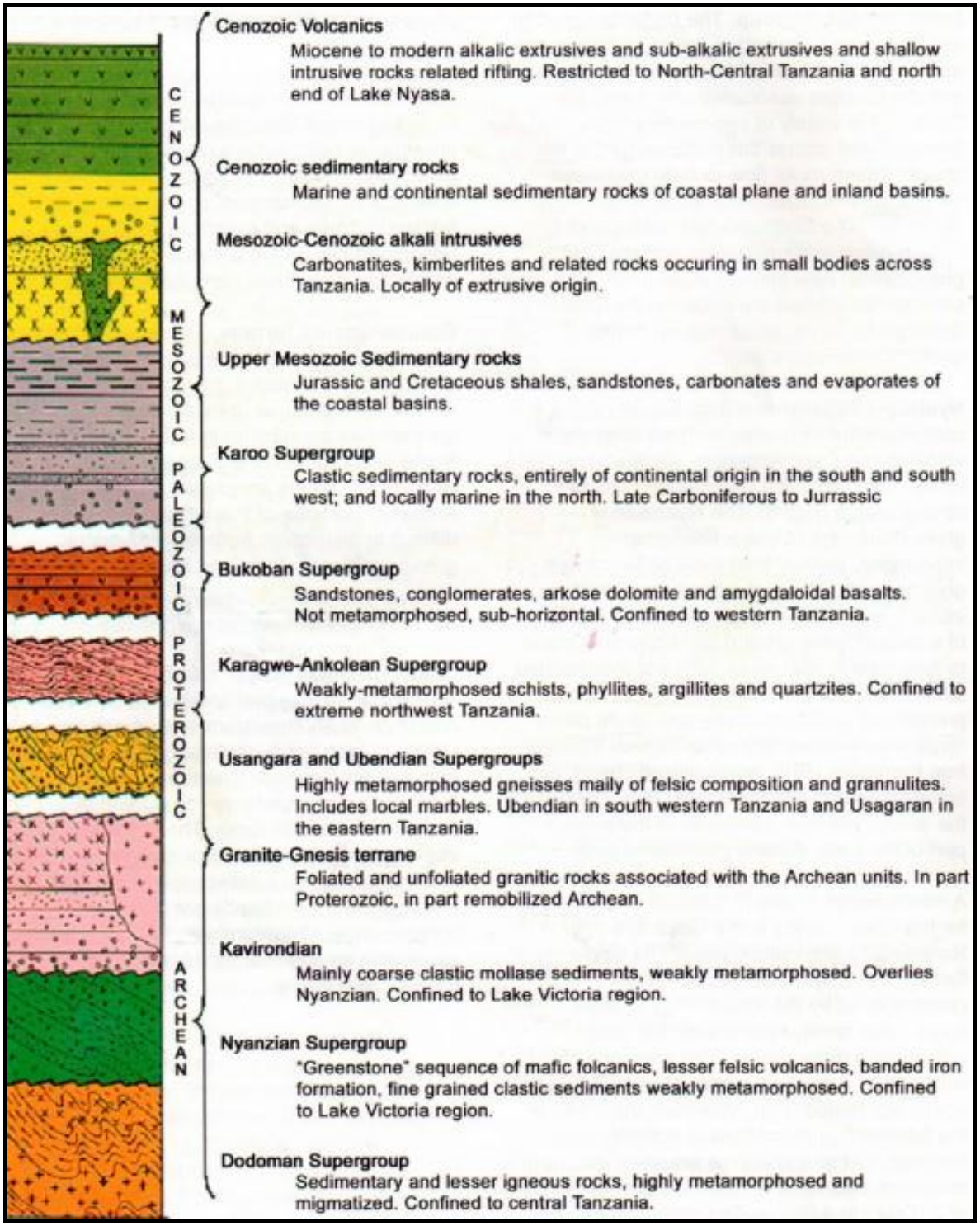

Figure 9. Simplified stratigraphic sequence of Tanzania geology and its economic significance (Semkiwa et al 2005).

3.3.2 Structure

The Kilindi Handeni Superterrane is believed to be of the same age as that of the Archaean lithologies ~2.7 Ga (Fig. 10). The recent work from Kabete (2008) cited in Groves (2010)

entails that the KHS lies on the same regional structural trend at NW – SE as the Sukumaland Corridor of the LVG. The rocks from this area believed to be overprinted by high grade metamorphic event caused by regional tectonic effects (Groves, 2010 & Kabete *et al*, 2012b).

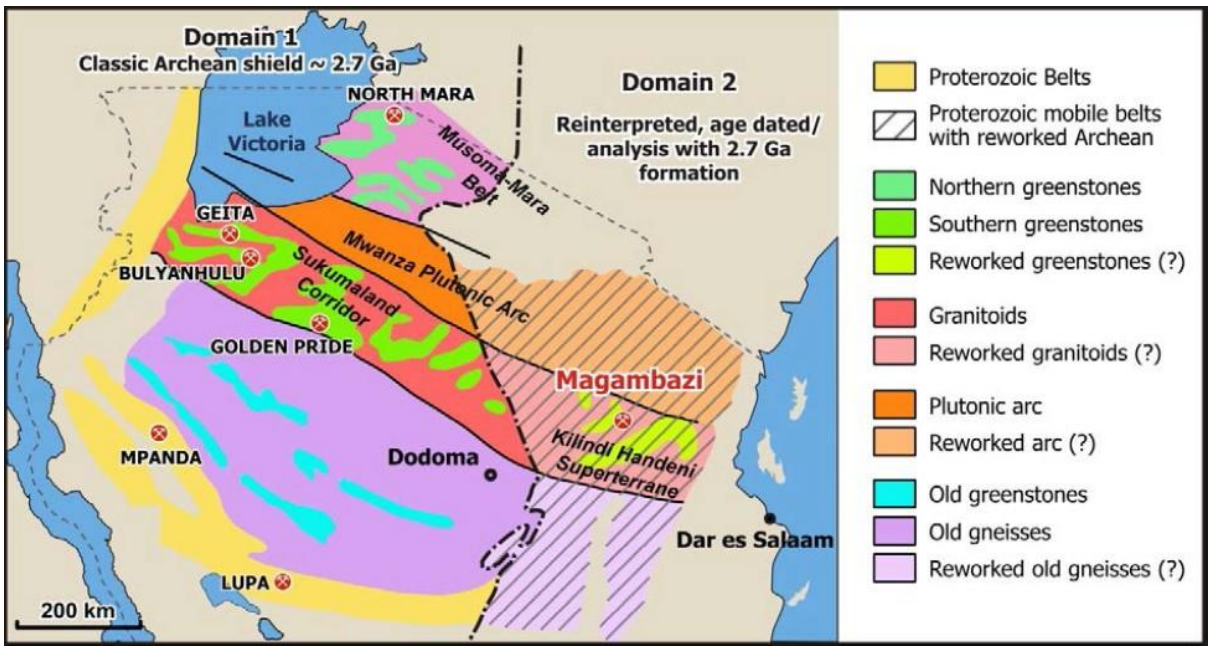

Figure 10. Schematic map of tectonic subdivisions of the Tanzania Craton with interpreted reworking concept model (Groves, 2010).

3.3.3 Metamorphism

Many lithological units from Archaean to Proterozoic rocks have been affected by regional metamorphism in Tanzania from low to high grade. These are caused by a series of tectonic events affecting part of the East Africa from regional to local scale. These tectonic events include: i) the Pan African events (Neoproterozoic), which influenced the whole MB between 615 to 650 Ma, ii) the breakup and assembly of Gondwanaland subsequent to the continent – continent collision, iii) the formation of the EARS in association with the volcanoes and great lakes resulted from the African and Somalian plates collisions, iv) the plate convergent and subduction of oceanic plate during the formation of Proterozoic rocks of Usagaran belt at 1.9 Ga and v) the Archaean event affected the craton at 2.5 -3.0 Ga (Kroner *et al*, 2004; Link *et al*, 2010; Stern, 1994; Sommer *et al*, 2005;Moller *et al*, 1998).

Rollinson (1982) suggested that the ultramafic rocks in many greenstone belts have been converted into talc schists and tremolite actinolite schists due to metamorphism. The basic volcanics rocks commonly have the following assemblages; actinolite-albite-chlorite-epidote

or at higher grade; hornblende - andesine - epidote - quartz. Also Windley (1995) documented that the metasediments are the typically schists containing the following mineral assemblages actinolite – chlorite - quartz, sericite-quartz and biotite-chlorite-quartz. These two suggestions could be related to greenstone rocks from the Nyanzian system.

Kroner *et al* (2004) suggested that part of the regions of EAO characterised by high grade metamorphic assemblages of which its origin consists predominantly of much older Mesoproterozoic to Archaean continental crust that was strongly reworked (Fig. 11) during the Neoproterozoic, this has been observed by different scholars (Reddy *et al*, 2003; 2004, Collins *et al*, 2004; Stern, 1994; Fritz *et al* 2009; Kabete *et al* 2012b).

Many scholars (Reddy *et al*, 2003; 2004; Collins *et al*, 2004 etc.) worked on geochronology of the Usagaran belt by using SHRIMP U-Pb zircon, suggested that amphibolite facies overprint older rocks than 2 Ga. Based on the U-Pb zircon ages from the eastern granulites of Tanzania Stern (1994) interpreted the time of granulite facies metamorphism and ranges from 650 Ma to 715 Ma. This metamorphism occurs at 8 to 13 Kbar and from 700 to 900 ^{o}C, whereas Fritz *et al* (2009) was precise to 850 ^{o}C and 11 Kbar for peak metamorphism. Kabete *et al* (2012b) on his recent age dating studies using SHRIMP zircon, qualitatively interpretation of the higher metamorphic-grade of the KHS correlated with regional structural data show the same structural trend ESE (Fig. 12).

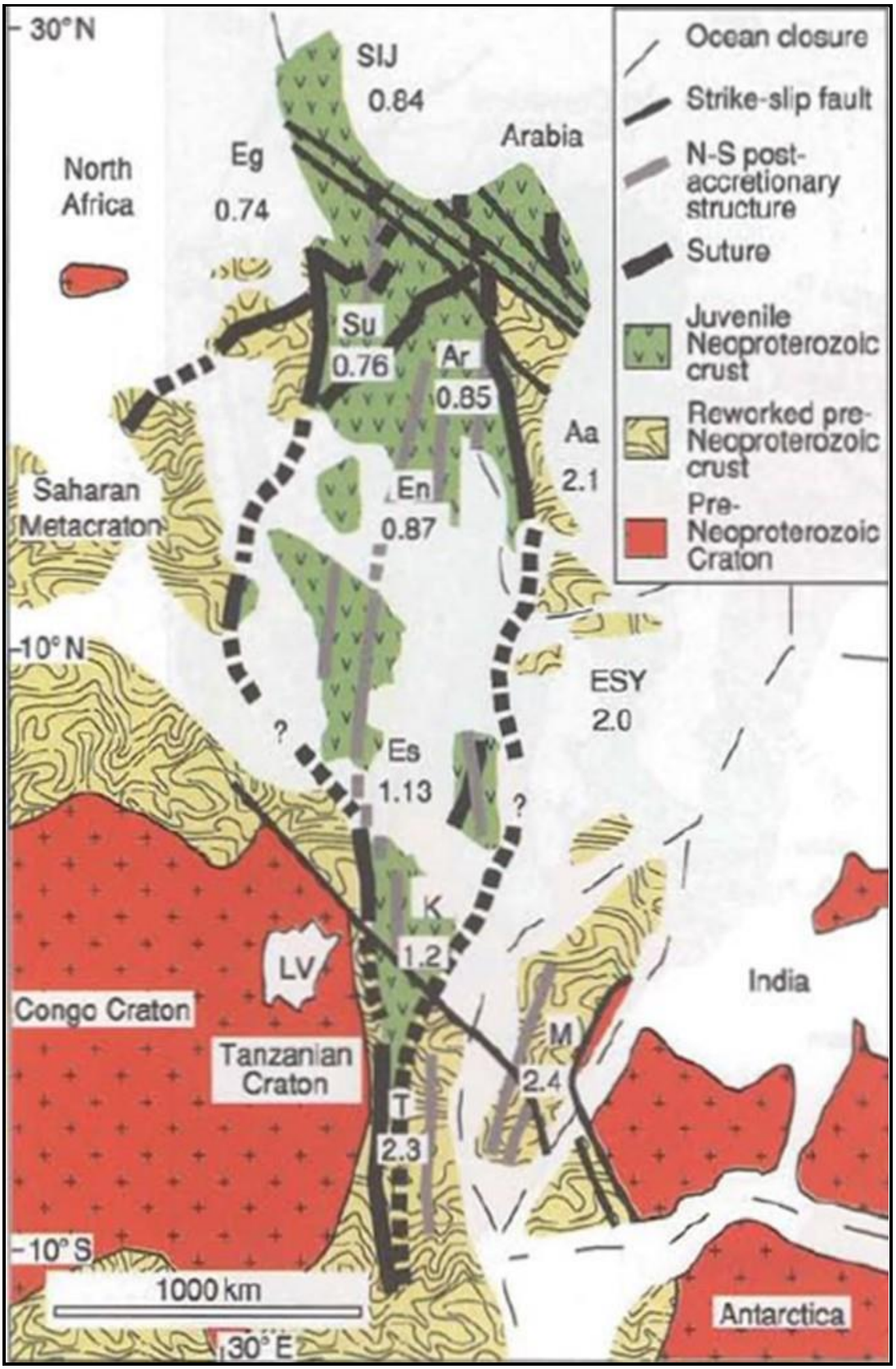

Figure 11. Reworked pre-Neoproterozoic crust in Pre-Jurassic configuration of elements of the northern part of EAO and surrounding regions. Regions include Egypt (Eg), Sudan (Su), Sinai-Israel-Jordan (SIJ), Afif terrane, Arabia (Aa), rest of Arabian Shield (Ar), Eritrea and

northern Ethiopia (En), southern Ethiopia (Es), eastern Ethiopia, Somalia, and Yemen (ESY), Kenya (K), Tanzania (T), and Madagascar (M). Numbers in italics beneath each region label are mean Nd-model ages in Gy, (Kroner et al, 2004).

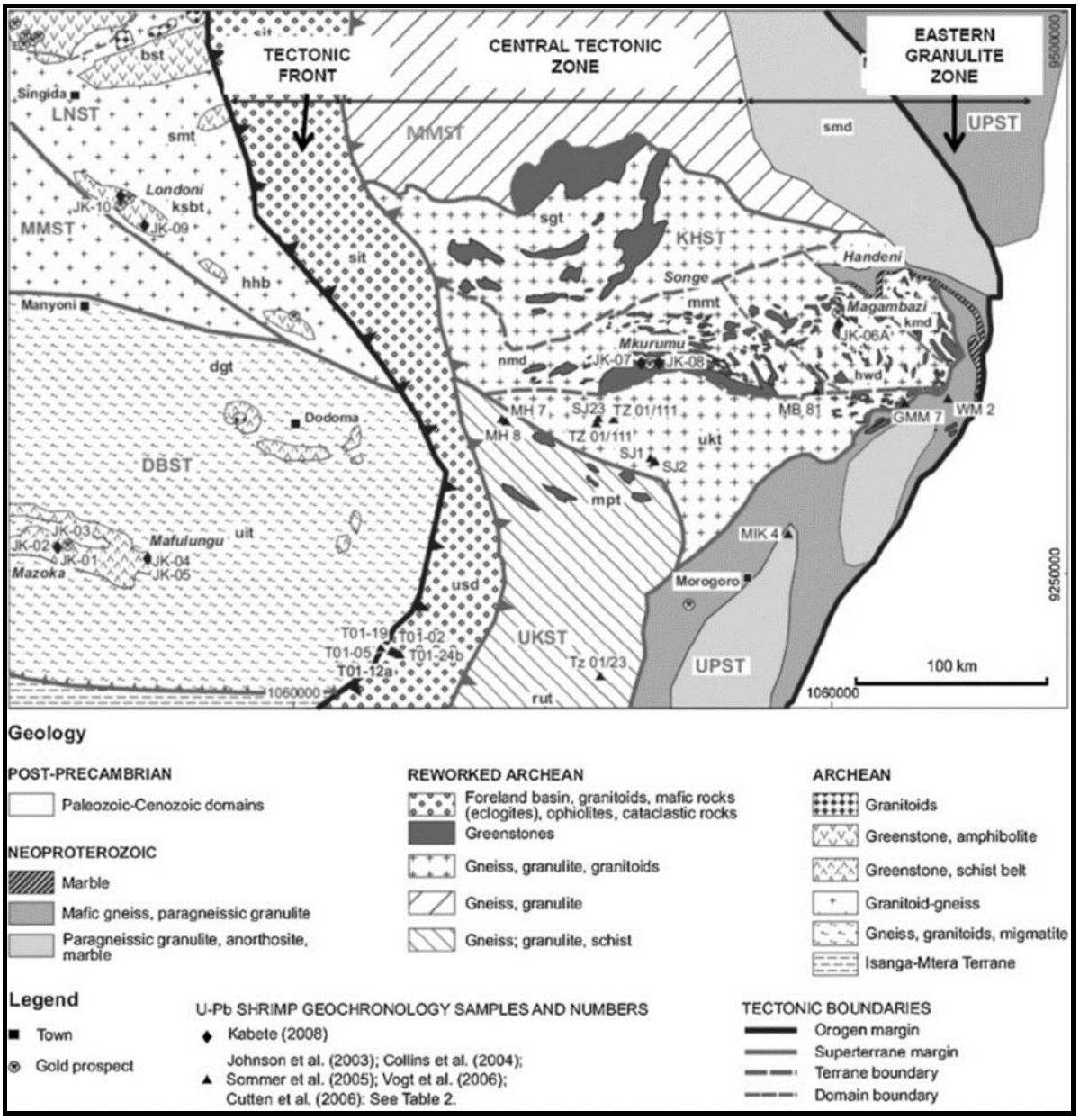

Figure 12. Regional geologic-tectonic map showing crustal blocks and belts which make up the south-eastern part of the Tanzania Craton and Southern EAO (Kabete et al, 2012b).

The KHS which is located in the Usagaran belt have been metamorphosed from amphibolite to granulite facies. The presence of mafic rocks in the KHS and the geochronological data suggested that the area under gone several metamorphism events. The process is referred as

overprint of Archaean rocks including the low grade rocks from the greenstone belt (Fig. 13) (Archibald, 2011; Howard, 2011; Fritz *et al*, 2009; Groves, 2010; Kabete *et al*, 2012).

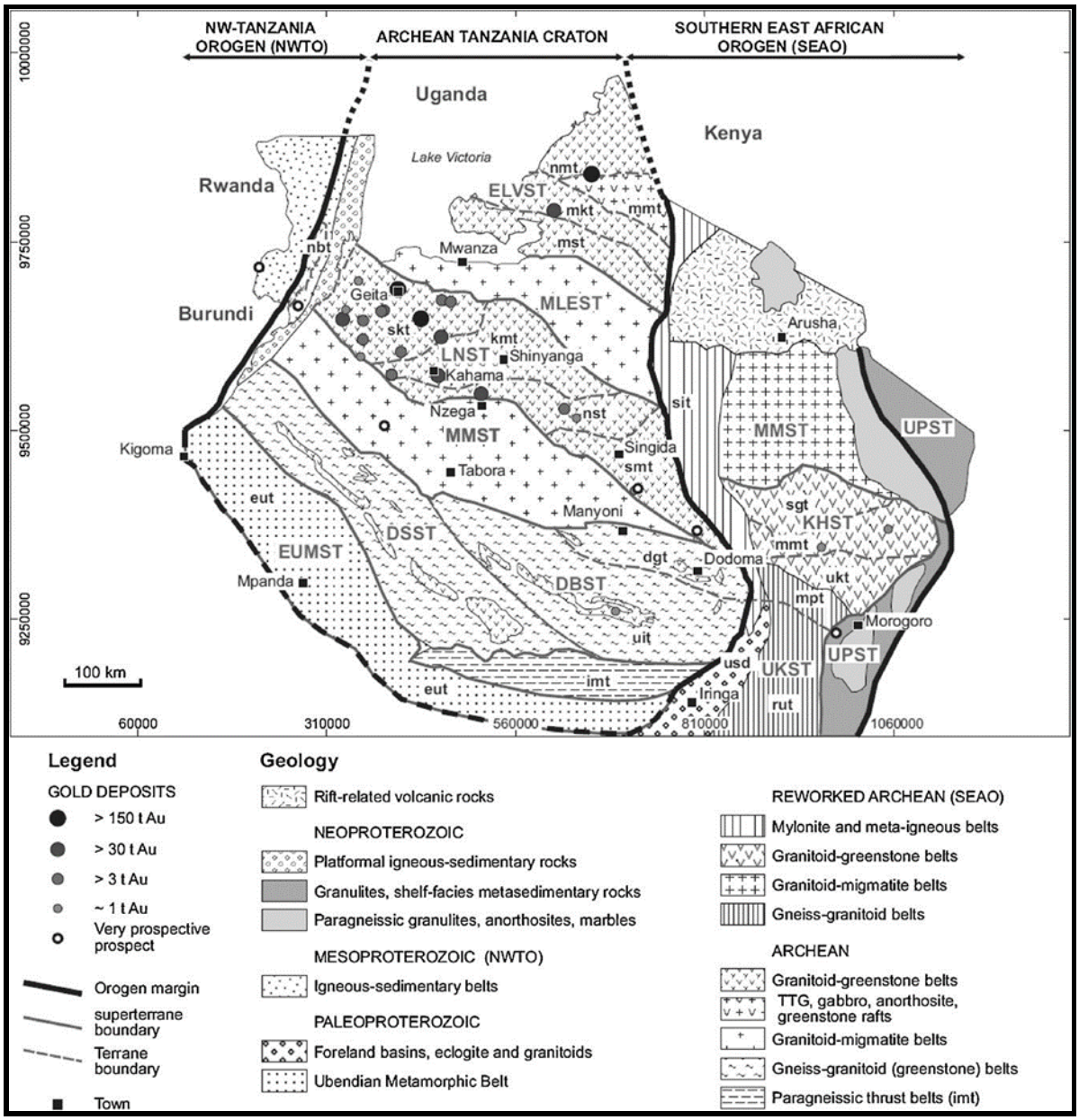

Figure 13. The Archaean Tanzania Craton and the blocks comprising it with the Proterozoic belts of Ubendian and Usagaran, which shows the reworked part of the Usagaran orogen including the KHS, (Kabete et al, 2012b).

CHAPTER 4 GEOLOGY OF THE HANDENI DISTRICT

4.1 INTRODUCTION

The Proterozoic lithologies of Tanzania are divided into two main belts, the Usagaran belt east of Archaean Tanzania Craton and the Ubendian belt west of the Archaean Tanzania craton. The KHS is located in the Usagaran belt east of the Archaean Tanzania Craton. Kabete *et al* (2012) dividing the KHS into two geological zones: the eastern granulite zone which contains the Neoproterozoic (outside the study area) and the central tectonic zone which is believed to have resulted from reworked Archaean Paleoproterozoic. This chapter discusses the local geology, structures and mineralization of Handeni project.

4.2 LOCAL GEOLOGY

The geology of Handeni district represents the geology of KHS which is classified as part of the Proterozoic Usagaran belt that occurs east of the Archaean Tanzanian Craton. The Usagaran belt is trending north – south and is dominated by high grade metamorphic rocks of amphibolite to granulite facies. It is characterized by a sequence of ultramafic to felsic volcanic flows, black shales and quartz bearing sedimentary rocks (Scheepers, 2010).

The Handeni project is characterised by the following lithological units: the granulite gneiss as the basement overlain by paragneiss and interleaved para-amphibolite rocks. These are overlain by amphibolite-mafic gneiss with abundant quartz veining. Garnet containing mafic rocks overlie the orthogneiss and rafts of amphibolite. The post kinematic intrusions are covered by saprolite and thick soil derived from weathered metamorphic rocks (Fig. 14) (Groves, 2010; Kabete *et al*, 2012).

Scheepers (2010) and Howard (2011) suggested that high grade metamorphism has converted the original lithologies to a variety of metamorphic equivalents including: biotite-hornblende-garnet-pyroxene gneiss, migmatitic augen garnet hornblende- pyroxene gneiss, quartzo-feldspathic hornblende-biotite-pyroxene gneiss, pyroxene-hornblende-biotite-garnet granulite (Fig. 15). The entire assemblage has been folded into a synform with a northwest-southeast axis, complicated by numerous faults, some of which are spatially associated with gold mineralization.

The geology of KHS represents a non-traditional exploration environment dominated by the high grade metamorphic rocks trending NW-SW. Historically the region has a potential for

coloured gemstones until early 2003 where artisanal miners discovered alluvial gold within the area. This was followed by a recent re-interpretation of the regional structural data (Kabete *et al*, 2012) which suggested that, the rocks from KHS lie on the same trend NW-SW as that of Nyanzian System hosting gold mineralisation.

The main host rocks are silicified garnet bearing amphibolite enclosed within a sequence of interbedded paragneiss and amphibolite as well as within the siliceous or quartz veins, (Scheepers, 2010; Archibald, 2011). Major and micro structures including ENE trending thrust faults, NW-SE shear zones, folds and NE-SW trending brittle and ductile faults zones are developed (Scheepers, 2011). The ore geology (host rocks) of the area characterised by the series of garnet to amphibolitic rocks, these include garnet silica rock, garnet rich bearing amphibolite and quartz veins (Fig. 15).

Gold mineralization in Handeni project is categorized as vein related structurally controlled. Groves *et al* (1998) categorized gold of this type as orogenic gold deposit which has been affected by the metamorphism. The gold mineralisation occurs in both native state and associated with sulphides such as pyrrhotite and arsenopyrites and is geometrically often in quartz veins, veinlets and scattered pods (Scheepers, 2010 and Archibald, 2011). Sulphide minerals related to gold mineralization include pyrrhotite, chalcopyrite and arsenopyrite (Scheepers, 2010). Other minerals related to gold mineralization are galena and locally graphite (Howard, 2011 and Groves, 2010).

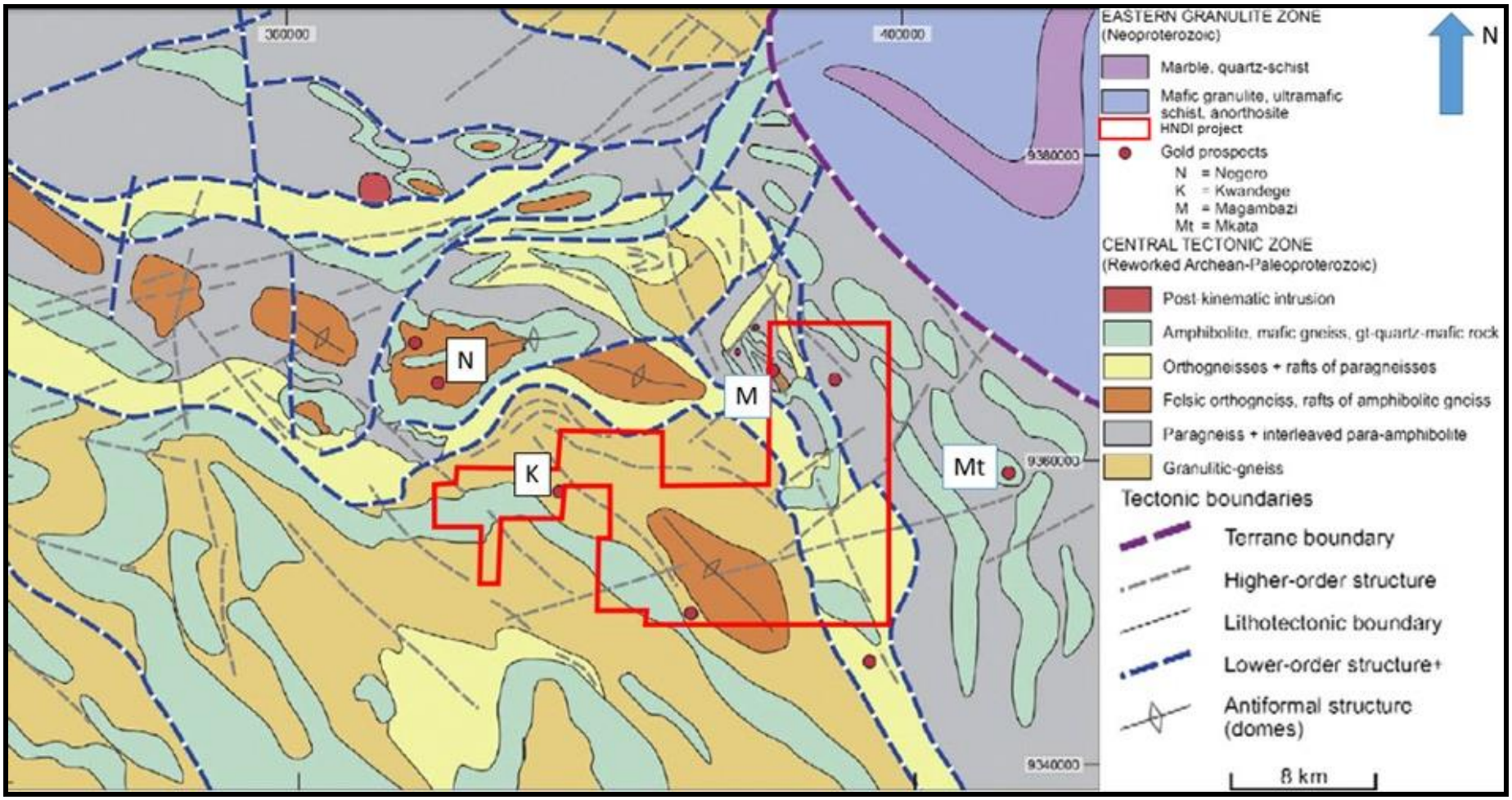

Figure 14. Geology of the Kilindi–Handeni Superterrane in the Southern East African Orogen. A result of qualitative interpretation of high-resolution magnetic and radiometric imagery interpreted in terms of geology (Kabete et al, 2012a).

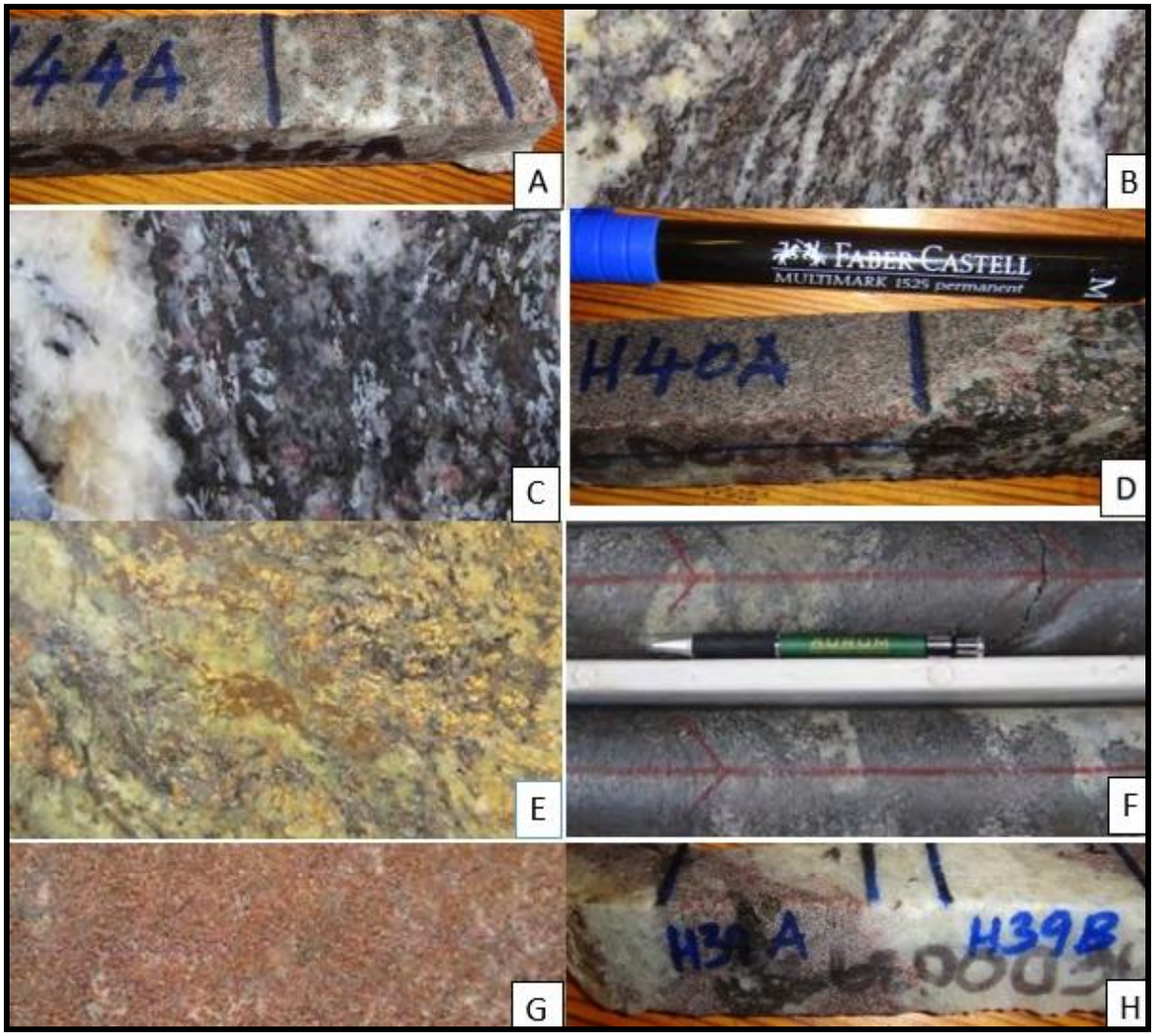

Figure 15. The lithologies available in the Handeni project, A- Garnet-bearing amphibolite, B - Feldspathic gneiss, C - Garnet-Sillimanite / Kyanite - bearing feldspathic gneiss, D - Garnet-silica rock at the contact with garnet bearing amphibolite, E - weathered sulphide zone containing graphite, F - Massive graphite with feldspathic gneiss, G – Silicified Garnet rock and H – Quartz vein with gradational contact in Garnet Silicified rock, (modified after Archibald, 2013).

4.3 LOCAL STRUCTURES

The Handeni project lithologies contain massive to disseminated sulphides which influenced Handeni Gold Inc. to conduct airborne magnetic and radiometric surveys. In addition ground electromagnetic and induced polarization surveys as well as foot borne radiometric surveys were done. Data from the surveys were interpreted and delineated geophysical targets which were then followed up by geochemical surveys.

Subsequent to the acquisition of airborne geophysical data (magnetics and radiometric survey), the data shows the same regional trend (NW-SE) as those interpreted in regional structural features in Figure 10. The common structure has the same trend as the regional structures interpreted in QDS 147 and 148 as well as recent qualitatively interpreted in Kabete *et al* (2012).

Local interpretation of the data correlate well with the old gold workings in both of the projects as illustrated in sub section 4.7.1 and 4.7.2 and in Figures 16 and 17 respectively. The local structural features exemplify their coincidence with old gold workings from both of the projects as shown in radiometric and magnetic data (Howard, 2011).

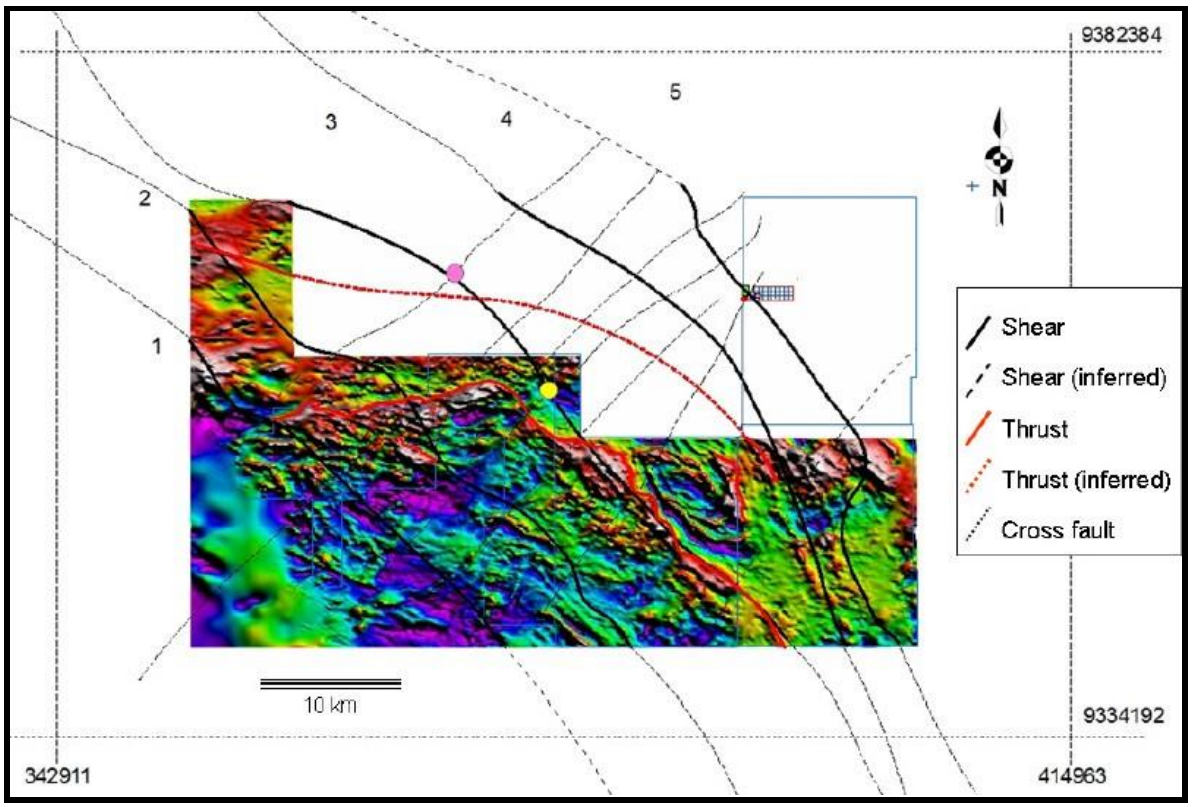

Figure 16. Interpretation of structures based on airborne magnetics data exemplifying their coincidence with known old gold deposits (pink and yellow dots) (Scheepers, 2010 and Howard, 2011).

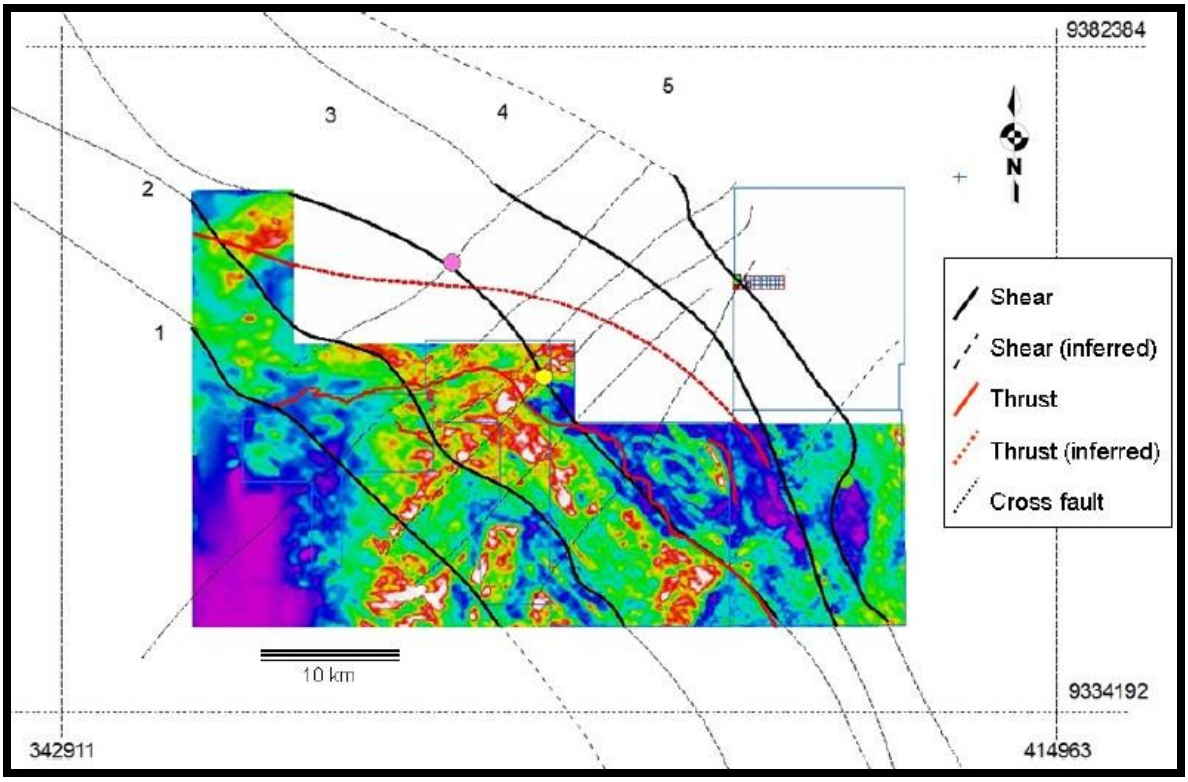

Figure 17. Interpretation of structures based on airborne radiometric data (total counts) exemplifying their coincidence with known old gold deposits (pink and yellow dots) (Scheepers, 2010 and Howard, 2011).

4.4 MINERAL RESOURCES OF HANDENI PROJECT

In contrast to Lake Victoria Goldfields (LVG) in northern Tanzania where gold occurs within the greenstone belts known as Nyanzian Superterrane, characterized by banded iron formation (BIF), amphibolite - green schist, porphyries and quartz reefs with favorable structural settings. Gold mineralization in Kilindi - Handeni region is hosted in garnet-amphibolite zones within the amphibolite to granulite facies metamorphic assemblages (Howard, 2011).

In terms of resources and reserve from the Proterozoic age, the recent resource estimate from East Africa Metals (previous Canaco Resource Inc.) within the Usagaran belt are presented in Table 3. East Africa Metals announced (0.721 Ma of gold) on its project contiguous to HNDI project (the study area) in Handeni district. Also un-reported amount of lead and silver are present in relation to gold mineralization (Archibald, 2013).

Table 3. East Africa Metals at Handeni district, summary of the resource, estimated at 0.5 g/t as on May 2012, (Archibald, 2013).

CATEGORY	INDICATED RESOURCE			INFERRED RESOURCE		
Cut-off grade (grams/tonne gold)	Tonnes (000s)	Average grade (Au-g/t)	Contained gold (ounces)	Tonnes (000s)	Average grade (Au-g/t)	Contained gold (ounces)
0.30	19,685	1.23	777,500	9,256	1.09	324,500
0.40	17,218	1.36	750,300	7,831	1.23	308,800
0.50	**15,186**	**1.48**	**721,300**	**6,683**	**1.36**	**292,400**
0.60	13,392	1.60	689,900	5,593	1.52	273,400
0.70	11,884	1.72	658,700	4,791	1.67	256,800
1.00	8,593	2.07	570,600	3,058	2.14	210,700
Total	**85,958**	**1.58**	**4,168,300**	**37,212**	**1.50**	**1,666,600**

CHAPTER 5 METHODOLOGY

5.1 INTRODUCTION

This chapter presents the methods used in this research. Investigation of various metamorphic assemblages observed in these samples resulted in the definition and characterization of the potential precursor units to the Handeni metamorphic assemblages, which will lead to protolith recognition. An important aspect of the investigation is the characterization of gold mineralizing events. Investigating the alteration assemblages and particularly those related to gold mineralization by conducting microscopic studies and electron microprobe analysis led to the understanding of the timing of the gold mineralization in the study area.

5.2 DATASET

Research was conducted on core samples collected from holes drilled at the Kwandege and Magambazi East prospects (Fig. 18). Three subsets of data were produced from the core samples namely: i) ore microscopic data, ii) XRF(X-Ray Florescence) generated major and trace elements data to determine whole rock geochemical compositions of samples and iii) mineral compositions from the electron microprobe analysis, iv) major and trace elements by X ray for the whole rock geochemical composition.

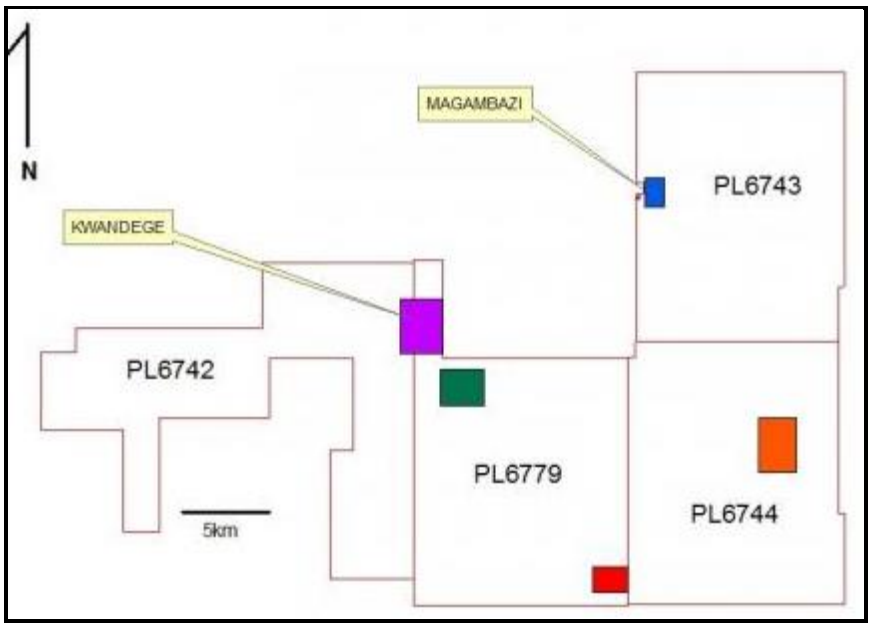

Figure 18. Four HNDI prospecting licenses with Kwandege and Magambazi projects as well as new targets Mjembe (orange), Target 6 (green) and Target 5 (red) (www.handenigold.com/latest-news)

5.3 GEOLOGICAL INVESTIGATION

The Handeni project is located in a high relief area with high rainfall resulting in dense vegetation cover which in turn contributes to a thick regolith cover, high rainfall also contributes to the formation of significant overburden within streams and valleys which hinder's the finding of outcrops. Occasional outcrops are found on high ridges or mountainous areas. These factors significantly affected the geological investigation especially the mapping process, stream sampling and occasionally soil sampling due to the development of thick horizon A and a thick saprolith zone.

The regional geological mapping was conducted by the Geological Survey of Tanzania (Quarter Degree Sheet –QDS 147 and 148) and recently updated from Kabete (2008) in Archibald (2012). Core logging for the Handeni project was done on site at the Kwandege and Magambazi East locations (Fig. 18). Logging focused on lithology, colour variation of individual units, grain size variations, foliations, mineralogical variation, alteration and any structural features of interest including foliation, dip, faults and shear zones.

5.4 DRILLING AND SAMPLING

HNDI conducted the diamond drilling program on its two projects Kwandege and Magambazi East based on targets generated by airborne and ground geophysics as well as geochemical anomalies. Thirty five (35) quartered cores were sampled based on details logs (from HNDI) and a total of 16 samples were selected (Table 4) to represent: host rock, ore, quartz veins and the contact between the ore and host rock to ensure the understanding of the lithology and distribution of mineralization.

Table 4. Representative samples used in this research for microprobe and XRF analyses.

HOLE ID	SAMPLE	FROM	TO	THICK.	MAJOR MINERALS	UNIT
MZD 01	H01A	29.0	29.5	0.5 m	Garnet feldspathic amphibole	Mafic Granulite
MZD 01	H7A1	35.0	35.5	0.5 m	Garnet feldspathic amphibole	Mafic Granulite
MZD 01	H7A2	35.0	35.5	0.5 m	Garnet amphibole plagioclase	Garnet Silica
MZD 01	H13A	38.0	38.5	0.5 m	Garnet feldspathic amphibole	Mafic Granulite
MZD 20	H39A	123.0	123.5	0.5 m	Garnet amphibole plagioclase	Garnet Silica
MZD 20	H40A	123.5	124.0	0.5 m	Garnet amphibole pyroxene	Garnetiferous Granulite
MZD 25	H44A	70.5	71.0	0.5 m	Garnet amphibole pyroxene	Garnetiferous Granulite
MZD 28	H54A	43.5	44.0	0.5 m	Garnet amphibole pyroxene	Garnetiferous Granulite
KW2-07	H78A	48.5	49.0	0.5 m	Garnet feldspathic amphibole	Mafic Granulite
KW2-08	H79A	72.0	72.5	0.5 m	Garnet feldspathic amphibole	Mafic Granulite
KW2-08	H79B	72.0	72.5	0.5 m	Garnet feldspathic amphibole	Mafic Granulite
KW4-02	H81A	61.0	61.5	0.5 m	Calcite amphibole pyroxene	Hornblende Pyroxenite
KW4-02	H83A	62.0	62.5	0.5 m	Calcite amphibole pyroxene	Hornblende Pyroxenite
KW1-05	H97A	28.0	28.5	0.5 m	Garnet amphibole pyroxene	Garnetiferous Granulite
KW2-01	H113	128.0	128.5	0.5 m	Calcite amphibole pyroxene	Hornblende Pyroxenite
KW2-01	H124	134.0	134.5	0.5 m	Garnet feldspathic amphibole	Mafic Granulite
KW2-01	H123	133.5	134.0	0.5 m	Garnet amphibole pyroxene	Garnetiferous Granulite

5.5 MICROSCOPY

Thin section preparation was done at the Rhodes University's Geology department. The core samples were cut at 48 mm x 26 mm sizes, grinding one side and glued onto a thin transparent glass of about 1.44 µm, followed by cutting the other side to about 2.2 mm (the thickness of glass and sample). The glued sample was subsequently grinded (by Struers Accutom 50) to 1.49 µm by first using the 90 µm diamond cup wheel and then 40 µm diamond cup wheel. Following the 40 µm grinding, the thin section is polished in a Leco Grinder Polisher GPX 200 polishing machine, which was the final stage to produce a polished thin section of about .440 µm thickness, ready for microscope works (J. Hepple pers com.).

Investigation of the polished samples under both transmitted and reflected light were conducted and photomicrographic images were taken by using suitable attachments to standard polarizing petrographic microscope using Leica Application Suit (LAS EZ) version 1.4.0. Mineral groups of interest including sulphides, pyroxene, amphiboles, garnet etc. were selected and marked for further analysis. Microscope data is used to understand the mineralogical assemblages and protolith of the rock. This data provides a better understanding of metamorphic processes and assemblages and the relationship of ore minerals with host rock including the relative timing of mineralizing events.

5.6 ELECTRON MICROPROBE

The electron microprobe also known as the electron probe micro analyzer (EPMA) uses secondary X-Rays generated by a focused (on the point of analytical interest) electron beam. The EPMA data acquisition was performed at Rhodes University, Department of Geology, on a Jeol JXA 8230 Superprobe, using 4 WD spectrometers. The analytical conditions employed were: acceleration voltage 15 kV, probe current 20 nA and spot beam size (< 1 micron). Qualitative analysis (WDS total scan) used 50 ms dwell time, at 50 microns step. For each element, the quantitative analysis run at 10 sec counting time on peak and 5 sec on each upper and lower background, respectively. Natural standard were used (refer appendix I). For element concentration below 5%, a large diffracting crystal with high sensitivity was used for quantitative analysis. The ZAF matrix correction method was used for quantification.

5.7 BULK ROCK GEOCHEMISTRY

Major elements are geochemically defined as elements that constitute a large proportion (up to 99% by weight) of the rocks. Rollinson (1993) recommended ten major elements which are (Si, Ti, Al, Fe, Mn, Mg, Ca, Na, K and P) traditionally present as oxides in major element chemical analysis, whereas a large quantity of trace elements are present among the geochemical elements despite their low abundances. Each of the elements represent unique chemical properties. They are presented in concentrations of less than 0.1% wt (less than 1,000 ppm). Normally they constitute a very small fraction of the rock (Rollinson, 1993).

The remainder of each representative core samples (approximately 30 gm) used to prepare thin sections were crushed and milled to a fine powder by using a jaw crusher and finished in a bow mill or carbon steel rolling mill (HERZOG-Lab Crushing Swing Mill). Subsequently 15 g of the finely powdered material of each sample were subjected to a finer grinding for about 45 minutes in a Pulverisette agate Swingmill from Fritsch.

Preparation of fusion discs for major elements analysis, ideal 0.28 grams out of approximately 4 grams of the oven-dried powdered sample were mixed with 1.5 grams of (spectroflux 105) lithium tetraborate and 0.02 grams of NaNO3 and heated at 1000 ^{o}C for 10 minutes to make glass beads. Hygroscopic water (H_2O^-) and loss on ignition (LOI) were determined after heating the 4 grams of powder sample to 110 ^{o}C and 1050 ^{o}C respectively. Table 5 below shows the representative samples for major elements with their precise measurement.

Preparation of pellet for trace elements analysis was: five grams of the very fine powder for each sample were added with boric acid and form two powder layers, by using the hydraulic pressing machine from the Geology laboratory, the two layers were pressed and form a pellet of about 120 mm thick.

The whole rock geochemical composition (major and trace elements) was determined by Philips PW1410 automatic wavelength dispersive XRF spectrometer. X-rays were generated from Rh – Rhodium (K – alpha) X ray tube operated at 50 kV and 50 mA. All the work have been done at the geology departmental laboratory, Rhodes University. Major and trace elements will be used in supporting the recognition of the protoliths.

Table 5. Quantities of the representative samples preparation for major elements analysis.

Sample Number	Empty crucible-gm	Cruicible+sample-before heat-gm	Weight of powder-gm	Cruicible+sample- after heat-gm	Loss of Water in gm	Percentage Loss of Ignition	Weight of dry sample-gm	Weight of NaNO3-gm	Weight of Flux-gm	Weight of sample in disc - gm
H01A	29.8368	34.0758	4.2390	34.0479	0.0279	0.6582	0.2840	0.0208	1.5013	0.2838
H40A	28.8539	33.3777	4.5238	33.3663	0.0114	0.2520	0.2862	0.0206	1.5028	0.2857
H44A	28.8923	33.3265	4.4342	33.3210	0.0055	0.1240	0.2831	0.0208	1.5025	0.2826
H54A	19.7146	23.3592	3.6446	23.1601	0.1991	5.4629	0.2837	0.0205	1.5047	0.2828
H78A	16.8215	21.5932	4.7717	21.3213	0.2719	5.6982	0.2846	0.0210	1.5016	0.2843
H79A	18.5822	23.6425	5.0603	23.5450	0.0975	1.9268	0.2866	0.0205	1.5024	0.2861
H81A	20.3228	25.6464	5.3236	25.4282	0.2182	4.0987	0.2823	0.0211	1.5012	0.2821
H83A	28.8092	33.6358	4.8266	33.4150	0.2208	4.5746	0.2851	0.0204	1.5031	0.2845
H97A	24.8695	29.7712	4.9017	29.6307	0.1405	2.8664	0.2847	0.0219	1.5048	0.2838
H113	18.4510	24.3862	5.9352	23.6226	0.7636	12.8656	0.2862	0.0220	1.5071	0.2849
H123	18.1602	22.9110	4.7508	22.8880	0.0230	0.4841	0.2831	0.0210	1.5073	0.2817
H124	27.2972	31.1342	3.8370	31.1156	0.0186	0.4848	0.2846	0.0205	1.5006	0.2845

5.8 DATA PROCESSING TOOLS

The data have been processed by various computer based software packages, these include: Microsoft excel package for (Data analysis, correlation, graphing and other plots) by Microsoft (2012) and other packages such as Minpet for mineralogical and petrological data processing system by Richard (1995) and Igpet for major and trace elements data processing and graphics by Carr (1995).

CHAPTER 6 RESULTS

6.1 INTRODUCTION

This chapter presents the results from the detailed geological logging, ore microscope work, electron microprobe data and geochemical analytical data from XRF analyses.

6.2 CORE LOGGING

Main lithological units and detailed logging on a specific unit for the representative holes were identified. From the logging, a generalized lithological sequence for rocks encountered has been constructed (Fig. 19). The fact that the various lithologies have been subjected to intensive folding, shearing and faulting over short distances renders the construction of a stratigraphic column difficult. Descriptions of the core are also presented in Figure 20.

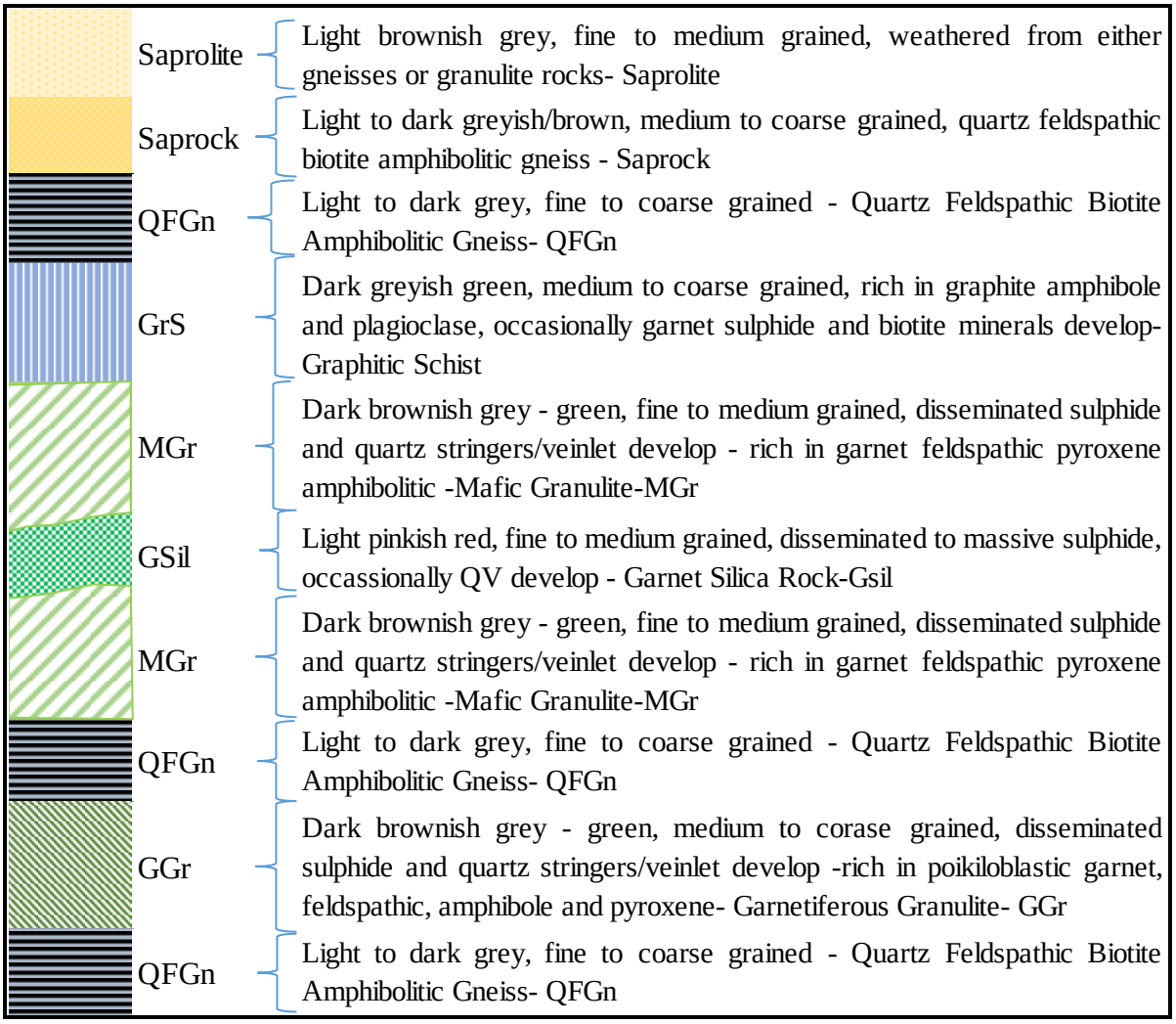

Figure 19 Generalized section showing the interpreted potential lithological sequences of Handeni project rocks.

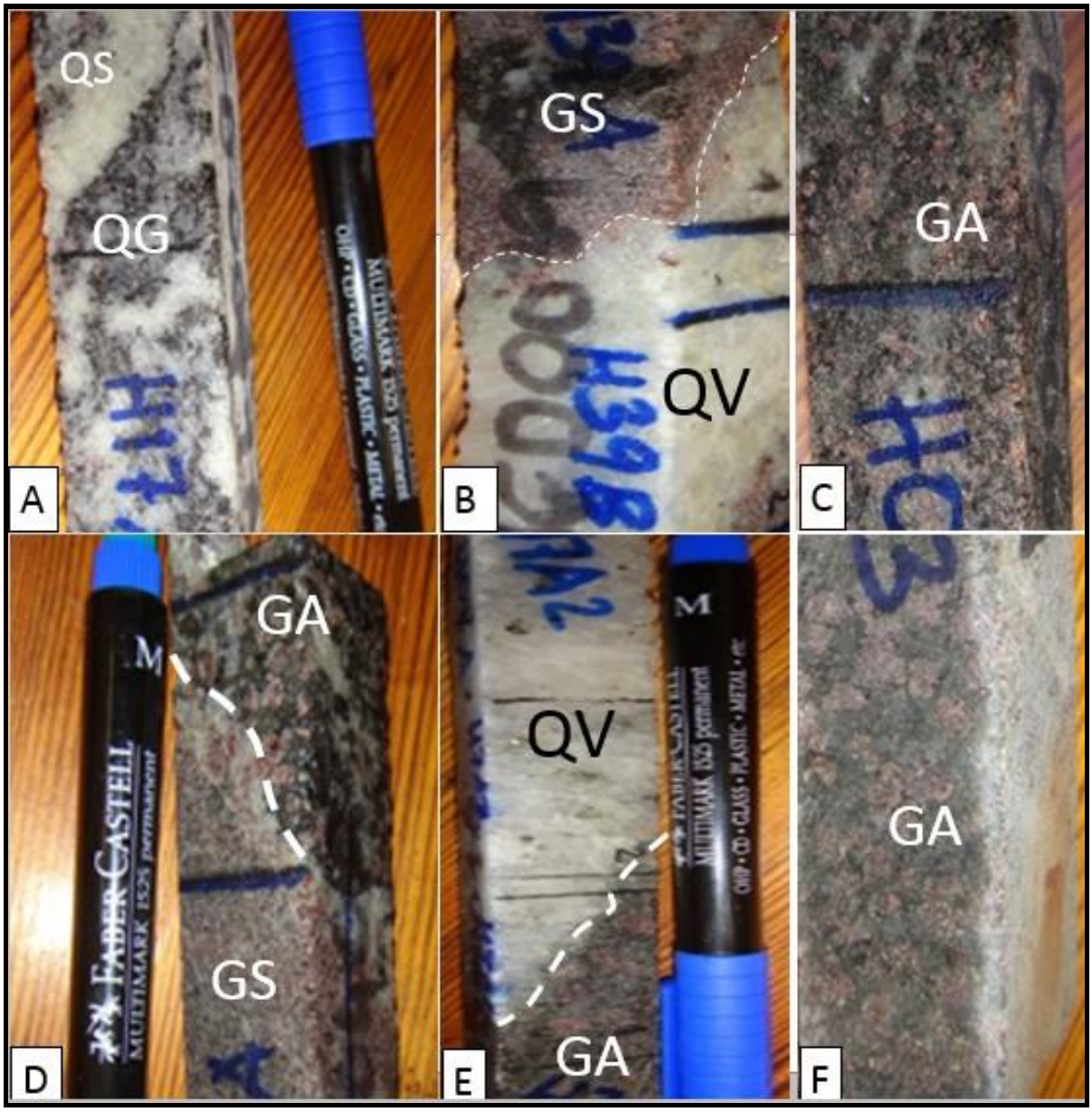

Figure 20. A) Quartz feldspathic biotite amphibole gneiss- QG with quartz stringers the dominant hanging and the footwall unit B) Garnet silicified rock –GS showing undulating contact with quartz vein –QV, C) Garnet feldspar amphibole pyroxene granulite –GA medium to coarse grained "ore rock" D) Undulating contact between the GS and medium grained to coarse grained GA, E) the undulating contact between the medium to coarse grained GA and Qv and F) Coarse to gritty (poikilitic texture) feldspar garnet amphibole pyroxene granulite.

6.3 PETROGRAPHY OF HANDENI ROCKS

6.3.1 Quartzofeldspathic Gneiss1

Quartzofeldspathic Gneiss (QFGn, Fig. 20A) is characterized by fine to medium grained foliated rocks categorized as the country rock and subsequently subdivided into two types;

quartz feldspathic amphibolite gneiss and migmatitic quartz feldspathic amphibolite gneiss. Both have the same minerals in composition varying in textures and grain sizes. Their mineral assemblage is made up of amphiboles, plagioclase (andesine and labradorite) quartz and occasionally biotite and pyroxene. Occasionally disseminated sulphides (pyrite and pyrrhotite) developed as inclusions (Fig. 21 and 22) which suggests a late crystallization following plagioclase, amphibole and pyroxene.

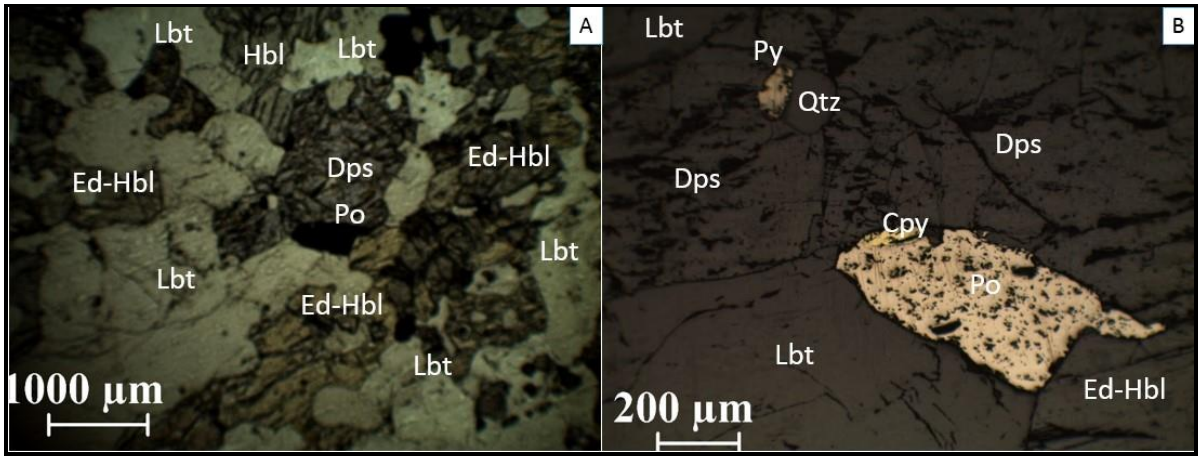

Figure 21. Photomicrograph under A) transmitted- B) reflected light crossed polar showing feldspar amphibole, with inclusions of pyrrhotite Po, pyrite –Py and chalcopyrite –Cpy in edenite hornblende-Ed-Hbl, plagioclase labradorite-Lbt and near margin of diopside-Dps and Quartz-Qtz.

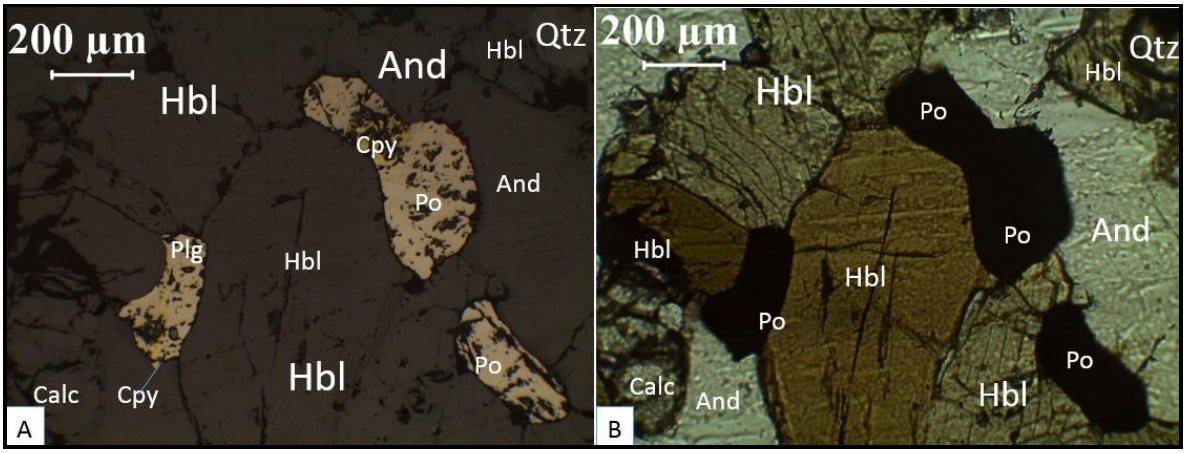

Figure 22. Photomicrographic image of migmatitic quartz-Qtz feldspathic (plagioclase-andesine-And) amphibolite (hornblende-Hbl) gneiss with intergrowth of sulphides (pyrrhotite-Po and chalcoyrite-Cpy) and calcite –Calc. A)Reflected and B) transmitted crossed polar images.

6.3.2 Graphitic Schist

Graphite amphibolitic schist (GrSc) is not encountered in many of the holes due to extensively folding of the lithologies and occasionally pinch out. It is characterized by dark greyish green colour presence of massive to disseminated graphite flakes and medium to coarse grained amphiboles with occasionally disseminated garnet, sulphide and pyroxene.

6.3.3 Garnet Silicified Rock

Garnet Silicified rock (GSil, Fig. 20 B) is characterized by medium pinkish grey colour, fine to medium grained size and massive to granulitic texture. Its main minerals are garnet and quartz in a groundmass made up of plagioclase and quartz. Quartz vein or stringers as well as massive to disseminated sulphides pyrrhotite, pyrite and chalcopyrite develop (Fig. 23).

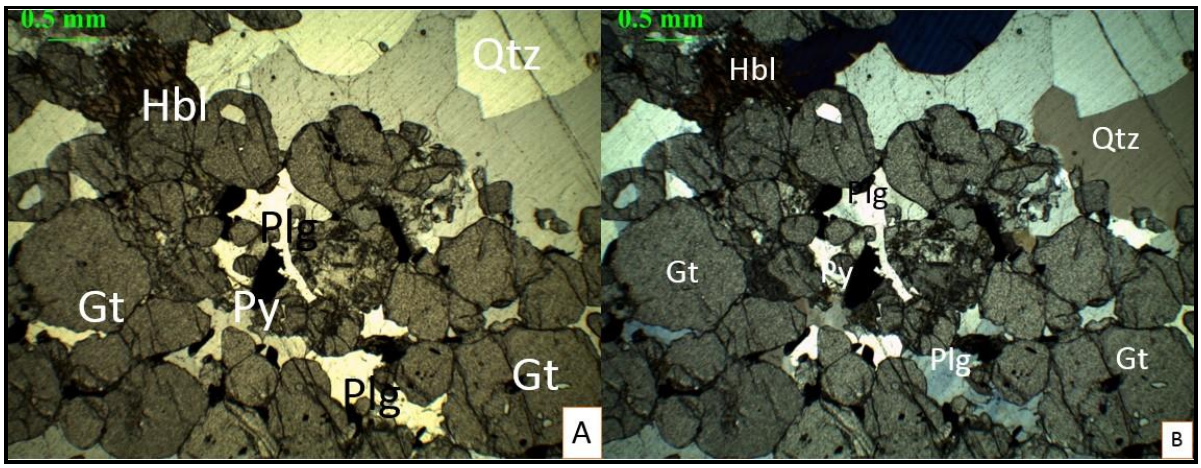

Figure 23. Photomicrographic image of garnet silicified rock showing massive almandine garnet grains with the groundmass quartz and plagioclase.

6.3.4 Mafic Granulite

Mafic Granulite (MGr, Fig. 20 C - E) is a granulite rock characterized by dark brownish green colour, fine to medium grained, granoblastic texture with massive structure, interlayered with QFGn, generally showing no foliation. The most common mineral assemblage is pyroxene (diopside), amphiboles (hornblende), plagioclase, garnet (almandine) exhibiting rounded and fracturing features, which are replaced by plagioclase and occasionally quartz and biotite minerals (Fig. 24 & 25). Hornblende and pyroxene are the dominant mineral forming the groundmass of the rock. Massive to disseminated sulphide minerals (pyrite, pyrrhotite, chalcopyrite, and pentlandite) developed as the replacement of the plagioclase and silica within the margin zones of the hornblende - or garnet - and pyroxene. Alteration and accessories

minerals developed, these include calcite and (ilmenite and titanite) respectively (Fig. 26 & 27).

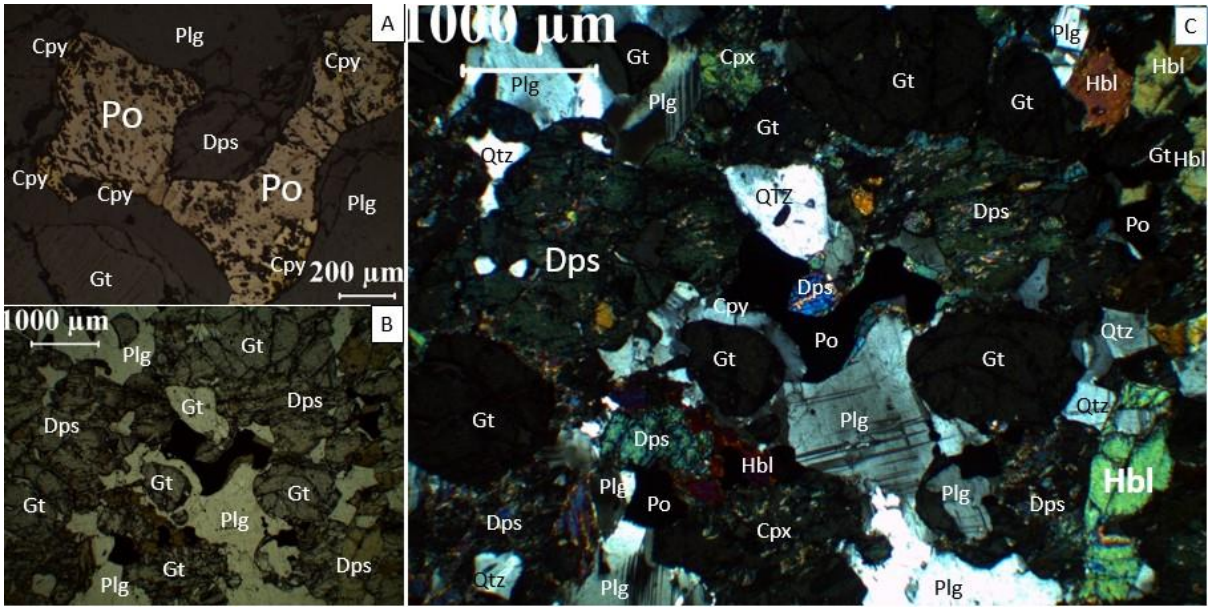

Figure 24. Photomicrographic images of medium grained granulite rock showing pyrrhotite – Po with anhedral chalcopyrite – Cpy at its margin replacing the plagioclase Plg (polysynthetic deformation twinning) intergrown in the margin between the fracturing garnet Gt and coarse subhedral clinopyroxene-diopside (DPS), hornblende Hbl and quartz – Qtz. Crossed polar images with A) reflected and C) transmitted light where B is plane polarized transmitted light.

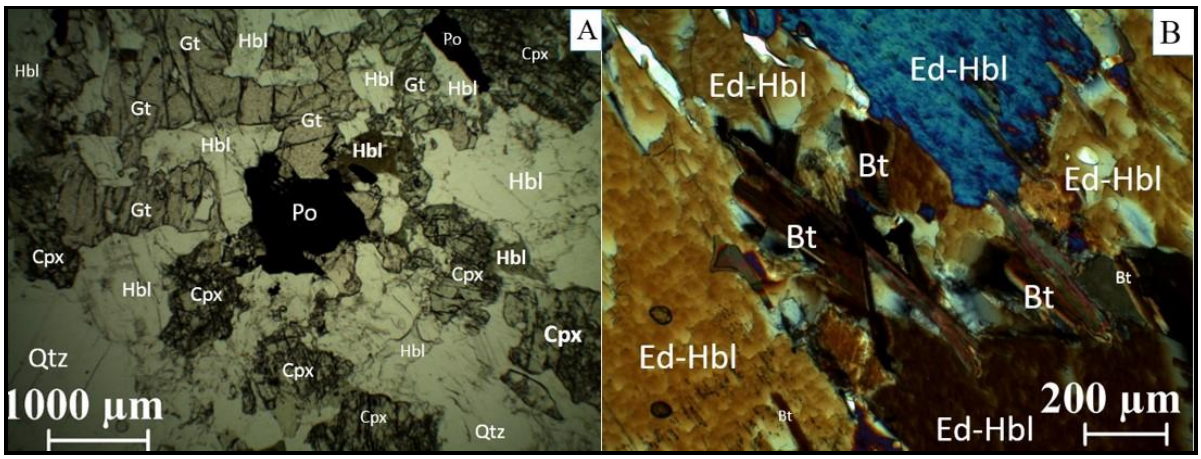

Figure 25. Photomicrographic images of medium grained garnet amphibolite pyroxene granulite showing corona garnet – Gt symplectite largely in between the edenite hornblende - Hbl and rare the clinopyroxene –cpx, pyrrhotite-Po replacing plagioclase intergrowth between the margins of garnet and clinopyroxene –Cpx, quartz –Qtz are rarely developed under transmitted light plane polar and B) under crossed polar reflected light, granulite dominated

by hornblende – Hbl shows coarse grained euhedral to subhedral crystals intergrown with brownish idiomorphic biotite –Bt flakes.

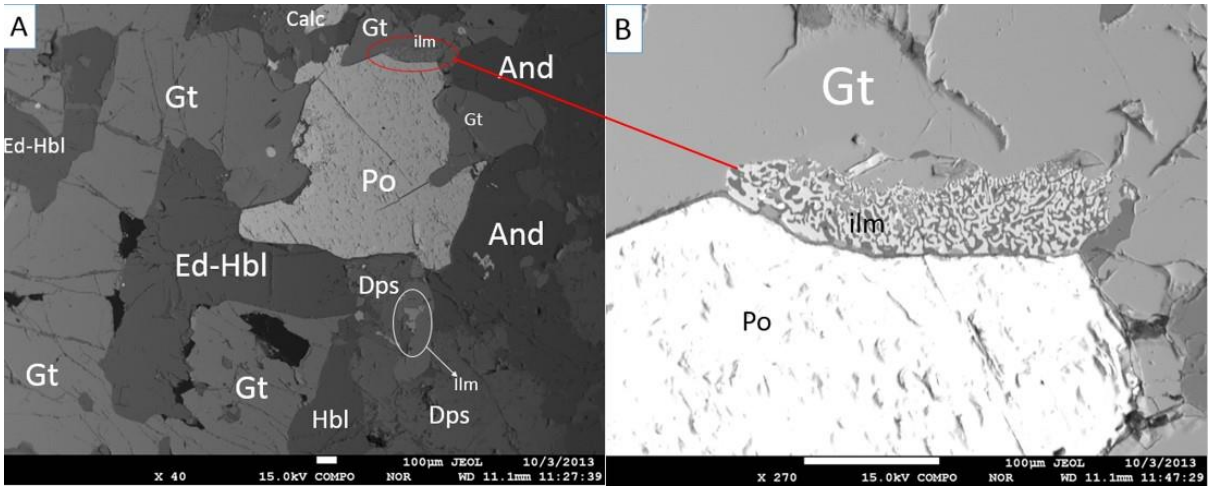

Figure 26. Backscatter electron images of medium grained garnet-amphibole-pyroxene granulite taken at 100 micron 40 X magnification showing the garnet corana –Gt symplectitic intergrowth of edenite hornblende and Ilmenite –ilm, intergrown in garnet and diopside clinopyroxene- Dps B) a 100 micron 270 X magnification shows euhedral ilmenite grains intergrown with the garnet corona and pyrrhotite – Po.

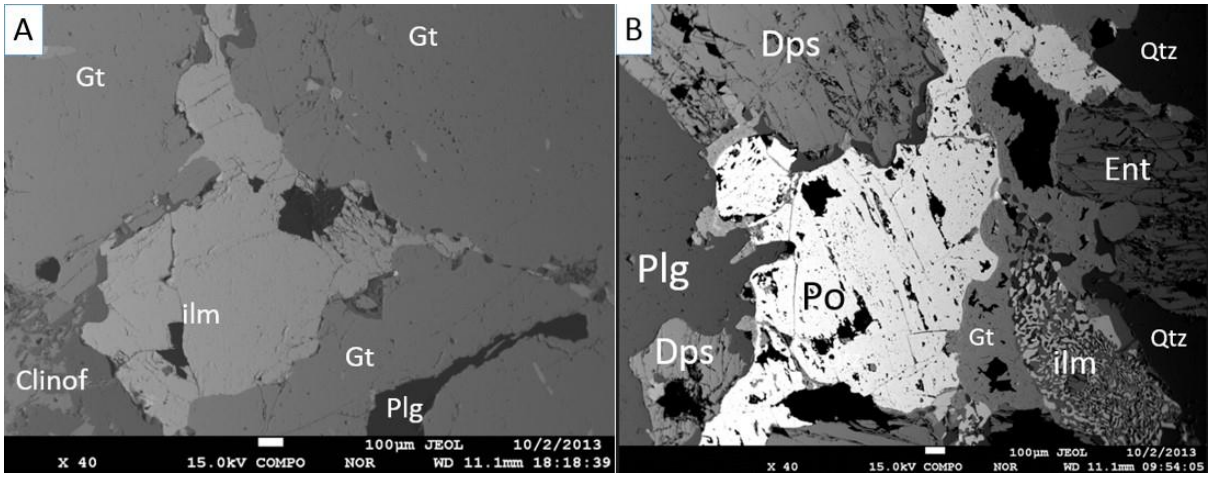

Figure 27. Backscatter electron images of medium grained garnet-amphibolite-pyroxene granulite at 100 micron 40 X magnification showing ilmenite grain replacing the plagioclase during the fracturing of garnet, as well as clinoferrosilite Clinof and B) at 100 micron 40 X magnification showing the intergrowth of the pyrrhotite, which replaces plagioclase- Plg between the diopside –Dps and garnet grain as well as the intergrowth of the ilmenite grains between the garnet quartz- Qtz and enstatite- Ent grains.

6.3.5 Garnetiferous Granulite

Garnetiferous Granulite (GGr, Fig. 20 F) is a granulite rock that exhibits dark brownish green color and medium to coarse graines, with poikilitic texture and granular structure. Its common mineral assemblages are pyroxene (both diopside and enstatite), amphibole (hornblende as edenite dominant), coarse grained garnet as almandine, plagioclase and quartz. Massive to disseminated sulphide minerals developed in these rocks as well. These include pyrrhotite, pyrite, chalcopyrite and occasionally arsenopyrite. Alteration minerals such as calcite are developed as an inclusion occasionally in hornblende as well as biotite with round to elongated shape developed as inclusions in hornblende. Other inclusion minerals which develop in these rocks are chalcopyrites in pyrrhotite, quartz and plagioclase in garnet (Fig. 28 & 29).

The most significant differences between the mafic granulite and garnetiferous granulite units are the variation of the grains sizes, the MGr has fine to medium while GGr has medium to coarse grained, ilmenite and titanite occasionally developed in MGr whereas than GGr does.

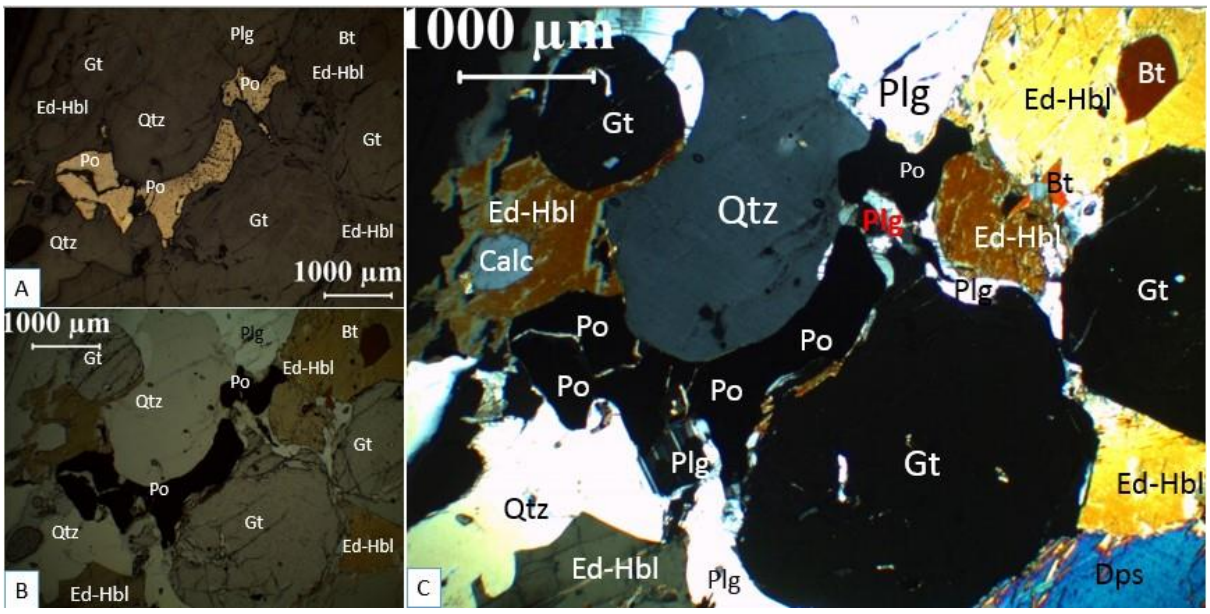

Figure 28. Photomicrographic image of coarse grained garnet plagioclase amphibole pyroxene granulite showing the late crystallization of plagioclase followed by sulphide minerals as well as inclusion of biotite and altered mineral calcite. A) The reflected light crossed polar, B) transmitted light plane polar and C) transmitted light crossed polar, all image are of the same granulite unit. Garnet Gt edenite hornblende Ed-Hbl biotite Bt and calcite –Calc inclusion on hornblende, quartz Qtz plagioclase (Plg) ,diopside clinopyroxene Dps and sulphide (pyrrhotite Po) replacing the plagioclase.

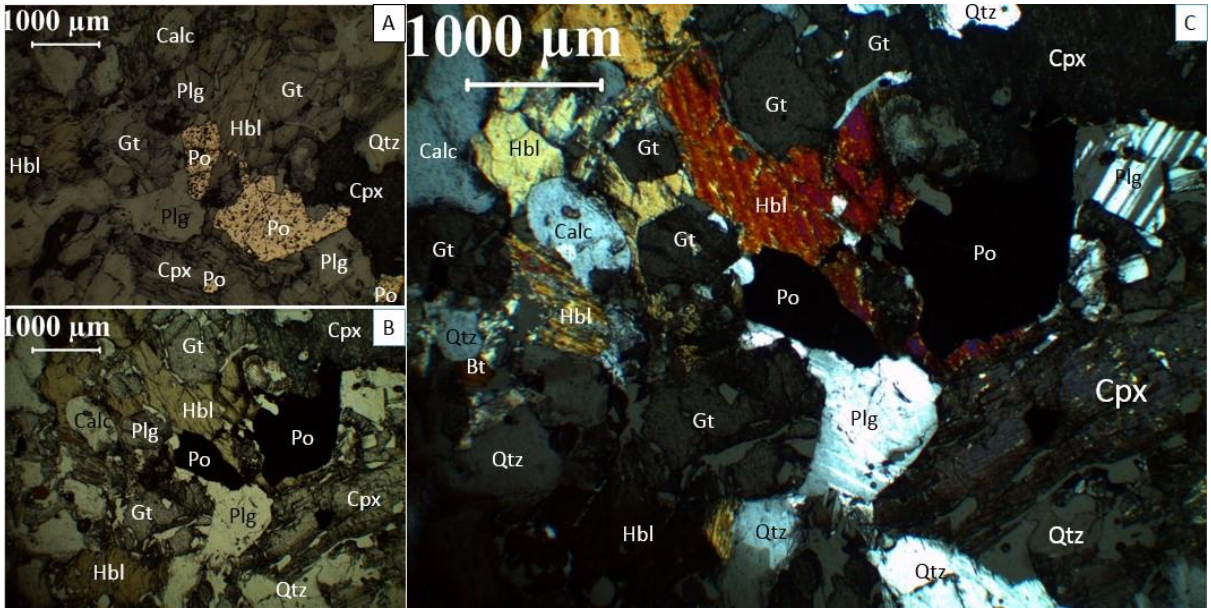

Figure 29. Photomicrographic images showing coarse grained garnet plagioclase amphibole pyroxene granulite with sulphide -pyrrhotite Po as inclusion in hornblende Hbl and plagioclase Plg or silica filling the garnet fracture zones. Other mineral includes clinopyroxe.

6.3.6 Hornblende Pyroxenite

Hornblende Pyroxenite (HP) is a magnesium rich unit characterized by a light greyish green colour, fine to medium grain sized, and weakly foliated structure with massive texture. The typical mineral assemblages of these units is (in order of decreasing abundance) pyroxene dominantly orthopyroxene (enstatite), hornblende, magnesite and occasionally plagioclase calcite and biotite (Fig. 30 & 31).

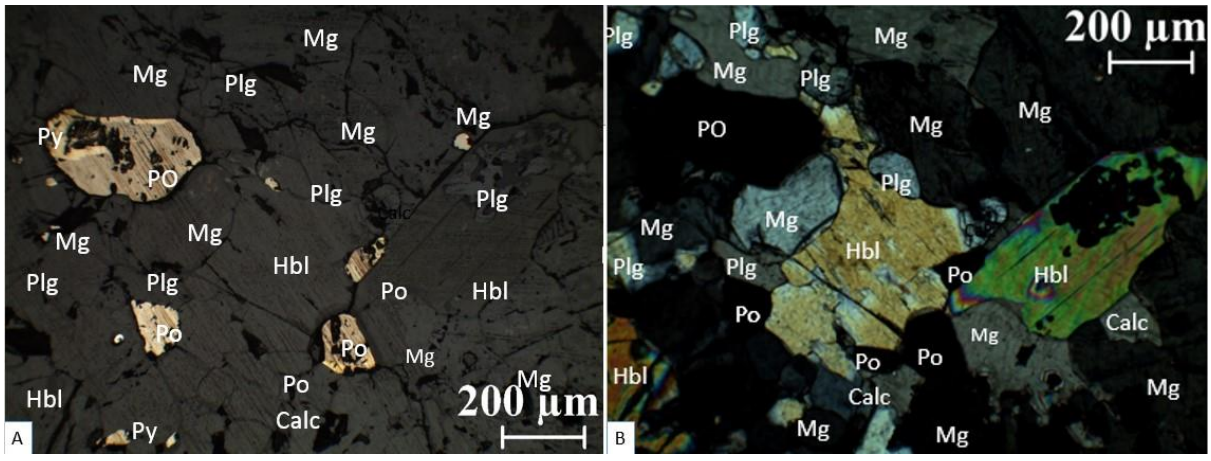

Figure 30. Photomicrographic images of biotite amphibole pyroxene magnesite showing the massive sulphide pyrrhotite Po within the marginal zones of magnesite Mg and hornblende

Hbl. Other mineral include pyrite Py and calcite Calc. Images A) under reflected light crossed polar B) transmitted light crossed polar, Hbl crystallize after Mg.

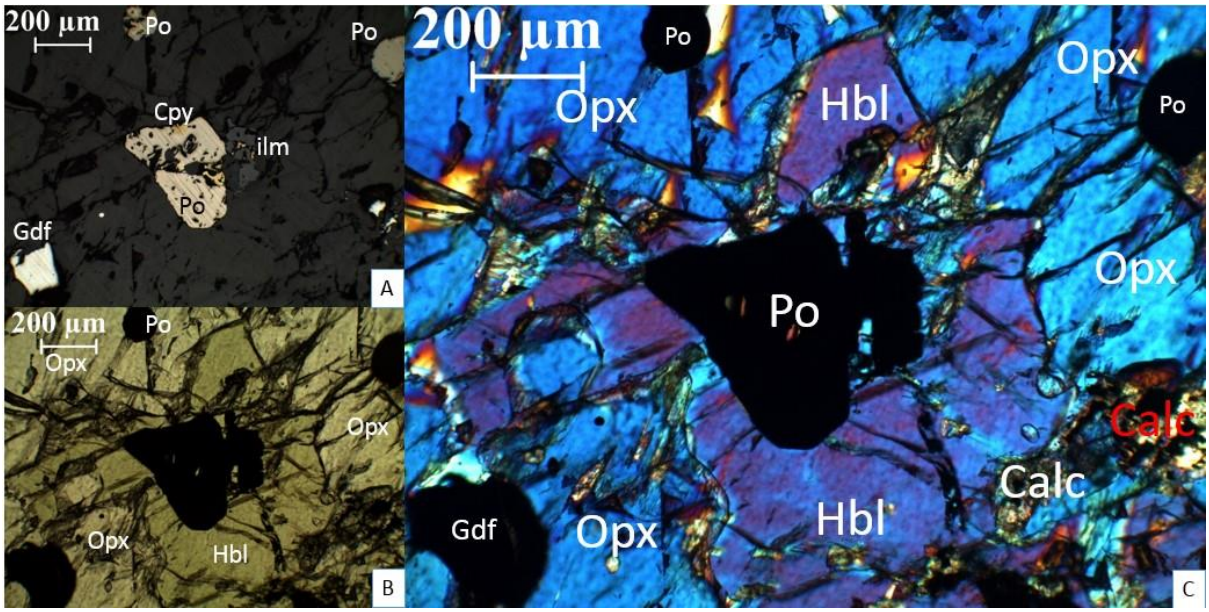

Figure 31. Photomicrographic images showing the abundance of orthopyroxene-Opx hornblende -Hbl and calcite – Calc minerals with inclusion of pyrrhotite-Po chalcopyrite- Cpy and gersdorffite-Gdf sulphide minerals.

Mafic minerals grains show late crystallization phase after the magnesite Figure 31. Abundance disseminated sulphides (pyrrhotite, chalcopyrite, pentlandite and gersdorffite) are developed as inclusion in these rocks suggesting late crystallization too (Fig. 32).

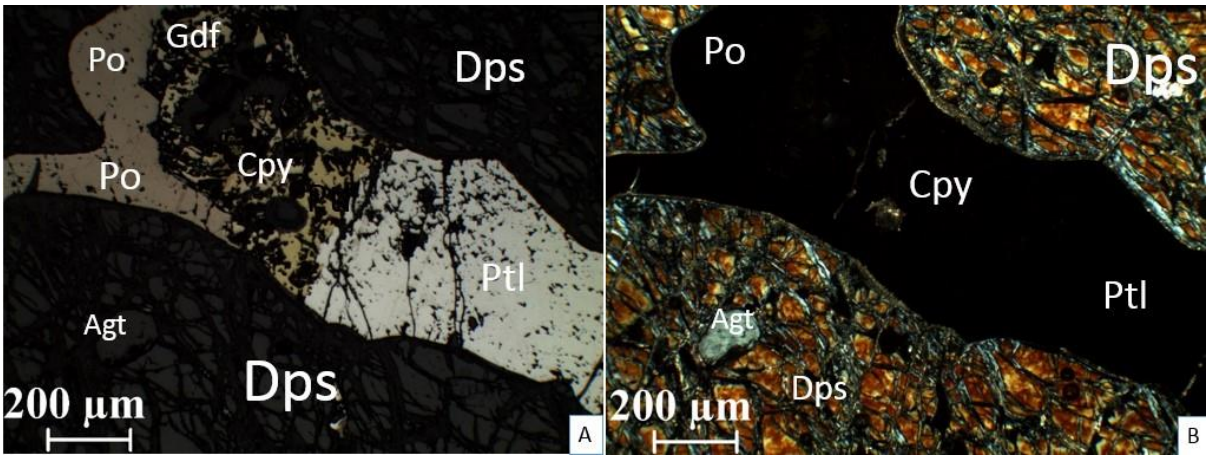

Figure 32. Photomicrographic image of biotite amphibole pyroxene magnesite taken at A) under reflected light plane polarized and B) transmitted crossed polar, showing intergrowth of tetra sulphides (chalcopyrite-Cpy crystallizes early followed by gersdorffite-Gdf, pyrrhotite-Po and Pentlandite-Ptl) they are both developed as inclusion in diopside- Dps.

6.4 MINERAL CHEMISTRY OF HANDENI ROCKS

Rocks encountered are composed of both major and accessories minerals including the sulphides and alteration minerals. These could be categorized into three groups as silicates, sulphides and carbonates. The silicates minerals, in decreasing order of abundance, include pyroxene, amphiboles, feldspar (plagioclase), garnet, quartz, biotite, titanite and ilmenite. Sulphides minerals in order of decreasing abundance include pyrite, pyrrhotite, chalcopyrite, gersdorffite, pentlandite and arsenopyrite. Carbonate minerals encountered in these rocks are calcite magnesite and dolomite. Classification and characterization of the minerals of interest in this research are garnet, pyroxene, amphibole, plagioclase, biotite and sulphides. Based on their mineral composition data from the microprobe analyses (Table 6 - 12) subsequently the calculation of cation and anion (Dee *et al*, 1962, 1963 and 1992 and Robles *et al*, 2009) of each mineral, each group has been classified and plotted.

6.4.1 Pyroxenes

Pyroxene is commonly found in mafic rocks of Handeni project, including both clinopyroxene and orthopyroxene (Table 6 - 8). Clinopyroxene minerals include diopside as dominant mineral and occasionally augite which are commonly found in three units namely QFGn, MGr and GGr and occasionally near the gradation contact with HP unit. Orthopyroxene minerals developed in these rocks are dominated by enstatite type as well as clinoferrosillite and occasionally the clino-enstatite. Their distribution varies in these rock, commonly enstatite develop in HP units and clino-enstatite and clinoferrosillite develop in GGr units.

Clinopyroxene is commonly found in QFGn, MGr and GGr rocks and occasionally found in HP rocks. The clinopyroxene is of diopsidic composition in the classification of Marimoto *et al* (1998) and occasionally augite one developed as well (Table 6, Fig. 33). There is a small variation in the clinopyroxene components such as the X_{Mg} ($Mg/Mg + Fe^{2+}$) of these rocks ranges between 0.8 to 0.57 whereas the TiO_2 ranges between 0.0 to 0.34 wt%, Al_2O_3 ranges between 0.28 to 4.16 wt% and Cr_2O_3 ranges between 0.0 to 012 wt%. Occasionally inclusions of quartz are developed in clinopyroxene mineral grains.

E**nstatite** ($Mg_2Si_2O_6$) orthopyroxene commonly developed in HP units and very rare in MGr and GGr units (Table 7 - 8, Fig. 32). The enstatite is the dominant mineral in this group and vary in grain size from fine to coarse grained (Fig. 30 & 31). There is very small variation in its composition such as its magnesium number (Mg#) ranges from 0.88 to 0.84 whereas TiO_2 (0.1-0.02wt %) and Al_2O_3 (1.4-0.52 wt %).

Table 6. Composition of clinopyroxene from the representative samples.

Lithology	**GGr**						**MGr**				
Sample	**H7A1**			**H44A**			**H01A**	**H78A**		**H79B**	**H124**
Analytical number	**1**	**2**	**3**	**4**	**5**	**6**	**7**	**8**	**9**	**10**	**11**
wt% Coment	**Core**	**Core**	**Core**	**Core**	**Rim**	**Core**	**Core**	**Rim**	**Core**	**Core**	**Core**
SiO2	52.51	52.74	52.26	52.75	52.82	51.81	52.58	51.22	53.27	51.02	51.81
TiO2	0.34	0.33	0.30	0.21	0.17	0.32	0.30	0.23	0.00	0.01	0.01
Al2O3	3.26	3.46	4.00	2.07	2.09	4.16	4.10	2.88	0.28	0.98	0.74
FeO	6.51	6.52	6.54	6.75	6.50	7.20	6.52	9.22	8.50	13.71	9.38
Cr2O3	0.08	0.00	0.02	0.12	0.04	0.08	0.06	0.03	0.05	0.00	0.06
MnO	0.08	0.13	0.08	0.09	0.03	0.14	0.03	0.09	0.14	0.13	0.15
NiO	0.00	0.01	0.01	0.01	0.00	0.02	0.00	0.00	0.00	0.00	0.00
MgO	13.69	13.83	13.36	14.29	14.31	12.92	13.71	12.44	13.81	10.01	12.35
CaO	22.66	21.97	22.49	22.57	22.76	21.59	22.14	22.32	23.35	21.79	23.31
Na2O	0.63	0.60	0.64	0.50	0.51	0.75	0.77	0.69	0.20	0.40	0.43
K2O	0.01	0.02	0.02	0.01	0.00	0.01	0.01	0.02	0.01	0.01	0.00
Total	**99.77**	**99.61**	**99.72**	**99.37**	**99.23**	**99.00**	**100.22**	**99.14**	**99.61**	**98.06**	**98.24**
Oxygen basis	6.00	6.00	6.00	6.00	6.00	6.00	6.00	6.00	6.00	6.00	6.00
Si	1.94	1.95	1.93	1.96	1.96	1.93	1.93	1.93	2.00	1.99	1.98
Ti	0.01	0.01	0.01	0.01	0.00	0.01	0.01	0.01	0.00	0.00	0.00
Al	0.14	0.15	0.17	0.09	0.09	0.18	0.18	0.13	0.01	0.04	0.03
Fe	0.20	0.20	0.20	0.21	0.20	0.22	0.20	0.29	0.27	0.45	0.30
Cr	0.00	0.00	0.00	0.00	0.00	0.00	0.00	0.00	0.00	0.00	0.00
Mn	0.00	0.00	0.00	0.00	0.00	0.00	0.00	0.00	0.00	0.00	0.00
Ni	0.00	0.00	0.00	0.00	0.00	0.00	0.00	0.00	0.00	0.00	0.00
Mg	0.76	0.76	0.74	0.79	0.79	0.72	0.75	0.70	0.77	0.58	0.70
Ca	0.90	0.87	0.89	0.90	0.91	0.86	0.87	0.90	0.94	0.91	0.96
Na	0.05	0.04	0.05	0.04	0.04	0.05	0.05	0.05	0.01	0.03	0.03
K	0.00	0.00	0.00	0.00	0.00	0.00	0.00	0.00	0.00	0.00	0.00
Total	**4.00**	**3.99**	**4.00**	**4.00**	**4.00**	**3.99**	**4.00**	**4.02**	**4.00**	**4.01**	**4.02**
WO	48.36	47.34	48.63	47.23	47.65	47.66	47.79	47.59	47.35	46.84	48.63
EN	40.66	41.47	40.20	41.60	41.68	39.69	41.18	36.91	38.97	29.94	35.85
FS	10.98	11.19	11.18	11.17	10.67	12.65	11.04	15.50	13.68	23.22	15.52

Analytical numbers 1 - 11 represent the clinopyroxene mineral (diopside) develop in garnetiferous granulite – GGr and mafic granulite – MGr. Wo, En and FS values were calculated following Richard (1995).

Table 7. Composition of orthopyroxene from the representative samples.

Lithology					**HP**					
Sample	**H81A**				**H83A**		**H113**			
Analytical number	**12**	**13**	**14**	**15**	**16**	**17**	**18**	**19**	**20**	**21**
wt% Coment	**Rim**	**Core**	**Core**	**Core**	**Core**	**Rim**	**Core**	**Core**	**Core**	**Rim**
SiO2	56.68	56.56	56.79	56.41	55.57	55.65	55.82	56.42	56.46	55.77
TiO2	0.04	0.07	0.10	0.03	0.07	0.02	0.06	0.06	0.05	0.06
Al2O3	0.90	0.88	1.34	0.92	1.38	1.40	1.04	0.58	0.52	0.59
FeO	8.45	8.45	7.84	8.01	11.05	9.95	7.96	8.60	8.47	9.26
Cr2O3	0.02	0.07	0.06	0.02	0.01	0.20	0.00	0.08	0.07	0.03
MnO	0.19	0.13	0.12	0.11	0.15	0.17	0.17	0.17	0.13	0.20
NiO	0.03	0.02	0.02	0.00	0.04	0.07	0.09	0.00	0.04	0.03
MgO	33.88	33.81	33.28	33.45	31.56	31.78	33.15	33.79	34.20	33.56
CaO	0.08	0.08	0.08	0.15	0.14	0.15	0.14	0.10	0.13	0.08
Na2O	0.00	0.00	0.00	0.00	0.00	0.00	0.00	0.00	0.00	0.00
K2O	0.00	0.00	0.02	0.02	0.01	0.02	0.01	0.02	0.02	0.02
Total	**100.27**	**100.07**	**99.65**	**99.12**	**99.98**	**99.41**	**98.44**	**99.82**	**100.09**	**99.60**
Oxygen basis	6.00	6.00	6.00	6.00	6.00	6.00	6.00	6.00	6.00	6.00
Si	1.97	1.97	1.97	1.98	1.96	1.96	1.97	1.97	1.97	1.96
Ti	0.00	0.00	0.00	0.00	0.00	0.00	0.00	0.00	0.00	0.00
Al	0.04	0.04	0.06	0.04	0.06	0.06	0.04	0.02	0.02	0.02
Fe	0.25	0.25	0.23	0.23	0.33	0.29	0.23	0.25	0.25	0.27
Cr	0.00	0.00	0.00	0.00	0.00	0.01	0.00	0.00	0.00	0.00
Mn	0.01	0.00	0.00	0.00	0.00	0.00	0.00	0.00	0.00	0.01
Ni	0.00	0.00	0.00	0.00	0.00	0.00	0.00	0.00	0.00	0.00
Mg	1.75	1.75	1.72	1.75	1.66	1.67	1.74	1.76	1.77	1.76
Ca	0.00	0.00	0.00	0.01	0.01	0.01	0.01	0.00	0.00	0.00
Na	0.00	0.00	0.00	0.00	0.00	0.00	0.00	0.00	0.00	0.00
K	0.00	0.00	0.00	0.00	0.00	0.00	0.00	0.00	0.00	0.00
Total	**4.01**	**4.01**	**3.99**	**4.01**	**4.01**	**4.01**	**4.01**	**4.02**	**4.02**	**4.03**
WO	0.15	0.15	0.15	0.28	0.27	0.29	0.27	0.19	0.24	0.15
EN	87.35	87.41	88.03	87.76	83.17	84.60	87.67	87.13	87.43	86.22
FS	12.50	12.45	11.81	11.95	16.56	15.12	12.07	12.69	12.34	13.64

Analytical number 12 to 21 represent the enstatite (orthopyroxene) develop in hornblende pyroxenite HP. Wo, En and FS values were calculated following Richard (1995).

Table 8. Composition of pyroxene mineral grain from representative samples.

Lithology	**HP**	**GGr**						
Sample	**H81A**	**H7A1**	**H97A**					
Analytical number	**22**	**23**	**24**	**25**	**26**	**26**	**27**	**28**
wt% Coment	**Rim**	**Rim**	**Core**	**Core**	**Rim**	**Core**	**Rim**	**Rim**
SiO2	43.07	52.38	53.82	50.54	53.12	52.48	53.05	53.62
TiO2	1.08	0.34	0.05	0.04	0.02	0.00	0.02	0.00
Al2O3	13.77	3.29	0.32	0.46	0.39	0.48	0.36	0.33
FeO	4.34	6.20	29.08	31.87	27.62	28.10	27.50	26.14
Cr2O3	1.01	0.06	0.01	0.09	0.06	0.04	0.02	0.04
MnO	0.08	0.00	0.18	0.21	0.14	0.16	0.15	0.20
NiO	0.05	0.00	0.00	0.00	0.00	0.02	0.00	0.01
MgO	18.21	13.54	15.44	15.62	15.56	14.50	15.07	15.82
CaO	11.10	22.64	0.26	0.47	0.24	0.20	0.26	0.21
Na2O	3.18	0.56	0.02	0.00	0.01	0.02	0.00	0.00
K2O	0.34	0.01	0.02	0.01	0.02	0.01	0.00	0.02
Total	**96.23**	**99.02**	**99.20**	**99.31**	**97.18**	**96.01**	**96.43**	**96.39**
Oxygen basis	6.00	6.00	6.00	6.00	6.00	6.00	6.00	6.00
Si	1.62	1.95	0.00	0.00	0.00	2.08	2.09	2.09
Ti	0.03	0.01	1.97	1.88	1.98	0.00	0.00	0.00
Al	0.61	0.14	0.00	0.00	0.00	0.02	0.02	0.02
Fe	0.14	0.19	0.01	0.02	0.02	0.93	0.90	0.85
Cr	0.03	0.00	0.00	0.00	0.00	0.00	0.00	0.00
Mn	0.00	0.00	1.20	1.34	1.16	0.01	0.01	0.01
Ni	0.00	0.00	0.00	0.00	0.00	0.00	0.00	0.00
Mg	1.02	0.75	0.01	0.02	0.01	0.86	0.88	0.92
Ca	0.45	0.90	0.81	0.83	0.83	0.01	0.01	0.01
Na	0.23	0.04	0.02	0.04	0.02	0.00	0.00	0.00
K	0.02	0.00	0.00	0.00	0.00	0.00	0.00	0.00
Total	**4.15**	**3.99**	**4.04**	**4.14**	**4.03**	**3.91**	**3.91**	**3.90**
WO	27.83	48.88	0.58	1.00	0.55	0.47	0.61	0.49
EN	63.52	40.67	48.19	46.00	49.70	47.54	48.98	51.45
FS	8.65	10.45	51.23	53.00	49.75	51.99	50.42	48.06

Wo, En and FS values were calculated following Richard (1995).

Analytical number;

- 22 -23 represent the augite (clinopyroxene) mineral developed in hornblende pyroxenite HP and garnetiferous granulite –GGr and
- 24 to 27 are clinoferrosillite (orthopyroxene) and 28 as clino-enstaite both developd in garnetiferous granulite – GGr.

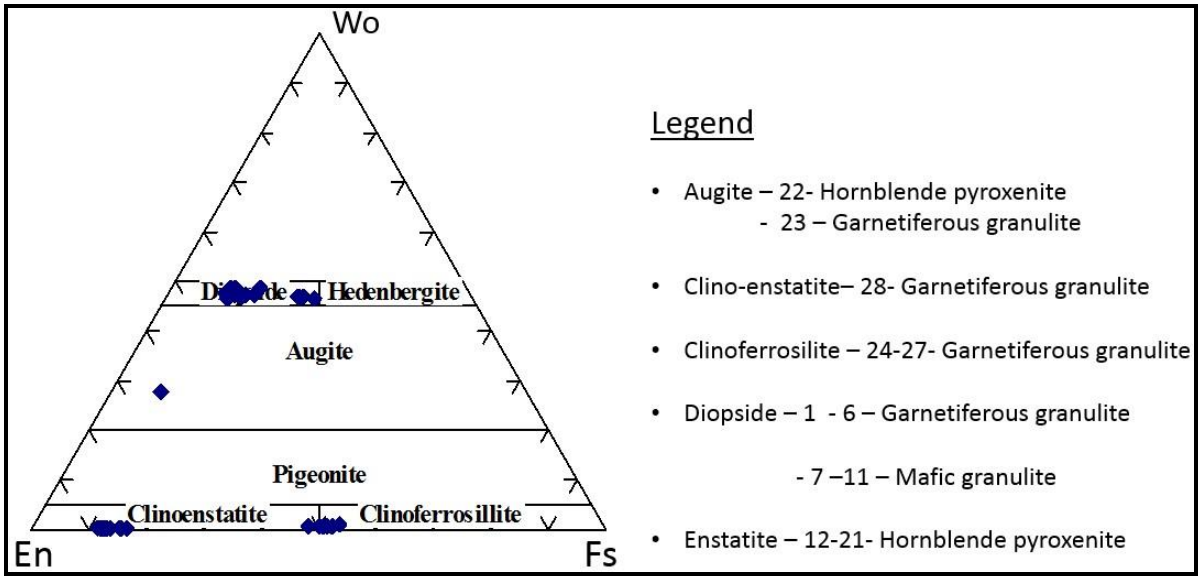

Figure 33 Ternary diagram showing the compositional classification of pyroxene minerals (after Morimoto et al, 1988). Abbreviation; Enstatite-En, Ferrosilite –Fs and Wollfsonite –Wo.

6.4.2 Feldspar Minerals

The dominant feldspar minerals in these rocks are plagioclase characterized as fairly sodic to intermediate between the sodium and calcium rich (Fig. 34). Plagioclase is the dominant mineral in these rocks followed by pyroxene and amphiboles. These minerals developed in both of the lithological units of Handeni project except in hornblende pyroxenite, which has less abundance of plagioclase (including silica).

Based on the classification (after Richard, 1995) of their mineral composition data in Table 9 and 10, three types of the plagioclase series are developed in these rocks namely; oligoclase, andesine and labradorite (Fig. 34). They are varying in grain sizes and shapes, most are fine to medium grained with irregular shape and commonly develop in the marginal zones between the grains of pyroxene-, garnet- and hornblende and within the fracture zones of garnet or pyroxene.

Andesine is the dominant plagioclase mineral developed in these rocks, they associate with pyroxene, amphibole and garnet as well as quartz and sulphide minerals. The composition of the main oxides (Table 9) of the analyzed andesine varies; CaO (8.9-6.2) wt% and Na_2O (7.5-6.3) wt % at average of 25.42 wt % of Al_2O_3 whereas the average ratios of Na/Ca is 1.65 and for Ca/Na is 0.91 as illustrated in the classification diagram (Richard, 1995) in Figure 34. The decrease of Ca could be due to the change in temperature as lowering the temperature the Ca rich plagioclase become progressively unstable.

Table 9. Composition of plagioclase from the representative samples H01A and H7A1.

Lithology	**Gsil**		**MGr**								
Sample	**H7A2**		**H01A**			**H13A**			**H78A**	**H124**	
Analytica numbe	**1**	**2**	**3**	**4**	**5**	**6**	**7**	**8**	**9**	**10**	**11**
wt%- Comment	**Core**	**Rim**	**Core**	**Core**	**Core**	**Core**	**Core**	**Core**	**Rim**	**Rim**	**Core**
SiO2	62.29	63.43	58.28	56.02	55.54	59.64	58.98	57.65	59.58	60.64	59.85
TiO2	0.00	0.00	0.00	0.00	0.02	0.00	0.03	0.00	0.07	0.00	0.01
Al2O3	23.43	23.28	25.71	27.91	27.84	25.08	25.28	26.20	24.79	24.05	24.18
FeO	0.06	0.08	0.13	0.06	0.00	0.07	0.01	0.00	0.13	0.03	0.01
MnO	0.00	0.00	0.00	0.00	0.03	0.01	0.02	0.00	0.01	0.01	0.00
MgO	0.01	0.02	0.00	0.00	0.00	0.00	0.00	0.00	0.01	0.00	0.00
CaO	5.30	4.78	8.09	10.39	10.01	7.08	7.29	8.51	6.68	6.07	6.12
Na2O	8.29	8.44	6.80	4.32	5.52	6.64	6.86	6.11	7.57	7.87	7.81
K2O	0.06	0.09	0.27	0.15	0.13	0.17	0.18	0.14	0.18	0.21	0.22
TOTAL	**99.44**	**100.12**	**99.28**	**98.85**	**99.09**	**98.69**	**98.65**	**98.61**	**99.02**	**98.88**	**98.20**
Oxygen basis	32	32	32	32	32	32	32	32	32	32	32
Si	11.08	11.18	10.50	10.14	10.07	10.73	10.65	10.44	10.72	10.90	10.84
Ti	0.00	0.00	0.00	0.00	0.00	0.00	0.00	0.00	0.01	0.00	0.00
Al	4.91	4.83	5.46	5.95	5.94	5.32	5.37	5.59	5.25	5.09	5.16
Fe2	0.01	0.01	0.02	0.01	0.00	0.01	0.00	0.00	0.02	0.01	0.00
Mn	0.00	0.00	0.00	0.00	0.01	0.00	0.00	0.00	0.00	0.00	0.00
Mg	0.00	0.01	0.00	0.00	0.00	0.00	0.00	0.00	0.00	0.00	0.00
Ca	1.01	0.90	1.56	2.01	1.94	1.37	1.41	1.65	1.29	1.17	1.19
Na	2.86	2.89	2.38	1.52	1.94	2.32	2.40	2.15	2.64	2.74	2.74
K	0.01	0.02	0.06	0.04	0.03	0.04	0.04	0.03	0.04	0.05	0.05
Total	**19.89**	**19.84**	**19.98**	**19.66**	**19.93**	**19.78**	**19.88**	**19.85**	**19.98**	**19.95**	**19.97**
AB	73.60	75.80	59.40	42.50	49.60	62.30	62.30	56.00	66.50	69.30	68.90
AN	26.00	23.70	39.10	56.50	49.70	36.70	36.60	43.10	32.40	29.50	29.80
OR	0.40	0.50	1.60	1.00	0.80	1.00	1.10	0.80	1.00	1.20	1.30

Table 9. Continue….Composition of plagioclase from representative samples H01A H7A2 and H78A.

Lithology	**GGr**										
Sample	**H7A1**						**H44A**		**H54A**		
Analytica numbe	**12**	**13**	**14**	**15**	**16**	**17**	**18**	**19**	**20**	**21**	**22**
wt%- Comment	**Core**	**Core**	**Core**	**Rim**	**Core**	**Rim**	**Core**	**Rim**	**Core**	**Core**	**Core**
SiO2	58.30	58.91	58.16	59.19	59.08	57.29	58.35	58.80	57.86	59.34	58.94
TiO2	0.01	0.00	0.01	0.00	0.00	0.00	0.00	0.00	0.00	0.00	0.00
Al2O3	26.04	26.11	25.90	25.58	25.31	26.85	25.28	25.09	25.13	23.95	24.36
FeO	0.10	0.03	0.00	0.04	0.00	0.18	0.01	0.00	0.12	0.00	0.05
MnO	0.03	0.00	0.00	0.01	0.00	0.02	0.02	0.00	0.00	0.02	0.00
MgO	0.00	0.01	0.00	0.01	0.00	0.00	0.00	0.00	0.00	0.00	0.00
CaO	8.52	8.29	8.26	7.76	7.44	8.90	7.65	7.36	7.37	6.16	6.32
Na2O	6.54	6.68	6.75	6.91	7.02	6.26	6.70	7.00	6.94	7.13	7.45
K2O	0.24	0.27	0.28	0.33	0.31	0.25	0.18	0.20	0.18	0.18	0.20
TOTAL	**99.78**	**100.30**	**99.36**	**99.83**	**99.16**	**99.75**	**98.19**	**98.45**	**97.60**	**96.78**	**97.32**
Oxygen basis	32	32	32	32	32	32	32	32	32	32	32
Si	10.46	10.50	10.47	10.59	10.63	10.30	10.60	10.65	10.58	10.87	10.77
Ti	0.00	0.00	0.00	0.00	0.00	0.00	0.00	0.00	0.00	0.00	0.00
Al	5.50	5.48	5.49	5.39	5.36	5.69	5.41	5.35	5.41	5.17	5.24
Fe2	0.02	0.00	0.00	0.01	0.00	0.03	0.00	0.00	0.02	0.00	0.01
Mn	0.01	0.00	0.00	0.00	0.00	0.00	0.00	0.00	0.00	0.00	0.00
Mg	0.00	0.00	0.00	0.00	0.00	0.00	0.00	0.00	0.00	0.00	0.00
Ca	1.64	1.58	1.59	1.49	1.43	1.71	1.49	1.43	1.44	1.21	1.24
Na	2.28	2.31	2.36	2.40	2.45	2.18	2.36	2.46	2.46	2.53	2.64
K	0.06	0.06	0.06	0.08	0.07	0.06	0.04	0.05	0.04	0.04	0.05
Total	**19.95**	**19.94**	**19.98**	**19.95**	**19.94**	**19.97**	**19.90**	**19.93**	**19.96**	**19.83**	**19.94**
AB	57.30	58.40	58.70	60.50	61.90	55.20	60.70	62.50	62.40	66.90	67.30
AN	41.30	40.10	39.70	37.60	36.30	43.40	38.30	36.30	36.60	32.00	31.50
OR	1.40	1.50	1.60	1.90	1.80	1.40	1.10	1.20	1.10	1.10	1.20

The Ab, An and Or end member were calculated following Richard (1995).

Analytical numbers;

- 1-2, 11 represent oligoclase plagioclase developed in garnet silica rock.
- 3, 6-10 represent the andesine mineral developed in mafic granulite rock.
- 12-22 represent the andesine plagioclase developed in garnetiferous granulite.
- 4-5 represent labradorite minerals developed in mafic granulite rocks.

Oligoclase occasionally develops in the siliceous rock such as in GSil and quartz veins and occasionally in mafic granulite rocks. Oligoclase is rich in sodium compared to andesine plagioclase which indicates the change in temperature to be from high to low. Labradorite is commonly developed in the mafic granulite rocks of the Handeni project commonly associated with amphiboles (Fig. 34).

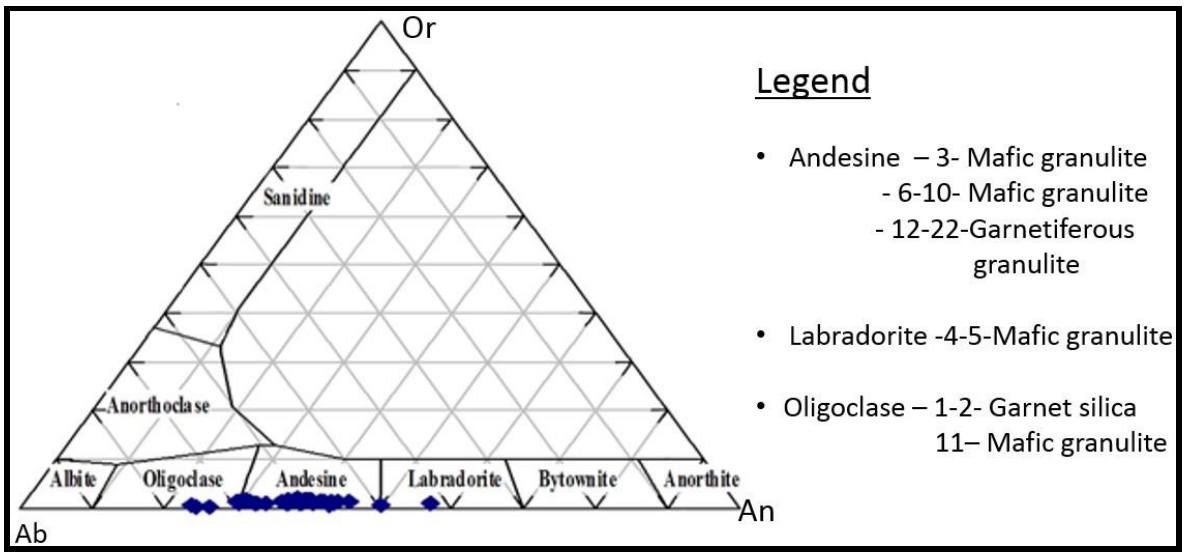

Figure 34. Ternary diagram showing the classification of the plagioclase modified after (Richard, 1995).

6.4.3 Garnet Minerals

Garnet minerals analyzed in these rocks commonly classify as almandine ($Fe_3{}^{2+}Al_2$ $(SiO_4)_3$) (Richard, 1995) Figure 35, they are characterized by fine to coarse grain size, exhibit zonation pattern steady with the retrograde overprint. They are dominantly in GGr, GSil, and MGr and occasionally in QFGn units. There is no trace of garnets developed in HP units. Occasionally, garnets develop corona textures which form symplectites with hornblende and clinopyroxene as well as plagioclase grains (Fig. 25 A). Garnet develop fracture zones which are occasionally replaced by quartz or plagioclase, occasionally inclusion of quartz develop in these rocks as well.

The chemical composition of garnet (Table 10) varies from the GSil, MGr to GGr units whereas the XMn remain fairly constant throughout. The average X_{Fe} (Fe^{2+}/Fe^{2+} +Mg) of MGr and GGr are 0.73 and 0.71 respective while the GSil shows decline X_{Fe} = 0.66. The GSil is silica rich compared to the two units MGr and GGr which support the Fe difference observed in MGr and GGr units. The garnets in MGr and GSil are rich in XAl (1.9) whereas low in GGr (0.75).

Table 10. Composition of garnet mineral from the representative samples.

Lithology	**Gsil**				**MGr**							
Sample	**H7A2**				**H01A**		**H13A**		**H79A**		**H124**	
Analytical number	**1**	**2**	**3**	**4**	**5**	**6**	**7**	**8**	**9**	**10**	**11**	**12**
Commet - wt%	**Core**	**Rim**	**Core**	**Rim**	**Core**	**Rim**	**Core**	**Rim**	**Rim**	**Core**	**Core**	**Rim**
SiO2	39.50	39.64	39.37	39.14	39.79	39.23	39.33	38.79	37.66	38.19	38.22	38.11
TiO2	0.06	0.08	0.02	0.00	0.04	0.04	0.06	0.06	0.04	0.08	0.00	0.12
Al2O3	21.61	22.00	21.85	21.68	22.21	21.76	22.02	21.93	21.11	21.03	21.38	21.22
FeO	21.31	22.80	21.25	22.38	20.89	22.08	20.99	22.04	28.08	27.58	25.07	26.63
MnO	0.72	1.12	0.75	1.04	0.51	0.68	0.54	0.58	1.37	1.39	1.18	0.84
MgO	6.23	6.44	6.28	6.43	7.14	6.38	6.76	6.39	2.84	3.32	2.99	3.66
CaO	10.68	9.44	10.71	9.22	10.20	9.71	10.17	9.71	8.45	8.05	11.17	8.97
Na2O	0.00	0.01	0.03	0.01	0.00	0.01	0.00	0.02	0.00	0.00	0.02	0.01
K2O	0.00	0.01	0.01	0.00	0.01	0.02	0.00	0.03	0.01	0.01	0.00	0.01
Cr2O3	0.01	0.02	0.05	0.03	0.00	0.11	0.00	0.00	0.02	0.04	0.03	0.06
NiO	0.03	0.00	0.00	0.00	0.00	0.00	0.00	0.00	0.00	0.00	0.00	0.00
Total	**100.16**	**101.55**	**100.32**	**99.92**	**100.79**	**100.02**	**99.86**	**99.53**	**99.56**	**99.68**	**100.05**	**99.62**
Oxygen basis	12	12	12	12	12	12	12	12	12	12	12	12
Si	3.03	3.01	3.01	3.02	3.01	3.02	3.01	3.00	3.00	3.02	3.00	3.01
Ti	0.00	0.00	0.00	0.00	0.00	0.00	0.00	0.00	0.00	0.00	0.00	0.01
Al	1.95	1.97	1.97	1.97	1.98	1.97	1.99	2.00	1.98	1.96	1.98	1.97
Fe	1.37	1.45	1.36	1.44	1.32	1.42	1.34	1.42	1.87	1.83	1.65	1.76
Mn	0.05	0.07	0.05	0.07	0.03	0.04	0.04	0.04	0.09	0.09	0.08	0.06
Mg	0.71	0.73	0.72	0.74	0.81	0.73	0.77	0.74	0.34	0.39	0.35	0.43
Ca	0.88	0.77	0.88	0.76	0.83	0.80	0.83	0.80	0.72	0.68	0.94	0.76
Na	0.00	0.00	0.00	0.00	0.00	0.00	0.00	0.00	0.00	0.00	0.00	0.00
K	0.00	0.00	0.00	0.00	0.00	0.00	0.00	0.00	0.00	0.00	0.00	0.00
Cr	0.00	0.00	0.00	0.00	0.00	0.01	0.00	0.00	0.00	0.00	0.00	0.00
Ni	0.00	0.00	0.00	0.00	0.00	0.00	0.00	0.00	0.00	0.00	0.00	0.00
Total	7.99	8.00	8.00	8.00	7.99	7.99	7.99	8.00	8.01	7.99	8.01	8.00
ALM	45.51	47.97	45.22	47.89	44.26	47.38	45.03	47.39	61.91	60.99	54.56	58.50
GROSS	29.19	25.38	29.04	25.18	27.69	26.36	27.95	26.75	23.81	22.68	31.05	25.06
PYROPE	23.72	24.15	23.82	24.53	26.96	24.40	25.85	24.49	11.16	13.09	11.60	14.33
SPESS	1.56	2.39	1.62	2.25	1.09	1.48	1.17	1.26	3.06	3.11	2.60	1.87
UVARO	0.03	0.06	0.15	0.09	0.00	0.34	0.00	0.00	0.06	0.13	0.09	0.19
XCa	29.20	25.50	29.20	25.30	27.70	26.70	28.00	26.80	23.90	22.80	31.20	25.30
XFe	45.50	48.00	45.30	47.90	44.20	47.40	45.00	47.40	61.90	61.00	54.60	58.50
XMg	23.70	24.20	23.90	24.50	27.00	24.40	25.80	24.50	11.20	13.10	11.60	14.30

Analysis number of almandine garnet representing the different units; garnetiferous granulite – GGr, mafic granulite – MGr and garnet silica – GSil.

Table 10 continue…. Composition of garnet mineral from the representative samples.

Lithology	GGr										
Sample	H97A		H54A		H44A		H97A	H44A			
Analytical number	13	14	15	16	17	18	19	20	21	22	23
Commet - wt%	Core	Rim	Core	Rim	Rim	Core	Rim	Core	Rim	Core	Core
SiO2	38.35	38.36	39.28	38.51	38.36	39.37	38.31	38.86	38.55	39.18	39.12
TiO2	0.05	0.03	0.04	0.01	0.05	0.00	0.01	0.03	0.05	0.02	0.00
Al2O3	21.47	21.31	21.90	21.78	20.93	21.63	21.25	21.59	21.74	21.50	21.62
FeO	27.87	29.36	23.88	23.37	24.53	23.99	29.73	23.59	23.47	23.85	23.21
MnO	0.43	0.34	0.79	0.96	0.88	0.93	0.51	0.76	0.84	0.82	0.77
MgO	5.83	4.95	6.00	5.55	6.33	6.12	4.07	6.19	6.00	6.25	6.17
CaO	5.27	5.25	9.12	10.02	7.83	8.04	5.94	8.69	8.09	8.03	8.55
Na2O	0.00	0.01	0.04	0.01	0.00	0.00	0.00	0.00	0.03	0.00	0.00
K2O	0.01	0.03	0.04	0.02	0.01	0.01	0.00	0.01	0.01	0.02	0.01
Cr2O3	0.02	0.06	0.00	0.03	0.09	0.01	0.12	0.07	0.04	0.00	0.08
NiO	0.02	0.00	0.02	0.00	0.00	0.00	0.01	0.01	0.00	0.00	0.00
Total	**99.31**	**99.71**	**101.09**	**100.26**	**99.00**	**100.11**	**99.95**	**99.80**	**98.82**	**99.66**	**99.52**
Oxygen	12	12	12	12	12	12	12	12	12	12	12
Si	3.01	3.02	3.01	2.98	3.01	3.04	3.02	3.01	3.01	3.03	3.03
Ti	0.00	0.00	0.00	0.00	0.00	0.00	0.00	0.00	0.00	0.00	0.00
Al	1.99	1.98	1.98	1.99	1.94	1.97	1.98	1.97	2.00	1.96	1.97
Fe	1.83	1.93	1.53	1.51	1.61	1.55	1.96	1.53	1.53	1.54	1.50
Mn	0.03	0.02	0.05	0.06	0.06	0.06	0.03	0.05	0.06	0.05	0.05
Mg	0.68	0.58	0.69	0.64	0.74	0.70	0.48	0.71	0.70	0.72	0.71
Ca	0.44	0.44	0.75	0.83	0.66	0.66	0.50	0.72	0.68	0.67	0.71
Na	0.00	0.00	0.01	0.00	0.00	0.00	0.00	0.00	0.00	0.00	0.00
K	0.00	0.00	0.00	0.00	0.00	0.00	0.00	0.00	0.00	0.00	0.00
Cr	0.00	0.00	0.00	0.00	0.01	0.00	0.01	0.00	0.00	0.00	0.01
Ni	0.00	0.00	0.00	0.00	0.00	0.00	0.00	0.00	0.00	0.00	0.00
Total	7.99	7.99	8.01	8.02	8.02	7.98	7.98	8.00	7.99	7.98	7.98
ALM	61.32	64.85	50.64	49.62	52.49	51.99	65.90	50.70	51.64	51.73	50.52
GROSS	14.79	14.67	24.78	27.16	21.18	22.29	16.49	23.71	22.68	22.31	23.60
PYROPE	22.87	19.49	22.68	21.01	24.14	23.64	16.08	23.72	23.53	24.16	23.94
SPESS	0.96	0.76	1.70	2.07	1.91	2.04	1.15	1.65	1.87	1.80	1.70
UVARO	0.06	0.19	0.00	0.09	0.29	0.03	0.38	0.22	0.12	0.00	0.25
XCa	14.80	14.90	24.80	27.30	21.50	22.30	16.90	23.90	22.80	22.30	23.80
XFe	61.30	64.90	50.70	49.70	52.50	52.00	65.90	50.70	51.70	51.70	50.50
XMg	22.90	19.50	22.70	21.00	24.20	23.70	16.10	23.70	23.60	24.20	23.90

The XCa, XFe and XMg values were calculated following Richard (1995).

Analytical number 1-40 representing the almandine garnet from the three main lithological units.

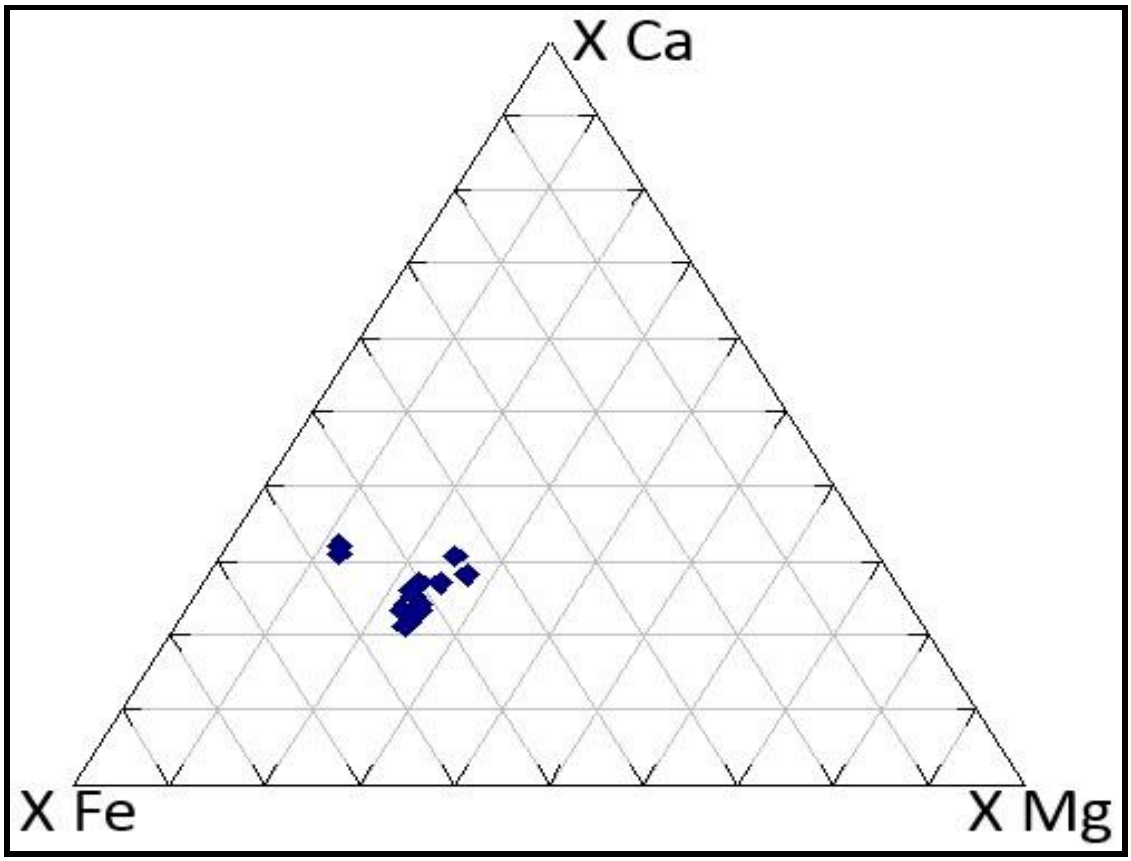

Figure 35. Ternary diagram showing the classification of garnet "almandine" 100 normalization of XCa, XFe and XMg from garnet composition (after Richard, 1995).

6.4.4 Amphibole Minerals

The dominant amphibole mineral developed in these rocks is calcic hornblende, based on the classification and nomenclature of (Leake, 1978 and Richard, 1995) of the amphibole composition (Table 11) three end members of hornblende calcic amphiboles are dominant namely edenite, pargasite and tschermakite (Fig. 36), commonly developed in MGr, GGr, HP and QFGn and rare in GSil unit.

The chemical composition of these hornblendes varies from parasite, tschermakite to edenite and exhibit the characteristics of retrograde metamorphism. Edenite minerals commonly develop in GGr and MGr rocks, pargasite in MGr and Tschermakite in GGr. They change in chemical composition from pargasitic to edenitic during retrograde metamorphism releasing considerable amounts of Al_2O_3 at an average of 12.4 wt %. The XMg (Mg/(Mg+Fe2+) ranges from 0.58 to 0.67, the content of CaO varies from 11.48 to 11.55 wt %, Na_2O varies from 1.61 to 1.5 wt % and TiO2 is less than 1.85 wt% whereas the K2O ranges from 1.04 to 082 wt % (Table 11). Most of the grains analyzed for amphibole show edenite and tschermakite exchange.

Table 11. Composition of amphibole (hornblende) as from the analyzed representative samples.

Lithology	**GGr**							**MGr**			**GGr**				
Sample	**H7A1**					**H97A**	**H44A**	**H13A**		**H54A**	**H7A1**	**H54A**			
Analytical number	**2**	**3**	**4**	**5**	**6**	**10**	**11**	**22**	**16**	**12**	**1**	**25**	**26**	**27**	**29**
Core/Rimim	**Rim**	**Core**	**Core**	**Core**	**Rim**	**Core**	**Core**	**Core**	**Core**	**Rim**	**Rim**	**Rim**	**Rim**	**Core**	**Rim**
SiO2	44.43	44.57	44.77	45.06	45.35	46.84	45.73	44.62	44.47	43.53	45.68	42.64	42.50	43.62	42.34
TiO2	1.85	1.80	1.76	1.62	1.52	1.05	1.33	1.77	1.76	2.01	1.66	1.81	1.75	1.43	1.39
Al2O3	12.89	12.74	12.43	12.22	11.94	9.53	11.66	11.79	12.70	12.45	11.47	13.15	13.28	12.06	13.36
FeO	11.65	10.58	11.51	11.60	11.58	12.39	10.67	11.91	10.90	13.07	10.65	12.43	13.68	14.29	14.88
MnO	0.17	0.07	0.05	0.03	0.07	0.04	0.07	0.05	0.00	0.11	0.05	0.14	0.09	0.16	0.13
MgO	12.98	12.53	12.91	13.30	13.22	13.47	13.40	13.05	13.10	11.19	13.72	11.00	10.79	10.85	9.91
CaO	11.71	11.78	11.54	11.48	11.52	11.09	11.75	11.58	11.54	11.31	11.97	11.41	11.29	11.38	11.26
Na2O	1.62	1.51	1.54	1.50	1.37	1.46	1.55	1.58	1.46	1.80	1.25	1.71	1.58	1.01	1.49
K2O	1.00	1.09	1.04	0.95	0.99	0.49	0.20	0.89	1.00	1.03	0.89	1.14	1.10	0.90	1.03
Cr2O3	0.11	0.12	0.13	0.07	0.05	0.08	0.22	0.07	0.09	0.03	0.15	0.07	0.07	0.02	0.08
NiO	0.01	0.00	0.00	0.00	0.00	0.06	0.01	0.00	0.00	0.00	0.00	0.03	0.02	0.00	0.00
Total	**98.40**	**96.79**	**97.69**	**97.83**	**97.60**	**96.50**	**96.59**	**97.30**	**97.01**	**96.52**	**97.49**	**95.51**	**96.14**	**95.71**	**95.86**
Oxygen basis	24	24	24	24	24	24	24	24	24	24	24	24	24	24	24
Si	6.73	6.82	6.81	6.84	6.89	7.19	6.97	6.83	6.79	6.77	6.92	6.69	6.66	6.85	6.69
Ti	0.21	0.21	0.20	0.18	0.17	0.12	0.15	0.20	0.20	0.24	0.19	0.21	0.21	0.17	0.16
Al	2.30	2.30	2.23	2.18	2.14	1.72	2.09	2.13	2.29	2.28	2.05	2.43	2.45	2.23	2.49
Fe	1.47	1.35	1.46	1.47	1.47	1.59	1.36	1.52	1.39	1.70	1.35	1.63	1.79	1.88	1.97
Mn	0.02	0.01	0.01	0.00	0.01	0.01	0.01	0.01	0.00	0.01	0.01	0.02	0.01	0.02	0.02
Mg	2.93	2.86	2.93	3.01	3.00	3.08	3.04	2.98	2.98	2.59	3.10	2.57	2.52	2.54	2.33
Ca	1.90	1.93	1.88	1.87	1.88	1.82	1.92	1.90	1.89	1.88	1.94	1.92	1.90	1.92	1.90
Na	0.48	0.45	0.45	0.44	0.40	0.43	0.46	0.47	0.43	0.54	0.37	0.52	0.48	0.31	0.45
K	0.19	0.21	0.20	0.18	0.19	0.10	0.04	0.17	0.19	0.20	0.17	0.23	0.22	0.18	0.21
Cr	0.01	0.01	0.02	0.01	0.01	0.01	0.03	0.01	0.01	0.00	0.02	0.01	0.01	0.00	0.01
Ni	0.00	0.00	0.00	0.00	0.00	0.01	0.00	0.00	0.00	0.00	0.00	0.00	0.00	0.00	0.00
Total	**16.24**	**16.15**	**16.19**	**16.19**	**16.16**	**16.09**	**16.07**	**16.22**	**16.17**	**16.23**	**16.12**	**16.25**	**16.25**	**16.10**	**16.23**
TSI	6.44	6.57	6.53	6.54	6.60	6.88	6.67	6.54	6.51	6.52	6.63	6.45	6.38	6.55	6.40
TAL	1.56	1.43	1.47	1.46	1.40	1.13	1.33	1.47	1.49	1.48	1.37	1.55	1.62	1.46	1.60
TFE3	0.00	0.00	0.00	0.00	0.00	0.00	0.00	0.00	0.00	0.00	0.00	0.00	0.00	0.00	0.00
TTI	0.00	0.00	0.00	0.00	0.00	0.00	0.00	0.00	0.00	0.00	0.00	0.00	0.00	0.00	0.00

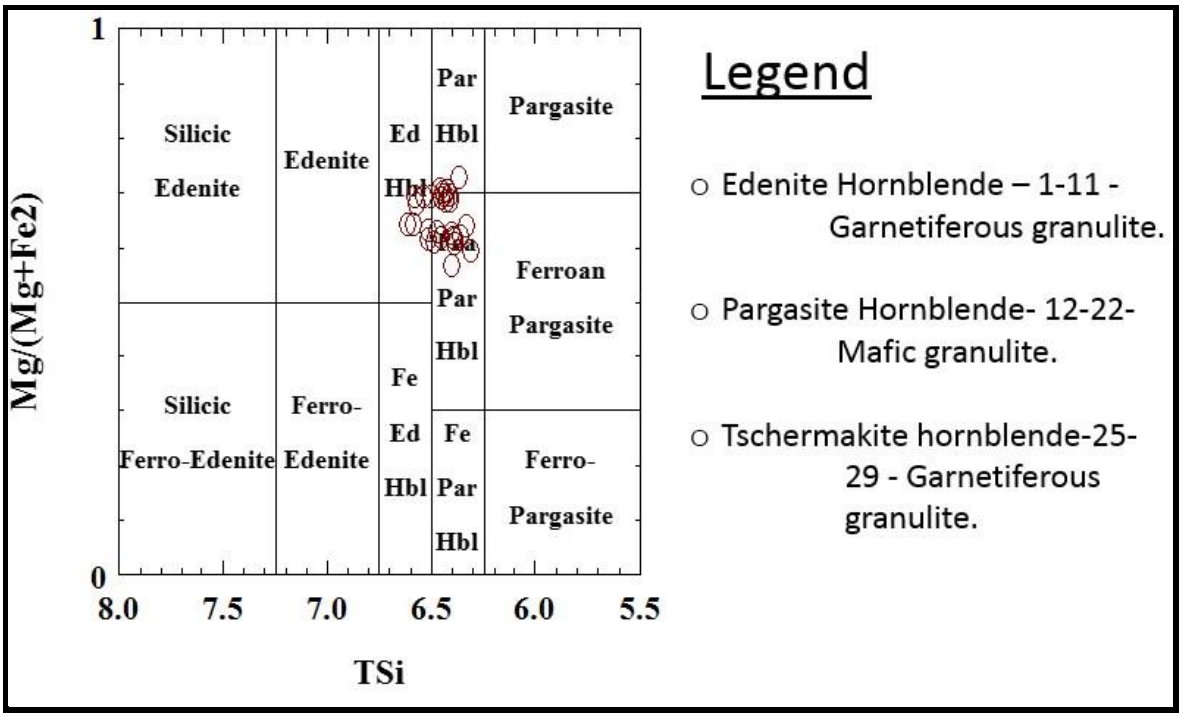

Figure 36 Classification of calcic amphibole or hornblende-Hbl mineral (modified from Leake, 1978 and Richard, 1995).

6.4.5 Quartz

Quartz commonly developed in margin zones of pyroxene or hornblende and garnet, also occasionally as individual grains mostly in a veins, which display a colorless hue and regular shape with medium to coarse grains. Commonly quartz grains are associated with garnet and plagioclase. In a vein, quartz shows C$^{>}$-parallel prism with sub grains boundary while in country rocks show basal plane parallel with sub grains boundary Figure 23. This implies that quartz from the veins were crystallized later than those from the country rocks (Kruhl, 1996)

6.4.6 Biotite

Biotite in these rocks is not commonly distributed in all of the units of the Handeni project, but is occasionally developed in GGr and rare in MGr and HP units. Biotite develops dark brownish flakes of fine to medium grain and occasionally occurs as inclusions in hornblende or pyroxene (Fig. 25 and 28). The chemical composition of biotite in these GGr rocks has a considerable amount of FeO and MgO about 15.13 wt % and 13.27 wt % respectively whereas the Fe-FeMg and Mg-FeMg of 0.39 and 0.61 respectively and its XMg (Mg/Mg+Fe2+) is 0.61 (Fig. 37). Their TiO2 range from 4.96 wt % to 3.78 wt % and K2O ranges between 9.01 wt % and 6.35 wt % giving the Al^{IV} of about 2.29 and the Al^{VI} of about 0.61equivalent to Mg-FeMg or XMg (Table 12).

Table 12. Composition of biotite mineral from representative sample H01A and H97A.

Lithology	**GGr**									
SAMPLE	**H40A**		**H97A**							
Analytical number	**1**	**2**	**3**	**4**	**5**	**6**	**7**	**8**	**9**	**10**
Comment-wt%	**Core**	**Core**	**Core**	**Rim**	**Core**	**Core**	**Core**	**Core**	**Core**	**Core**
SiO2	38.78	37.83	35.40	34.95	34.33	34.75	35.16	34.13	34.61	34.55
TiO2	4.67	4.66	4.96	4.94	4.48	4.01	3.78	4.31	4.54	4.54
Al2O3	16.18	15.86	15.00	15.08	14.76	15.00	15.35	15.05	15.22	15.39
FeO	12.70	12.43	15.97	15.91	15.69	15.41	15.68	15.43	16.09	16.00
MnO	0.02	0.01	0.04	0.02	0.00	0.01	0.00	0.00	0.01	0.00
MgO	15.85	15.26	12.95	12.69	12.06	12.73	13.20	12.64	12.44	12.84
CaO	0.00	0.02	0.00	0.00	0.03	0.06	0.00	0.04	0.04	0.00
Na2O	0.08	0.12	0.28	0.26	0.25	0.24	0.21	0.26	0.20	0.22
K2O	6.35	8.12	8.54	8.49	8.54	9.01	8.97	8.54	8.37	8.36
Cr2O3	0.08	0.10	0.11	0.05	0.08	0.14	0.10	0.13	0.06	0.11
NiO	0.01	0.01	0.09	0.11	0.09	0.09	0.00	0.00	0.06	0.00
Total	**94.72**	**94.40**	**93.35**	**92.50**	**90.31**	**91.46**	**92.44**	**90.54**	**91.63**	**92.01**
Oxygen basis	24	24	24	24	24	24	24	24	24	24
Si	5.88	5.83	5.68	5.66	5.70	5.70	5.70	5.65	5.66	5.62
Ti	0.53	0.54	0.60	0.60	0.56	0.50	0.46	0.54	0.56	0.56
ALIV	2.12	2.17	2.32	2.34	2.30	2.30	2.30	2.35	2.34	2.38
ALVI	0.77	0.71	0.52	0.54	0.59	0.60	0.62	0.58	0.59	0.57
Fe2	1.61	1.60	2.14	2.16	2.18	2.12	2.12	2.14	2.20	2.18
Mn	0.00	0.00	0.01	0.00	0.00	0.00	0.00	0.00	0.00	0.00
Mg	3.58	3.50	3.10	3.07	2.99	3.12	3.19	3.12	3.03	3.12
Ca	0.00	0.00	0.00	0.00	0.01	0.01	0.00	0.01	0.01	0.00
Na	0.02	0.04	0.09	0.08	0.08	0.08	0.07	0.08	0.06	0.07
K	1.23	1.60	1.75	1.76	1.81	1.89	1.85	1.80	1.75	1.74
Cr	0.01	0.01	0.01	0.01	0.01	0.02	0.01	0.02	0.01	0.01
Ni	0.00	0.00	0.00	0.00	0.00	0.00	0.00	0.00	0.00	0.00
Total	**15.76**	**16.00**	**16.21**	**16.21**	**16.23**	**16.32**	**16.33**	**16.28**	**16.21**	**16.24**
FE_FEMG	0.31	0.31	0.41	0.41	0.42	0.40	0.40	0.41	0.42	0.41
MG_FEMG	0.69	0.69	0.59	0.59	0.58	0.60	0.60	0.59	0.58	0.59

Calculation of the Fe-FeMg and Mg-FeMg were done following Richard (1995).

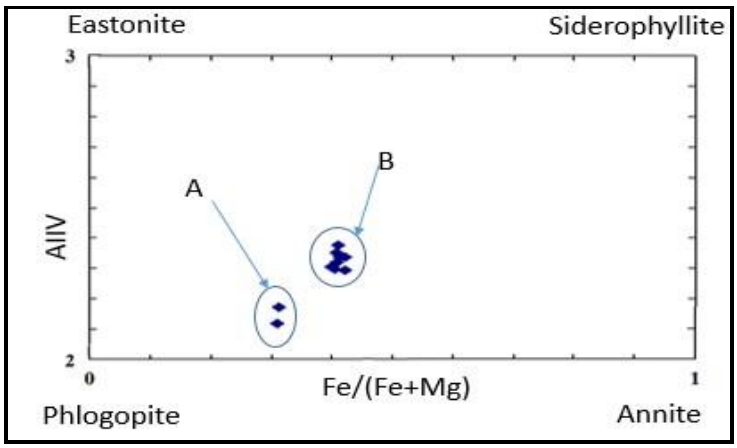

Figure 37. Classification of biotite (after Richard, 1995) in garnetiferous granulite showing the difference in iron abundance between coarse grained GGr (A) and gritty GGr (B) in garnetiferous granulite rock.

6.4.7 Sulphide Minerals

Dominant sulphides minerals present in these rocks include pyrrhotite chalcopyrite pyrite gersdorffite and occasionally pentlandite and arsenopyrite. The chemical compositions for the sulphide minerals are attached in appendices A - D. **Pyrites** show regular to irregular shapes associated with pyrrhotite and chalcopyrite. Pyrite occurs in all of the lithological units in Handeni project except in hornblende pyroxenite units, commonly in the margin of mafic minerals such as clinopyroxene and amphiboles (Fig 21).

Pyrrhotite is one of the dominant sulphide minerals occurring as disseminated granular crystals with a tabular or platy shape. They show late crystallization as plagioclase or quartz (Fig. 28) in the margin between the pyroxene and amphibole (hornblende) and rarely with garnet. Also, they commonly developed in MGr, GGr, GSil and HP rocks. They also rare occur as inclusion in pyroxene, occasionally shows intergrowth of chalcopyrite and pentlandite as well as gersdorffite (Fig. 32).

Chalcopyrite ($CuFeS_2$) is deep yellowish in color, fine to medium grained with regular to irregular shape (anhedral to euhedral) and developed as inclusions in the pyrrhotite grain (Fig. 24, 30A & 32A). Chalcopyrite is found as disseminated minerals commonly associated with pyrrhotite and crystallises in between the pyroxene and hornblende margins. Occasionally gersdorffite develops as inclusions in chalcopyrite. Chalcopyrite commonly occurs in MGr, GGr, HP and GSil rocks and occasionally develops in QFGn rock.

Gersdorffite (NiAsS) occurs with regular shape whilst exhibiting a phaneritic texture. Gersdorffite is commonly associated with chalcopyrites and pyrrhotite (Fig 32). It is developed in margin zones of pyroxene and hornblende or garnet, also as inclusion in chalcopyrite (Fig. 32A). Gersdorffite commonly developed in HP and disseminated in GGr and MGr units. **Pentlandite** ($(Fe, Ni)_9 S_8$) occasionally is intergrown with the chalcopyrite and the pyrrhotite and developed in HP and occasionally in GGr and MGr units regularly associated with pyrrhotite suggesting a magmatic relationship**.**

6.4.8 Carbonate minerals

Three types of carbonate minerals that have been encountered in these rocks are calcite, magnesite and dolomite (appendix Tables F-H for their chemical composition). M**agnesite** developed in HP rocks and is associated with pyroxene and orthopyroxene but not well developed in MGr GSil or GGr units. Magnesite averages about 34.12 wt % MgO shows

perfect cleavage and conchoidal fracture and does not show any relationship with sulphides in these rocks.

Calcite, $CaCO_3$ and dolomite, $CaMgCO_3$ associate with pyrite diopside quartz garnet magnesite and plagioclase being subjected to alteration after metamorphism. They normally develop as inclusions in quartz, garnet, hornblende and occasionally in pyroxene and commonly occur in MGr, GGr and QFGn (Fig. 24 and 29).

6.4.9 Minor or Accessory Minerals

Minor or accessory minerals occuring in these rocks include the following minerals: **Ilmenite** (its composition in appendix Table E) developed in the groundmass of the pyroxene and garnet which shows a symplectitic texture near the margin of garnet and quartz or pyrrhotite refer Fig. 26 B and 27 respectively. **Titanite**, $CaTiSiO_5$ (its composition in appendix I) is very fine grained and associated with diopside ilmenite calcite and occasionally with biotite. These minerals commonly developed in HP units and occasionally in MGr and GGr.

6.5 BULK ROCK GEOCHEMISTRY

The samples for geochemical analysis of the whole rocks were chosen to be petrographically homogeneous, without veinlets or intercalations of contrasting compositions. Some lithological units, like QFGn, GSil and quartz veins were not part of the bulk rock analysis, therefore rocks of only three main units were analyses namely MGr, GGr and HP and their compositions are given in Table 13 and 14.

The analyzed bulk rocks show average SiO_2 content that ranges from 42.31 to 56.09 wt % with a mean of 49.43 wt% whereas MGr has 50.57 wt%, GGr has 5015 wt % and HP has 46.72 wt %. The Mg# calculated as ($100Mg/Mg+Fe^{2+}_{total}$) for each units MGr, GGr and HP is 45.06, 44.10 and 85.04 respectively (Table 13).

The concentrations for Ni ranges from 4671.7 ppm to 1708.1 ppm, 93.0 ppm to 149.4 ppm and 108.3 ppm to 142.4 ppm for the HP, GGr and MGr respectively. These have corresponding similar ranges of concentrations as of Cr, from 1581.4 ppm to 1840.5 ppm, 142.1 ppm to 348.5 ppm and 189.3 ppm to 340.5 ppm respectively

According to Eskola (1939) bulk rock classification ACF of these rocks from the major elements (Fig. 38), the units GGr and MGr classified as pelitic rocks whereas the HP unit classified as the intermediate rocks corresponding to hornblende.

Table 13. Major element compositions (molar weight – wt %) of the whole rock analysis for the representative samples.

Lithology	**MGr**	**GGr**		**MGr**		**GGr**		**MGr**	**HP**		
Sample ID / Wt %	**H01A**	**H40A**	**H44A**	**H54A**	**H78A**	**H79A**	**H97A**	**H123**	**H124**	**H81A**	**H83A**	**H113**
SiO2	48.78	53.88	48.67	45.19	56.09	48.07	54.17	48.84	49.36	49.58	48.28	42.31
TiO2	1.06	2.12	1.21	1.36	0.76	1.39	0.73	1.45	1.51	0.37	0.35	0.38
Al2O3	14.55	14.13	14.86	14.66	7.67	13.30	10.67	14.87	15.47	1.93	2.09	2.61
Fe2O3	13.05	16.63	13.64	15.32	23.49	15.11	21.15	14.72	14.98	12.08	12.49	11.31
MnO	0.39	0.37	0.37	0.39	0.34	0.43	0.38	0.36	0.36	0.29	0.29	0.19
MgO	7.18	4.73	6.14	7.99	5.43	6.49	5.73	7.57	7.51	33.43	31.94	37.16
CaO	13.35	8.71	13.18	12.05	5.90	14.66	7.59	10.03	9.75	2.43	3.71	6.18
Na2O	1.70	0.62	2.66	2.14	2.17	0.20	0.88	2.34	2.57	0.00	-0.03	0.13
K2O	0.21	0.22	0.07	0.44	0.35	0.10	0.17	0.41	0.43	0.10	0.14	0.07
P205	0.10	0.21	0.09	0.10	0.12	0.18	0.13	0.20	0.16	0.05	0.05	0.06
LOI	0.66	0.12	0.25	5.46	5.70	1.93	2.87	0.48	0.49	4.10	4.58	12.87
Total	**101.02**	**101.72**	**101.14**	**105.10**	**108.02**	**101.86**	**104.46**	**101.27**	**102.56**	**104.35**	**103.89**	**113.28**
FeO	0.9*Fe2O3											
Mg# =	(100*Mg2+)/(Fe2+t+Mg2+)											
Mg#	52.38	36.24	47.36	51.06	31.60	46.22	35.15	50.71	50.07	84.70	83.64	86.79
FeO	11.74	14.96	12.28	13.79	21.14	13.60	19.03	13.24	13.48	10.87	11.24	10.18

MGr - Mafic granulite,

GGr - Garnetiferous granulite and

HP – Hornblende pyroxenite.

Table 14. Trace element in parts per million (ppm) of the whole rock for the representative samples of the Handeni project.

Lithology	**MGr**				**GGr**					**HP**		
Sample / Elements-ppm	**H 01A**	**H 78A**	**H 79A**	**H 124**	**H 40A**	**H 44A**	**H 54A**	**H 97A**	**H 123**	**H 81A**	**H 83A**	**H 113**
Co	49.00	69.10	33.70	54.20	70.60	76.80	68.00	33.10	53.00	141.70	194.50	100.20
Mn	1964.40	2304.40	1477.00	1677.60	1819.30	1813.30	1972.60	1711.50	1587.80	1190.70	1235.40	1088.60
Cr	340.50	189.30	231.40	203.90	142.10	348.50	269.20	236.70	193.10	1581.40	1840.50	1723.90
V	297.80	317.50	204.40	351.80	401.00	333.00	382.70	221.80	342.00	49.50	52.70	53.70
Zn	101.00	123.50	379.20	134.00	124.40	94.70	322.20	235.80	134.80	127.00	105.20	92.80
Cu	124.40	180.50	247.30	12.70	157.10	338.80	214.20	212.50	25.80	116.60	250.10	17.00
Ni	121.50	108.30	142.40	109.90	109.80	149.40	129.90	93.00	108.50	3596.40	4671.70	1708.10
Mo	0.90	1.90	4.10	0.20	1.90	1.00	0.70	2.60	0.10	0.70	1.50	0.20
Nb	3.00	5.20	3.00	4.00	13.90	3.90	3.80	3.60	4.80	1.20	0.40	0.70
Zr	48.30	72.80	39.20	80.30	108.70	56.90	65.40	45.80	75.00	7.90	4.90	7.10
Y	19.70	30.30	16.00	32.30	37.30	24.00	27.40	22.10	30.10	2.00	2.60	2.80
Sr	87.60	111.50	15.50	97.10	38.10	151.50	154.60	39.40	90.10	8.30	13.70	16.90
U	0.10	-1.10	1.00	-0.50	7.50	-0.70	0.30	0.60	-0.70	-0.40	0.20	0.10
Rb	1.40	1.40	60.50	7.50	4.30	0.80	5.40	2.70	6.90	3.50	5.90	0.70
Th	1.90	0.70	3.00	0.40	5.40	2.00	1.10	2.80	1.40	0.20	1.20	0.60
Pb	3.10	0.80	11.20	5.10	2.60	1.30	7.90	18.00	3.40	-0.10	1.20	2.00

MGr=Mafic granulite, GGr= Garnetiferous granulite and HP= Hornblende pyroxenite

100 normalizing of ACF perimeters, A = $((Al_2O_3+Fe_2O_3) – (Na_2O + K_2O))$ and C = $(CaO-3.33(P_2O_5))$ and the F= (MgO + FeO + MnO) (Fig. 38).

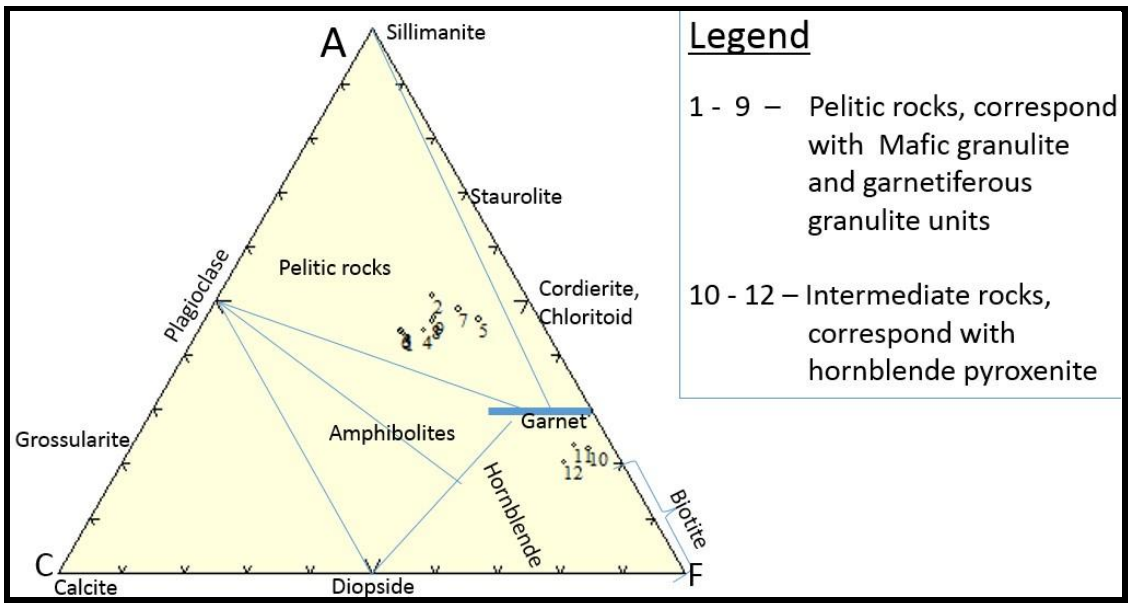

Figure 38. A 100 normalized ACF diagram classification of the bulk rock composition of the Handeni project rocks (after Eskola, 1939 and Winter, 2001).

The normalized AFM diagram (after Irvine *et al*, 1971) of these rocks demonstrate the nature of the Fe and Mg rich of the GGr and MGr rocks as well as the HP rocks respectively (Fig. 39).

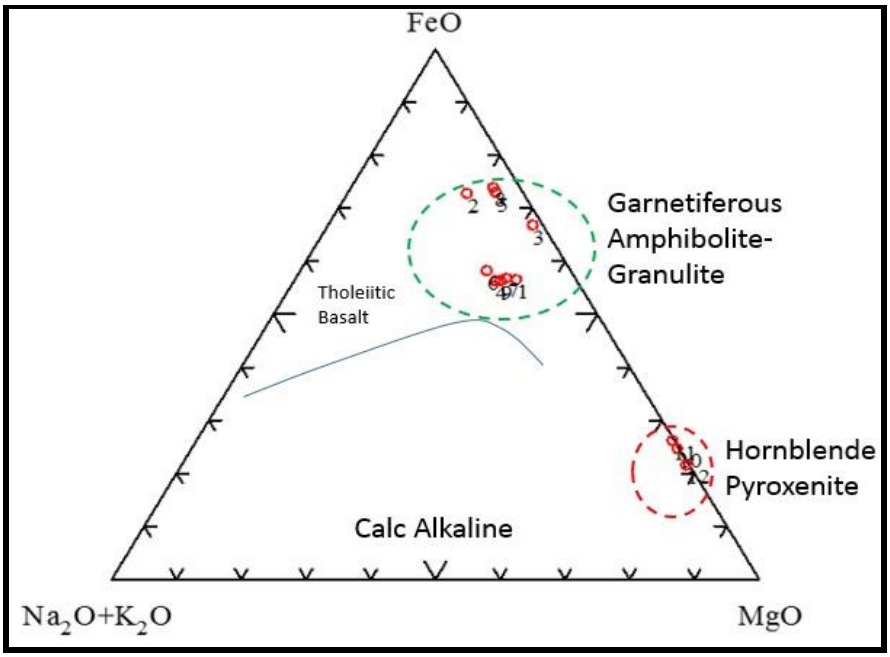

Figure 39. The AFM diagram of the Handeni project rocks (after Irvine et al, 1971 and Carr, 1995).

Fe_2O_3 show positive correlation with SiO_2 while MgO shows negative correlation, the rest has no correlation (Fig. 40).

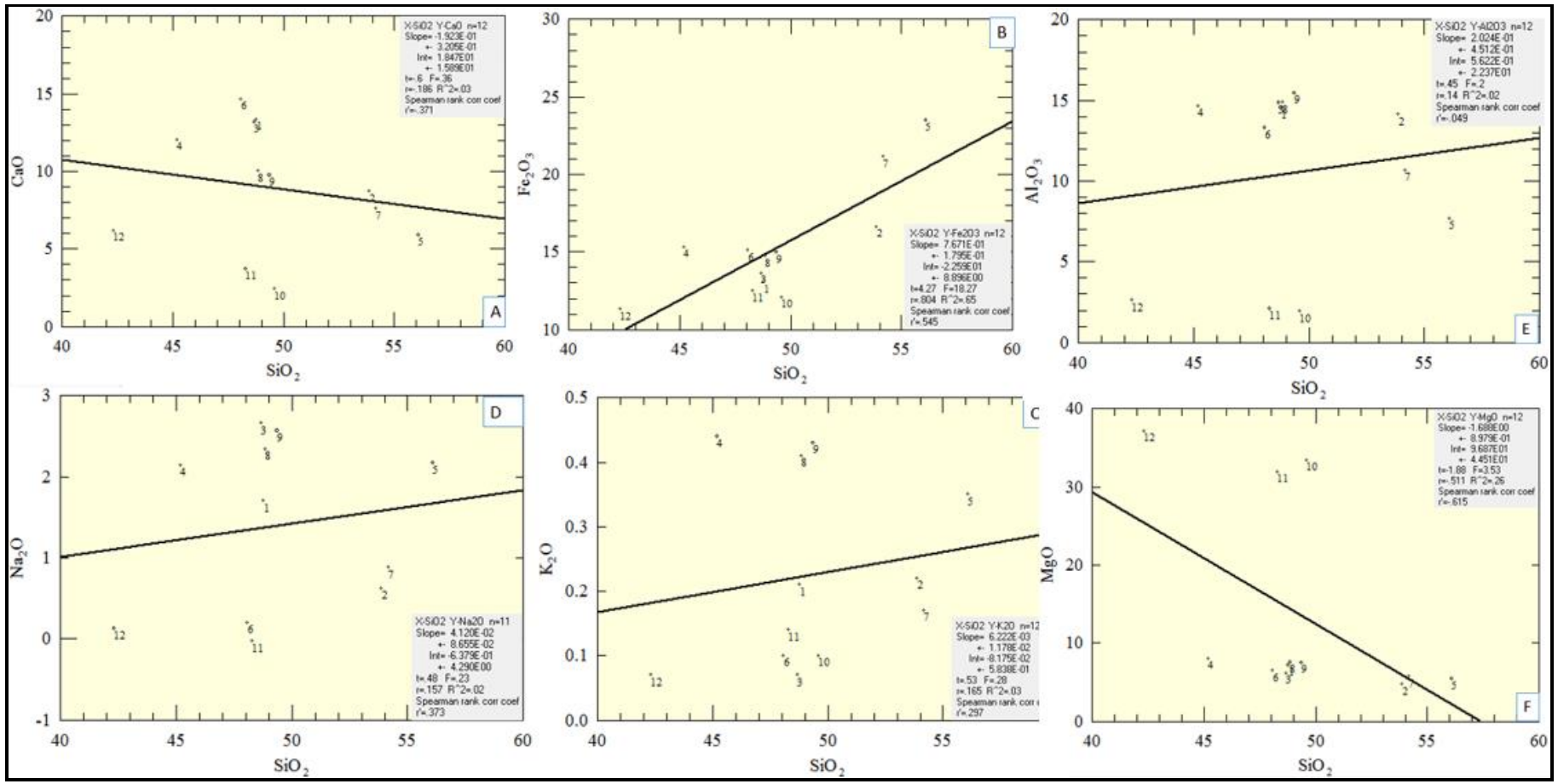

Figure 40. Major elements variation diagrams (after Carr, 1995) for the representative samples from Handeni rocks. Lithological units are presented by analytical number 1, 5-6 and 9 represent mafic granulite rocks, 2-4 and 7-8 represent garnetiferous granulite rock and 10-12 represent hornblende pyroxenite rocks.

Cr and Ni show negative correlation with SiO_2 from both units while Cu, V and Nb show weak positive correlation in all units (Fig. 41).

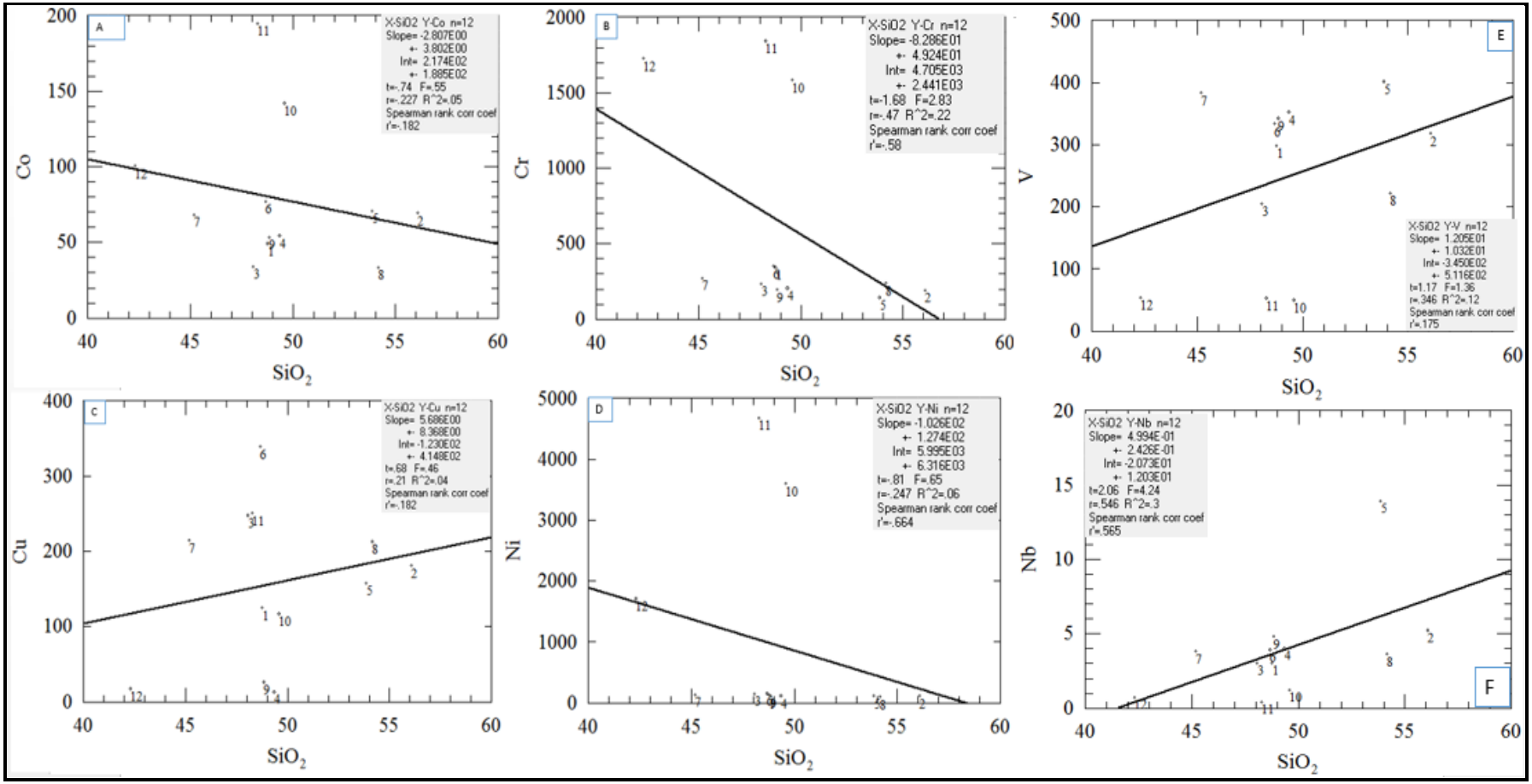

Figure 41. Trace elements variation diagrams (after Carr, 1995) as related to bulk rock composition. Lithological units are represented by analytical numbers: 1- 4 mafic granulite, 5-9 garnetiferous granulite and 10-12 hornblende pyroxenite.

In summary, the rocks from Handeni project are categorized by fine to coarse grained, intermediate to mafic rocks, which were highly affected by metamorphism. Mafic rocks include the MGr, GGr and HP units while an intermediate rocks include GSil and QFGn units. Major minerals dominating the assemblages are pyroxene, amphiboles, plagioclase garnet and disseminated sulphides. Sulphide minerals include pyrite, pyrrhotite, chalcopyrite, gersdorffite and pentlandite. Alteration minerals developed as calcite, sericite and dolomite. Few accessory minerals such as ilmenite and titanite also occur. The sulphide minerals such as pentlandite, gersdorffite and pyrrhotite as well as rare silicate minerals have characteristics of magmatic segregation. This has been observed from positive trace concentrations of Ni and Co.

Two suggestions have been proposed regarding the protolith of the rock based on the major composition and trace elements concentration of the bulk rock, petrology and mineralogy of each unit: i) these rocks are either of basaltic composition based on Le Bas *et al* (1986) TAS classification or ii) characterized as pelitic rocks based on Eskola (1939) classification of metamorphic rock' point of view. It is important to note that, pelitic rocks have high alumina. It is difficult to be conclusive without considering the effect of the intense metamorphism affecting these rocks, as outlined in chapter seven's discussions.

CHAPTER 7 DISCUSSION

7.1 INTRODUCTION

Chapter eight discusses the results of the geochemical analysis, petrology, mineralogy and rock composition as well as the metamorphism related to the minerals present in these rocks. The relationship between gold occurrences and the mineralization found within these rocks at Handeni district (Handeni project) will also be discussed.

7.2 MINERALOGY AND PETROLOGY OF HOST ROCKS

7.2.1 Mineralogy of the key lithological units

The key units of the Handeni project are characterized by the following minerals: i) silicate minerals include pyroxene, hornblende, plagioclase, garnet and quartz, ii) sulphide minerals including pyrrhotite, pyrite, chalcopyrite and gersdorffite. Minor and accessory minerals also present in these rocks include biotite, ilmenite, titanite, pentlandite, arsenopyrite, magnesite as well as calcite and dolomite (alteration minerals).

The following mineral assemblages can be deduced from the above minerals:

i) Pyroxene – Hornblende - Plagioclase – Garnet $\pm$ Sulphide + Quartz commonly found in garnetiferous amphibolite/granulite rock.
ii) Pyroxene - Hornblende - Magnesite $\pm$ Sulphides $\pm$ Biotite $\pm$ Plagioclase $\pm$Ilmenite $\pm$ Titanite commonly found in Hornblende pyroxenite rock.
iii) Quartz – Feldspar- Amphiboles $\pm$ Biotite $\pm$ Sulphides $\pm$ Garnet commonly found in Quartzofeldspathic gneiss rock.
iv) Garnet – Silica (Plagioclase + Quartz) $\pm$ (Hornblende + Biotite) commonly found in Garnet Silica rock.

7.2.2 Petrology of the host rocks

The mineral assemblage, pyroxene (clinopyroxene and orthopyroxene), amphibole (hornblende), plagioclase and garnet form the major mineral composition of the analyzed rocks. Based on this assemblage, five rocks types could be postulated from the petrology study namely: i) Garnetiferous granulite - GGr, ii) Garnetiferous amphibolite (mafic granulite) - GA iii) Hornblende pyroxenite - HP, iv) Garnet silicified rock – GSil and v) Quartzofeldspathic gneiss - QFGn.

Disseminated sulphide minerals are distributed throughout the rocks. Rocks rich in garnet are commonly characterized by well disseminated sulphide minerals. Whereas, those characterized with less abundant or no garnets are characterized by sporadic disseminated sulphide minerals, excepting the hornblende pyroxenite, which is characterized by well disseminated sulphide minerals despite lack of garnet minerals. Four major host rocks are identified in the Handeni project: garnetiferous amphibolite, garnetiferous granulite, garnet silicified rock and the hornblende pyroxenite.

Quartzofeldspathic gneiss is the thickest and most prolific unit in this area with less economic importance and can be categorized as country rock. Other units are of more economic importance with regard to the contents of sulphide minerals and gold recovered. These are garnet silicified rock, garnetiferous amphibolite, garnetiferous granulite and hornblende pyroxenite. These units overly the quartzofeldspathic gneiss, but due to extensive deformations including folding and faulting, it is difficult to maintain the stratigraphic sequence.

Garnetiferous granulite has abundant pyroxene whereas the garnetiferous amphibolite is rich in hornblende minerals. They both are characterized by disseminated sulphide minerals dominated by pyrrhotite, chalcopyrites and pyrites. Garnetiferous amphibolite and garnetiferous granulite are comprised of major and minor minerals including pyroxene, hornblende, plagioclase, quartz and garnet and occasionally biotite. They are the major host rocks (for gold) which are characterized with the occasional intrusion of quartz veins and stringers.

Garnet silicified rocks exhibit massive structure, fine to medium grained texture, and are characterized by disseminated sulphide minerals. Sulphides include pyrrhotite, chalcopyrite, pyrites, arsenopyrite and occasionally gersdorffite. Other major minerals include, garnet, quartz, plagioclase occasionally disseminated hornblende. GSil rock develops in between the quartzofeldspathic gneiss and the garnetiferous amphibole or granulite.

Hornblende pyroxenite is the magnesium rich rock composed of pyroxene, hornblende, magnesite, and plagioclase and disseminated sulphides. Pyrrhotite, chalcopyrite, pentlandite and gersdorffite are commonly sulphide minerals in these rocks. Occasionally biotite and quartz are developed. HP rock exhibits the primary magmatic characteristic with high abundance of base metals including Ni, Cr and Co, sporadic pyrite has been developed in this unit.

Hence, the Handeni project is characterized by the major four hosting rocks, Magambazi East dominated by garnet silicified rock, garnetiferous amphibolite and garnetiferous granulite, whereas the Kwandege project is dominated by the same rocks as Magambazi East as well as hornblende pyroxenite rocks.

7.3 PROTOLITH RECOGNITION

7.3.1 Bulk Rock Geochemistry

The Handeni project area geology is dominated by mafic to intermediate rocks of basaltic compositions. Considering the whole rock geochemistry, petrology and mineralogy results from this research showing that these rocks are characterized by the mineral assemblage; gersdorffite, pentlandite, pyrrhotite, pyroxene, magnesite, ilmenite, titanite, garnet and plagioclase which are the characteristic of basaltic rocks.

On the other hand, the mineral assemblage biotite, garnet (almandine), plagioclase, quartz, oligoclase and occasionally sillimanite or kyanite, is the common assemblage in pelitic rock (Malisa and Muhongo, 1990). Sillimanite and kyanite minerals develop in quartzofeldspathic gneisses rocks, which were not analyzed by XRF due to their inhomogenous nature.

Based on these two subsets of mineral assemblages and the fact that these rocks were affected by high grade metamorphism, three suggested mineral assemblages can be deduced from the available minerals:

- Pyroxene (clinopyroxene and orthopyroxene) – plagioclase – garnet – hornblende – quartz $\pm$ biotite $\pm$ sulphides (Basaltic assemblage).
- Hornblende – magnesite – pyroxenite $\pm$ sulphides $\pm$ biotite $\pm$ plagioclase (Basaltic assemblage).
- Garnet (almandine) – plagioclase (andesine + oligoclase) $\pm$ biotite (oligoclase) - quartz and occasionally sillimanite or kyanite which suggest similar assemblage as pelitic rocks of sedimentary origin or sediments from metamorphosed basalt.

According to Le Bas *et al* (1986) on the total alkali silica (TAS) classification of the igneous rocks, three rocks types of basaltic origin are suggested namely basalts, basaltic andesite and picro basalt (Fig. 42) from the normalization of the major element results. This classification has been done at the water free basis and normalizing to 100.

MGr and GGr have an average magnesium number (Mg#) of 44.53 whereas the Fe^{3+} - Fe^{2+} ratio is at an average of 1.10 and its Fe-Mg ratio of about 2.07 (Table 13). These three aspects reveal that, these rocks related to mafic and ultramafic intrusive, which support the suggested Le Bas *et al* (1986) classification as they have similar characteristic as basaltic rocks. It is important to note that basalt has equivalent chemical composition as gabbro, both have the same basaltic chemical composition (Babievskaya *et al* 2011). The main difference is by grain sizes, gabbro (phaneritic) and basalt (aphanitic) (Winter, 2001).

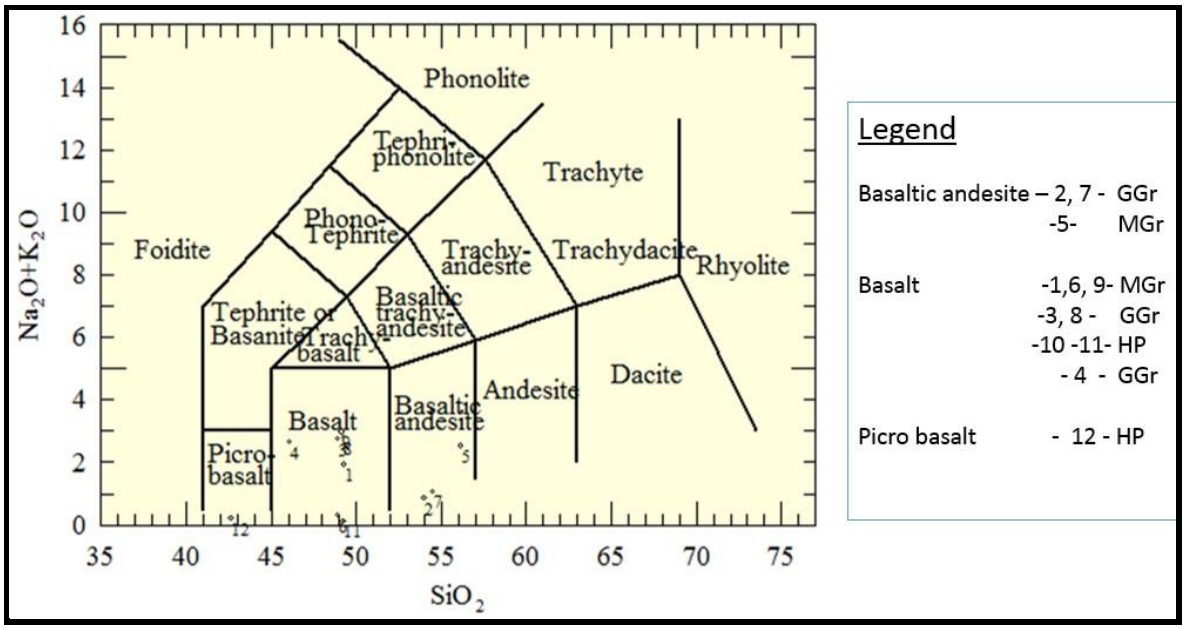

Figure 42. TAS diagram classification of the bulk rock composition from Handeni project rocks (after Le Bas et al, 1986). Numbers from the legend represent analytical units, hornblende pyroxenite-HP, garnetiferous granulite – GGr and mafic granulite – MGr (GA).

7.3.2 Parageneses and metamorphic events

Based on the microscope observations and geochemistry results of the analyzed rocks, silicate minerals crystallized first followed by sulphide minerals. The sequence could be proposed as follows: pyroxene crystallized first followed by the amphiboles (hornblende), plagioclase as the late stage of crystallization followed by garnets minerals. Sulphide minerals crystallized later following the crystallization of quartz or plagioclase in the margins of pyroxene and amphiboles and occasionally as inclusions (Fig. 27).

Chalcopyrite crystallized earlier followed by gersdorffite then pyrrhotite (Fig. 28), also, the research suggests that pyrrhotite and pentlandite crystallized at the same time. Figure 22 shows a good inclusion of chalcopyrite in pyrrhotite. The proposed sulphide crystallization sequence could be: chalcopyrite crystallized earlier followed by gersdorffite, gersdorffite followed by

the crystallization of pyrrhotite (Fig. 43) and pentlandite (Fig. 22 and 28). Commonly carbonate minerals are the products of mineral alteration due to the effect of metamorphism in the region.

According to the parageneses of the minerals above and the whole rock chemical characteristic of the analyzed rocks, a proposed petrogenetic sequence will be: basalt as the early formed crust, followed by the late intrusion of igneous rocks (intermediate to mafic rocks) and then overlain by sedimentary rocks derived from the oceanic basin sediments before the onset of metamorphism.

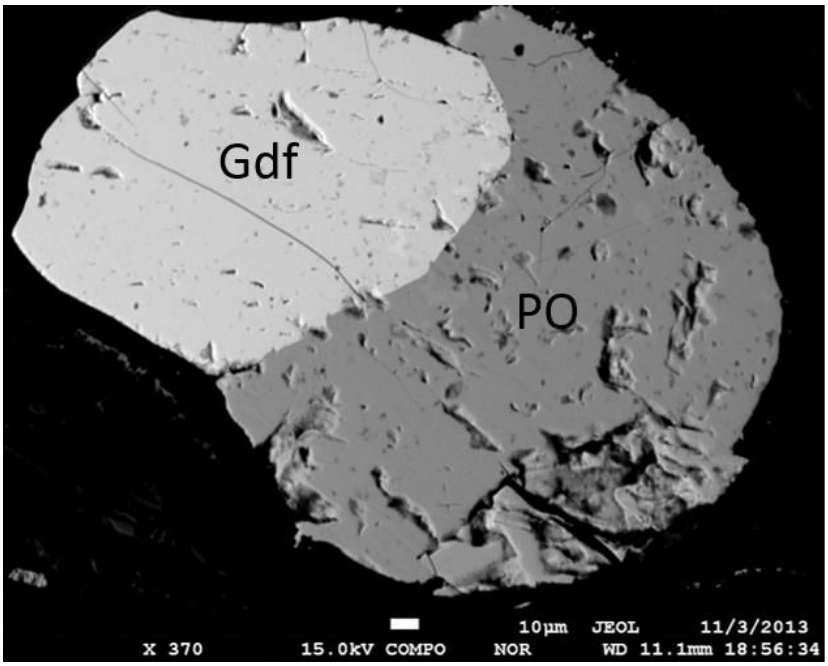

Figure 43. Backscatter electron image taken at 10 micron of 370 X magnification (JEOL) showing the crystallization of gersdorffite (Gdf) earlier than pyrrhotite (Po) in hornblende pyroxenite rock. The rimmed sulphide suggest that it existed prior to the metamorphism of the silicate minerals surrounding it.

Three phases of events were related to the metamorphism of the Usagaran belt. First phase was during the intrusion of the Archaean rocks into Tanzania Craton at approximately 2550 Ma ago (Moller *et al*, 1995). It is important to note that the Usagaran belt is located east of the Tanzania craton and west of the MB. Thus the metamorphosed product from Archaean rocks were founded in Usagaran belt as well as in MB, which are related to the emplacement episodes associated with these belts (Reddy *et al*, 2003).

The second phase of regional metamorphism in the Handeni area is related to a subduction event occuring during the early Proterozoic dated > 1.9 Ga which resulted in the formation of

the Usagaran belt, followed by plate convergence and subduction of the oceanic plate. The evidence of eclogites (Moller *et al*, 1995) reflect the occurrence of high grade metamorphism, probably from a mafic rocks typically of basaltic origin. The third phase of regional metamorphism occurred during the Pan African (Neoproterozoic) event which is related to the orogenic belts and the whole MB and Gondwana break up and its assembly. During the Gondwana assembly between 510 and 570 Ma following the Pan African tectonothermal event which affected the emplacement of MB (700 – 800 Ma) resulted to metamorphism dated between 615 and 650 Ma (Moller *et al*, 1995, Stern 1994 and Moller *et al*, 2000).

Thus, reviewing from the first phase of metamorphism to the third phases, one can suggest that the area was subject to low to high grade metamorphism. The mineral assemblage contains, hornblende-plagioclase-quartz – biotite- titanite- pentlandite found in GGr, MGr and HP, which suggests a magmatic minerals assemblage (Vyhnal *et al*, 1991). Also, the sulphide mineral assemblage of: chalcopyrite gersdorffite – pyrrhotite – pyrite and the associated pentlandite show typical characteristics of hydrothermal fluid. Thus, hydrothermal related minerals commonly developed in low grade metamorphic facies. The rimmed sulphides features suggest the re – metamorphism of the metamorphosed units.

7.3.3 Metamorphic Assemblages

Based on the mineral assemblages presented in section 3.3.1 of the rocks analyzed from the representative units in this thesis, a metamorphic facies series is deduced based on mineral content (Spear, 1993) and (Winter, 2001). Hodgson (1993) recommended that alteration zones such as progressive carbonatization, reflect the metamorphic facies with regard to the fluxes of heat. The presence of calcium silicate minerals (amphibole, diopside, garnet and calcite) reflect the high temperature facies whereas sericite and occasionally biotite reflect an intermediate temperature phase.

Thus, the two proposed metamorphic facies assemblages encountered in this area are;

- Amphibolite facies associates with hornblende + plagioclase (includes oligoclase $\pm$ andesine) + garnet + quartz, which involves these rocks: quartz feldspathic amphibolite gneiss, garnetiferous amphibolite and garnet silica rocks.
- Granulite facies, from the geothermobarometry calculations between garnet and pyroxene after (Ganguly, 1979), an average of 738 ^{o}C at 8 kb deduced. Therefore a granulite facies from the analyzed rocks are associated with pyroxene (orthopyroxene

and clinopyroxene) + hornblende + plagioclase ± garnet, which involve the garnetiferous granulite, hornblende pyroxene and garnetiferous amphibolite rocks.

7.3.4 Metamorphism

Two metamorphic facies series are encountered in these rocks as mentioned in previous section. These facies series would be presented in consideration of the two principal minerals being representative of all the units in this thesis, namely plagioclase and pyroxene. They are commonly distributed in all of these units.

According to Winter (2001) and Spear (1993), plagioclase rich in sodium is stable under low temperature and calcium rich plagioclase is stable under high temperature and vice versa, whereas increasing the temperature in amphibole (actinolite) simultaneously increases aluminium and alkalis as it loses water (becoming anhydrous) then it produces orthopyroxene and clinopyroxene:

- Albite ==> Oligoclase ==> Andesine implies a reaction occurred from low to high temperature.
- Pyroxene ==> Chlorite ==> Actinolite ==> Hornblende ==> Clinopyroxene and Orthopyroxene, this implies a reaction occurred from low to high temperature.

Thus, more Ca rich plagioclase, became stable at high temperatures and vice versa. Considering the presence of oligoclase, andesine and labradorite from the analyzed rocks, this implies that, albite was stable at low temperature (low grade), as temperature increased it attained more Ca either from calcite or titanite while decreasing in sodium until it become stable (Fig. 34). Refer plagioclase in the garnetiferous amphibolite and the garnetiferous granulite (Fig. 44) from the study area. Rock X at low temperature, Y intermediate (amphiboles rocks) and Z at high temperatures (granulites rocks). This reflects the metamorphism of the analyzed rocks.

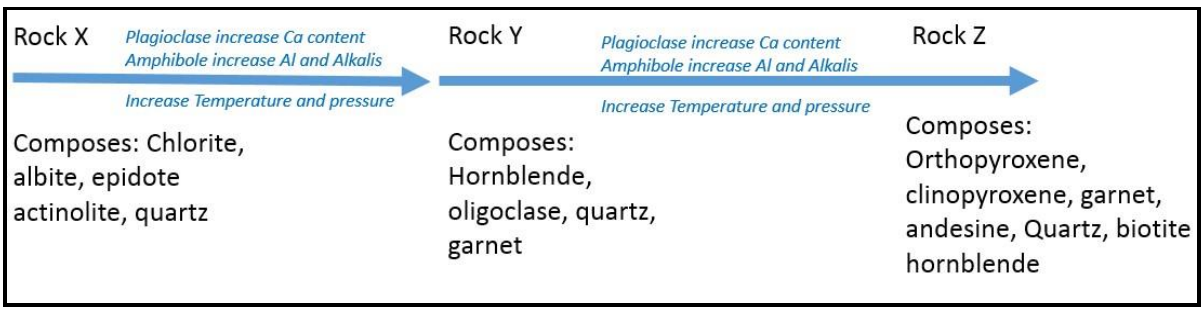

Figure 44. Schematic diagram showing the metamorphic sequence from greenschist to granulite facies, whereas rock X is in greenschist facies (not available in Handeni project), Y

is in amphibolite facies (represent GA, GSil and QFGn rocks) and Z in granulite facies (represent GG, GA and HP rocks) after (Winter, 2001 and Spear, 1993).

7.3.5 Protolith characterization

The bulk rock geochemical results (major and trace elements), petrology and mineralogy pave the way to the characterization and classification of the rocks comprising the Handeni area geology. The mineral composition of these rocks is related to igneous rocks with basaltic characteristics of either basalt or gabbro rocks. Commonly minerals used in discussing the characteristics of the protolith are plagioclase, pyroxene, garnet and amphiboles.

Andesine, which is the common plagioclase minerals in these rocks developed in both basalt and gabbro rocks. Labradorite and oligoclase are minerals commonly developed in gabbro rock and occasionally in basalt rock. Ozerov (2000) argued that plagioclase can be found as phenocrysts in basalt rocks whereas in gabbro it is found as a coarse grained groundmass, which is charachterstic of the analyzed rocks from the Handeni project.

The presence of pyroxene minerals including diopside (Ca rich pyroxene mineral) and enstatite (Mg rich pyroxene), are developed in gabbro or basalt rocks. In basalt rocks, commonly augite, pigeonite or occasionally orthopyroxene are present, but are not well developed in the analyzed rocks. In the Handeni project area, most of the analyzed rocks are characterised by the presence of diopside and enstatite (clinopyroxene and orthopyroxene) which are the pyroxene minerals developed in gabbro rocks.

Based on the bulk rock geochemistry, these rocks commonly contain high Si, Fe and Mg. They show an average magnesium number (Mg#) of 44.53 for the mafic rocks of garnetiferous amphibolite and garnetiferous granulite, which ranges from 31.6 to 52.38 and about 85.04 for the hornblende pyroxenite (Table 13). These show the relationship on how the magma evolved in relation to basaltic rocks.

The host rocks (garnet silicified rock, garnetiferous granulite and garnetiferous amphibole as well as hornblende pyroxenite) exhibit a brittle - ductile - brittle deformation structure as evidence with no micro foliations or folding developed during the event of deformations. The brittle structure of these rocks lead to the fracturing and flow of fluids which commonly resulted in the development of the alterations minerals (calcite and silicification), quartz veining and stringers. These are suggested to be characteristic of mafic to intermediate intrusive

rocks. The presence of magmatic minerals such as pyrrhotite, gersdorffite, pentlandite, pyroxene, magnesite, quartz, plagioclase and rare biotite, ilmenite and titanite, signify the characteristics of magmatic equilibrium (Vyhnal *et al*, 1991).

With regards to metamorphism, the analyzed rocks from Handeni project exhibit the amphibolitic to granulitic metamorphic facies (prograde metamorphism). The documented eclogite rocks in Usagaran belt dated 2 Ga (Reddy *et al*, 2003;2004), suggests a high grade metamorphism of either gabbro or basalt rocks. Hornblende is the dominant amphibole mineral present in these rocks, which is the most important constituent formed by metamorphism of basalt or gabbro rock. Almandine is the end member, iron rich garnet developed in eclogite as well as after metamorphism of a basaltic rocks.

The evidence of deformation (fold, fault, fracture and shearing) shows that these rocks underwent a series of metamorphic processes from low to high grade. Quartzofeldspathic gneiss shows strong foliations with micro to macro folding including sheath folding while the garnet silicified rock, garnetiferous amphibolite, garnetiferous granulite and hornblende pyroxenite show micro and macro fracturing replaced by silica- and occasionally sulphides and alteration minerals.

7.4 MINERALIZATION

7.4.1 Ore Minerals and Source of Mineralization

Gold mineralization in the Handeni project area's rocks is developed as free blebby gold in association with the following ore minerals: arsenopyrite, graphite and chalcopyrite as well as number of gangue minerals including quartz, plagioclase and K-feldspar with rare orthopyroxene and phlogopite. Other ore minerals include pyrite, pyrrhotite, chalcopyrites and occasionally carbonates and alteration minerals develop (Scheepers, 2010). Traces of base metal mineralization can be found in association with pyroxene, hornblende, plagioclase, pyrrhotite, pentlandite, and chalcopyrite.

Two possible models of the origin (source) of gold related to the geological settings are proposed below:

- Gold and sulphur were intracrystalline and mobilized from magmatic sulphides by the reaction of seawater with hot lava or they have been mobilized from the lower crust during a late granulitisation event and concentrate in the supercrustal domain like Lupin and Hemlo in Canada (Saager and Meyer, 1984 and Colvine *et al*, 1988). The presence

of magmatic minerals develop in the Handeni rocks like pentlandite, gersdorffite, pyrrhotite, pyroxene, magnesite, quartz, plagioclase, ilmenite, titanite and biotite, which commonly develop in low to medium metamorphic grade affected by extensive deformations, which resulting to high grade metamorphism. This is related to remobilization of current ore fluids in high metamorphic grade (reworked).

- Gold has been mobilized by hydrothermal fluid flow during the low to medium grade metamorphism from the crust by upwell of the saline water through the fracture zones caused by the deformation event and re-metamorphosed to high grade by the second event resulting in amphibolite and granulite domains like in Yilgram block in Australia (Ridley *et al*, 1995). The quartz veins carrying gold mineralization in handeni project are related to low grade metamorphic, which have been affected by deformation resulting to high grade metamorphism. These have been evidenced by occasionally thin discontinuous quartz veins (Figure.20) developed in the amphibolite and granulite units develop in Handeni area, which can be related to that of Yilgram block.

7.4.2 Ore Composition

The ore rocks from the Handeni project are mafic rocks exhibiting high Fe content and high Fe - Mg ratios, which are similar to those found in the volcanic rocks of greenstone belts. They are commonly comprised of garnet, amphiboles, pyroxene, quartz, plagioclase and their associated sulphide minerals including pyrite, pyrrhotite, chalcopyrite gersdorffite and pentlandite and occasionally arsenopyrites and carbonate minerals.

7.4.3 Mineral Alterations

According to Rose and Burt (1979) mineral alteration is the change in chemical composition of the mineral to more stable conditions in response to fluctuation of the PTx with the presence of the fluids. Fyfet *et al* (1978) proposed three sources of alteration fluids i) hydrothermal fluid derived from the prograde devolatilization of the rocks, ii) metamorphic fluid commonly derived from the dehydration reaction and / or mobilization of pore fluids and intergranular fluids films resulting in metamorphic fluid in low to medium grade metamorphic terrane, iii) magmatic fluid generated when silicate magma reaches vapor saturation and a vapor phase exsolves from the silicate melt and crystals systems.

Two common types of alteration have been encountered in the Handeni project rocks; carbonatization and silicification. Thus, considering the different phases of metamorphism occurring in the area, the alterations of carbonatization type are associated with the replacement

of the magnesite resulted to dolomite and calcite minerals. Dolomite and calcite are commonly encountered in garnetiferous amphiboles and garnetiferous granulite as well as in hornblende pyroxenite rocks. Silicification; silica increases in modal quartz, quartz veinlet, or quartz stringers and occasionally quartz veining, which are commonly developed in garnetiferous amphiboles, garnetiferous granulite and garnet silica rocks. Occasionally plagioclase altered to sericite, however neither oxidation nor alkali metasomatism have been developed in those analyzed samples.

7.4.4 Timing of Mineralization

The timing of mineralization in this area is most likely related to gold mineralization and the host rocks in terms of deformations, alterations, metamorphism grade and the protolith of the rock. Colvine *et al* (1988) proposed that concentration of gold is related to major tectonic events as well as the possibility of the re-concentration during much later tectonism. Also, Groves *et al* (2000) argued that if the area is affected by regional metamorphism, plutonism and early phases of orogenic deformation in the immediate host rocks, mineralized gold veins were developed at a later stage.

The occurrence of native gold and other sulphide minerals, in a narrow discontinuous quartz veins or stringers (high Fe or Mg rich rocks) of mafic to ultramafic rocks as suggested in previous subsections, are related with mineralized fluid derived from hydrothermal fluid infiltration. From the concentration of the major elements (Table 13), it can be deduced that the host rocks were able to dehydrate and de–gas without the loss of metals during the gradual increment of the temperature and pressure.

The high Fe and Fe/Mg ratios increase the ability of gold precipitation in a low temperature environment. Therefore, gold mineralization in these rocks is related to early precipitation (low temperature environments) before the rocks were re-metamorphosed to high grade metamorphic rocks of amphibolite to granulitic facies. Although the alteration minerals of these rocks does not show any relation of metamorphic overprint but are rather related to retrograde metamorphic assemblages (garnet-hornblende-carbonate/calcite).

The presence of alteration minerals (calcite, sericite and dolomite), sulphide minerals (chalcopyrite, pyrrhotite, gersdorffite) and the positive correlation between Zn and Co represent the relation with hydrothermal fluid. This suggests a relationship of gold mineralization and hydrothermal activity that developed during and after peak metamorphism.

Colvine *et al* (1988) suggested that, if the mineralized fluid was of metamorphic origin it originated from a higher grade metamorphic terrane, specifically the zone of granulitisation.

In summary, the Handeni project is characterized by mafic volcanic rocks. These rocks are composed mainly of garnet, pyroxene, hornblende, plagioclase, quartz and occasionally biotite, carbonate and other minor and accessories minerals. These rocks exhibit medium to coarse grain texture and massive to granulitic structure. The area characterized by four host rocks namely: garnet silicified rock (GSil), garnetiferous amphibolite – GA (which previously mentioned as MGr), garnetiferous granulite (GGr) and hornblende pyroxenite (HP), which are of igneous mafic intrusive of basaltic composition (gabbro).

The area has been affected by numerous phases of metamorphism both contact (thermal) and regional metamorphism. Regional metamorphism caused by the tectonic events including the intrusion of Archaean Tanzania Craton (3 Ga) to the continental crust and other series of younger tectonic events. These younger events include the formation of Usagaran belt after the subduction of oceanic plate (1.9 Ga), the whole of Pan African (650 – 620 Ma), formation of Mozambique Belt (700 - 800 Ma), and the whole of the Gondwana events (510-570 Ma). Regional tectonic events resulted in different deformation features including folds, shears and faults. The basaltic rocks from Handeni project show a relationship with other fragmented rocks from the Archaean Tanzania Craton. These fragments from the eastern part of Archaean Tanzania Craton were re-metamorphosed (reworked) following the subduction of the oceanic plate. These rocks are characterized by micro and macro deformation features as well as rimmed minerals, which supporte the hypothesis of re-metamorphism.

The magmatic, sulphide-carrying gold mineralization intruded the low grade metamorphosed rocks during a period of contact metamorphism (Grove *et al,* 1998), which was as a result of the intrusion of the Archaean Tanzania Craton (2.5 – 3 Ga) to the crust. Mineralization in this area is associated with sulphide minerals, quartz, garnet and mafic minerals. It is associated with low grade metamorphic terrane related to hydrothermal fluid. Occasionally intrusion of quartz veins show the late crystallization of quartz which are fairly related with hydrothermal flow, sporadically these veins carry gold mineralization. This suggests that, gold were mobilized and precipitated in long/thick quartz vein during the low grade metamorphism, then re-mobilized by high grade metamorphism which is later precipitated in discontinuous thin quartz veins develop between the margins of graphitic (reduced environment) and

amphibolite/granulite units. Also, occasionally free gold precipitate in garnet quartz or/and amphibole/granulite units.

CHAPTER 8 EXPLORATION

8.1 INTRODUCTION

This chapter reviews gold exploration program conducted in the Handeni project area in its entirety and reflects gold deposition during the low grade metamorphic phase as well as gold deposition occurring as rocks were re metamorphosed by later events. Exploration methodologies applied, exploration significance with regards to gold deposition in high grade metamorphic terrane as well as proposed targets parameters *for* future exploratory approaches are included. The following exploration methods will be discussed in this section namely: geological mapping, remote sensing, geophysical survey (airborne and ground), regional and local structures and geochemical surveys.

8.2 GEOLOGICAL MAPPING

In any exploration program the desktop study and literature review is the cornerstone for evaluating an area for mineral prospecting. This will be followed by ground evaluation survey and geological mapping for reconnaissance survey before conducting a more detailed geological survey. Mapping forms the foundation of exploration, by collecting basic information including the kinematics of structures, mineral characteristics such as metal associations and timing of mineralization, alteration patterns and the locations of the known gold occurrence such as old working pits.

Geological mapping of the entire prospect area of the Handeni project was not well achieved, due to the fact that the prospects are characterized by dense vegetation and thick regolith cover, which results from the heavy rainfall and hinders many of the outcrops. That factor contributes to the difficulties in conducting a geological mapping program at a regional scale. As the result, this leads to lack of identification and delineation of lithologies of different compositions and competency. Besides, only interested selected areas from the geophysical data were mapped in detail. At some point, the structure framework within the Handeni project becomes difficult, thus the use of remote sensing data, geophysical data interpretation and satellite images becomes useful in interpreting the geological outlay of the area.

8.3 REMOTE SENSING

Remote sensing (Landsat and radar images) and other satellite imagery interpretations are useful tools in supporting exploration program especially for the area covered by thick

vegetation. The identification and mapping of regional and local fracture patterns as well as the hydrothermal altered rock associated with many ore deposits can be interpreted by using remote sensing data (Sabins, 1999).

In a regional scale, the satellite imagery is important in identifying the lithological boundaries such as the distribution of granitoid and against the greenstone, linear features and other structural significant features. It is important in areas with intense deformation and stronger tectonic uplift and generally regional structural evolution such as at Handeni project. Mallet (2009) suggested some common features used in processing the satellite imagery data for structural interpretations:

- Single band 5 composite imagery suitable edge enhanced and contrast for topographic and tectonic features,
- False color composite imagery using bands 1-4-7 with equally filtered and stretched for the topographic expression and the highly reflective granitoid and felsic volcanic areas. False color 4-1-7 composite imagery, which can provide better visual contrasts than 1-4-7 and
- False color decorrelation stretch imagery using components 4-5-6, which are commonly used in differentiating between the greenstone belt and the granitoid.

Sabins (1999) suggested that digitally processed Landsat thematic mapper (TM) can be used to identify alteration minerals in relation to hydrothermal deposit. Altered minerals include iron and clays minerals as well as alunite. Also the hydrothermal zoning can be related with species of iron and clay minerals following the interpretation of hyperspectral images. Both TM and hyperspectral imagery cannot provide better interpretation of silicification alteration. This also reflects to other minerals like quartz, even quartz veins have no diagnostic spectral features in the visible and reflected IR wavelength by these systems. Silica content could be recognized by the multispectral thermal IR images.

The use of remote sensing (satellite imagery, radar imagery), recognition of alteration assemblages, and interpretation of regional and local structure could be of more significance. This can be done by combining the geological mapping and the interpretation geophysical data especially in an area like Handeni district.

8.4 GEOPHYSICS

Following the geological mapping and the remote sensing data, the use of geophysical methods is an essential tool for regional exploration. This will help to narrow the prospect and enhance the interpretation of the structures and induced structures for mineralization, commonly in the area where there is thick vegetative cover. Different methods were employed on the Handeni project including airborne and ground geophysical surveys using electromagnetic (EM), induced polarization (IP), as well as magnetic and radiometric surveys. The first phase involved a regional geophysical survey at high resolution of 200 m line spacing and 80 m flight height with N – S direction. It was done by the fixed wing Cessna 210 conducted by the Council for Geosciences of South Africa, followed by a second phase involving ground magnetic, EM and IP surveys (Scheepers, 2010).

Significant outcomes with regards to these methods utilized on the Handeni project were the organization and identification of the structures, conductor minerals and mineralised zoning. The EM survey was successful in the identification of conductor anomalies, which are related to disseminate sulphide mineralization or graphitic zones where they possibly intersect the structural anomalies. IP was used in the area where mineralization is related to massive sulphide, graphite and some oxide which potentially shows good electrical conductivity.

Commonly, major and minor structures and preferred structural sites related to mineralization were identified and delineated subsequently to the interpretation of magnetic data collected during both airborne and ground magnetic surveys. Radiometric surveys were also conducted and data were interpreted even though it was not possible to recognize the lithological units and other alterations due to intensive deformation, however the areas showing high potassium correlated well with other structural features.

8.5 STRUCTURE

The Handeni project has been affected by intensive deformation resulting in many structural features including folding (open folds, syncline fold and sheath folds) on macro and micro scales, faults and shearing as well as brittle – ductile features. Groves *et al* (2000) suggested that near the large scale structure, deposits are normally placed in second and third order structures commonly transcrustal first order compressional or transpressional structure. Even though mineralized structures are characterized by the syn- and post- mineralization displacement commonly gold deposit have plunge extended downward.

Groves *et al* (2000) proposed four types of structural features associated with ductile - brittle controlling structures in relation to gold deposits in deformed areas, these are:

- Foliation zones
- Ductile turbidite sequences on the fold hinges and overturned limbs.
- Stockwork network or breccia zones in competent rocks or fracture arrays.
- Brittle faults to ductile shear zones with both low angle to high angle reverse motion and strike slip or oblique slip motion.

The above structural features need to be considered in the deformed area like Handeni although the variations in high pressure could lead to cyclic fault value behavior resulting in flat – lying extensional veins and equally cross-cutting steep fault vein.

8.6 GEOCHEMISTRY

Geochemical surveys play a major role in mineral exploration. They assist in delineating the mineralized area, initial indicator of mineralization grade and the most significant is the indication of pathfinder elements in relation with the mineral of interest. Geochemical surveys should be deployed after the interpretation of remote sensing, geophysical data and geological mapping. This involves different sampling methods within different soil media and is conducted via soil sampling, grab sampling, trenching, pitting and producing rock chips (drilling).

Geochemical soil sampling is preferred in areas covered by the superficial deposits following the orientation surveys. These include:

- The landscape analysis (to be aware with insitu or transported media)
- Alluvial soil will give false anomalies,
- Sampling media (soil horizon, stream or laterite),
- Evaluation of analytical procedures and facilities
- Determination of the indicator elements (pathfinder elements).

Soil sampling should be conducted in phases after the orientation survey. Reconnaissance phase involves the identification of analytical method to be used, suggested initial batch of sample to be analyzed by mobile metal ion (MMI) to determine the spatial distribution of elements and better analytical method to use. Therefore, the following phases of detail soil sampling will be organized.

Groves *et al* (2003) recommended the assaying of a broad spectrum of mineralization related elements including Au, Ag, As, W, Mo, Sb, Cu, Pb, Zn, Ba, Bi, Cr, Co, Ni, Ti, V and Sc will give the indication of the pathfinder elements relating to the mineralization (gold). Knowing the geology (rocks type, alteration minerals) of the area will also save the analysis cost by analyzing the expected minerals forming the rocks. Handeni project is characterized by mafic intrusive rocks of gabbroic origin which intensely affected by deformation and metamorphism.

Analyzing for Au, Ag, As, B, Bi, Pb, Zn, Cu, Sb, Te, W, Cr, Co, Ni, Ti, V and Sc will give a wide range information in relation to hydrothermal and magmatic with regards to gold mineralization. Following the positive results from soil sampling from both phases (reconnaissance and details survey) with the combination of geophysical and remote sensing data, the anomalous area will be identified and trenching or pitting will be deployed to study or confirmed the bed rock and structural studies prior to drilling. Trenching will establish the extent length, width and grade of mineralization. Also, it is a useful tool in mapping lithologies structures and alterations zones. Drilling provides potential information which is related to mineralization, alteration (fresh minerals) and lithological studies in vertical section (sequence). It is the useful tool in 3D geological modelling and resource calculations as well as reserve estimation.

Based on the XRF analysis for the bulk rock of the rocks analyzed in this research from Handeni project, there is good correlation (table 15) > 0.7 such as Co with Cr or Ni, Cr with Ni, V with Nb or Zr or Sr or Y. Also, good correlation at > 0.5 for Zn with Mo or Rb or Pb as well as Cu with Mo (Table 15). There are positive correlations between Ni and Co, whereas, Ni shows negative correlation with Mn and MgO (Fig. 45 and 46), which suggests that Ni is associated with sulphide mineralization. Therefore, this provides a clue that, the mineralization is sulphide related.

Table 15. Correlation of the bulk rock trace elements from Handeni project.

	Co	Mn	Cr	V	Zn	Cu	Ni	Mo	Nb	Zr	Y	Sr	U	Rb	Th	Pb
Co	1															
Mn	-0.56	1														
Cr	0.87	-0.80	1													
V	-0.67	0.82	-0.90	1												
Zn	-0.43	0.10	-0.36	0.14	1											
Cu	0.10	0.25	-0.12	0.05	0.32	1										
Ni	0.95	-0.70	0.92	-0.83	-0.31	0.03	1									
Mo	-0.26	0.12	-0.27	-0.05	0.61	0.58	-0.15	1								
Nb	-0.38	0.49	-0.60	0.70	-0.03	0.01	-0.51	0.17	1							
Zr	-0.62	0.73	-0.85	0.94	0.05	-0.07	-0.76	0.01	0.85	1						
Y	-0.68	0.79	-0.90	0.96	0.10	-0.03	-0.81	0.02	0.77	0.98	1					
Sr	-0.38	0.74	-0.59	0.75	0.00	0.19	-0.58	-0.34	0.16	0.54	0.62	1				
U	-0.08	0.05	-0.19	0.27	0.05	0.06	-0.14	0.30	0.82	0.45	0.33	-0.30	1			
Rb	-0.28	-0.17	-0.19	-0.08	0.73	0.23	-0.14	0.71	-0.07	-0.07	-0.08	-0.31	0.08	1		
Th	-0.35	0.21	-0.44	0.38	0.22	0.34	-0.37	0.57	0.77	0.49	0.42	-0.17	0.86	0.26	1	
Pb	-0.57	0.10	-0.41	0.12	0.73	0.20	-0.40	0.56	-0.01	0.08	0.17	-0.09	0.06	0.40	0.33	1

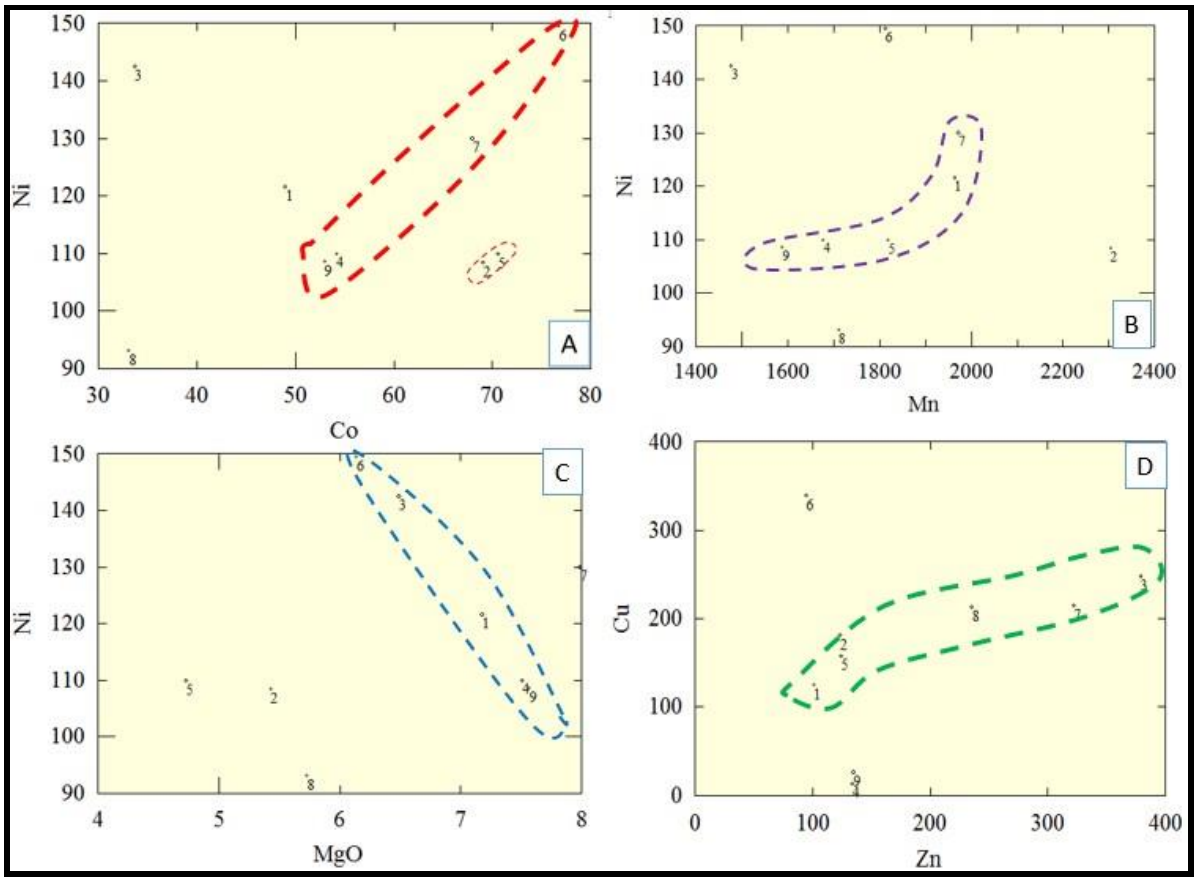

Figure 45.Correlation diagrams (after Carr, 1995) of trace elements from bulk rock analysis, 1-4 represent garnetiferous amphibolite unit and 5-9 garnetiferous granulite unit. Figures show A) magmatic signature, B) Mn savages Ni, C) sulphide mineralization and D) hydrothermal fluid signature.

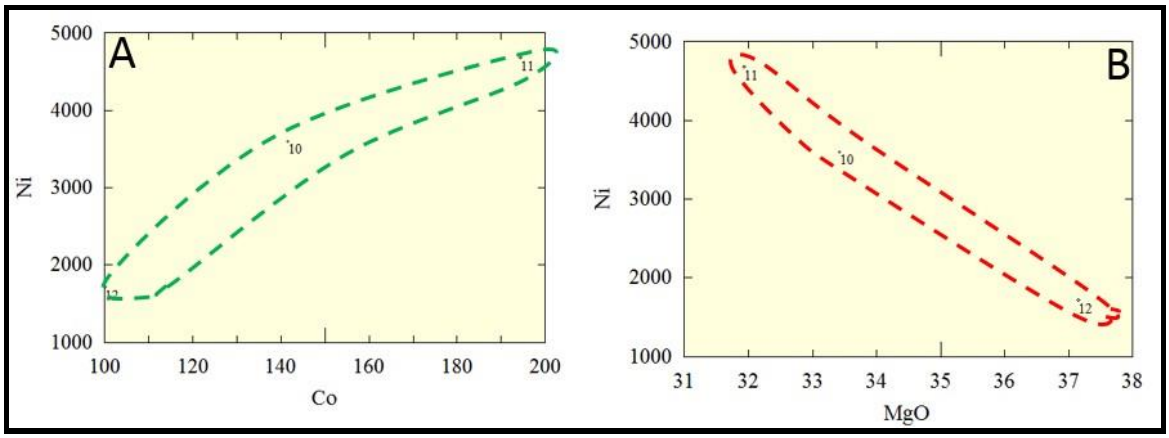

Figure 46. Trace and major elements correlation from bulk rock analysis. Figures (after Carr, 1995) shows A) Ni and Co represent a magmatic signature and B) Ni mineralization related with sulphide.

Different analytical methods were suggested for gold analysis during the exploration phase depending on the lithologies and mineralization types. These methods include MMI or ICP-MS for soil samples and ICP-AES for rock samples. For gold trace element analysis, bulk sample cyanide leach (BSCL) and mini BLEG will be suitable method after ICP-MS or MMI. Whereas for gold concentrations, the atomic absorption spectrometry (AAS) will be appropriate method after the ICP-AES (Levinson, 1974).

8.7 PROPOSED TARGET GENERATION

Various scholars (Groves *et al*, 1995; 2000; 2003; Barnicoat *et al*, 1991; Cox *et al*, 1979; Goldfarb *et al*, 2005 and Phillips *et al*, 2009) have conducted research on gold mineralization in metamorphic terranes from low to high grades. Groves *et al* (1995) suggested that in orogenic deposit, gold mineralization is sited in the lower order shears which may or may not show relationship with the large scale deformation zones although structures are the controlling factors.

Colvine *et al* (1988) recommended that the distribution and form of the gold bearing structure will depend on the deformed structure (brittle to ductile) of the body. Also, structural sites of gold deposition change with depth. This implies that a vertical zonation to the geometry of gold deposit provides elements of prodictability. Mafic rocks are characterized by high magnesium and iron concentrations as well as high density CO_2 and are compositionally uniform regardless of whether the local rocks provide a good target for gold precipitation. In Handeni area, the rocks with characteristics as discussed above are garnetiferous granulite, garnetiferous

amphibolite and hornblende pyroxenite. During metamorphism the ambient fluid normally consists of high density CO2 such as amphibolite or granulite rocks.

Reddy *et al* (2003) proposed that the Usagaran rocks represent the features from the depleted mantle Nd model ages of 2.7 to 3.1 Ga and 2. 1 to 2. 5 Ga from post tectonic granites which implies significant components of Tanzania Archaean rock is common throughout the eastern part of Tanzania. It is potentially known that the Archaean rocks consist of greenstone rocks (Nyanzian System), which hosts the gold mineralization in Tanzania, especially the south and east of Lake Victoria.

In summary, the base metals minerals (Ni, Co, Cr and Cu) show negative correlation with MgO which implies the sulphidic nature of the mineralization (e.g. Fig. 46 B). Mineralization is sulphide hydrothermal related. Host rocks are the hornblende pyroxenite, garnetiferous amphibolite, garnetiferous granulite and garnet silicified rocks. Proposed potential mineralization sites are fracture zone, shear zones, trough zones of the folds and occasionally in the fold limbs close to the crests or troughs. Emphasis should be on mapping the macro folds with targeting the quartz veins despite their dimensions or continuations.

CHAPTER 9 CONCLUSIONS AND RECOMMENDATIONS

9.1 CONCLUSIONS

The Handeni project is comprised of Proterozoic rocks from the Usagaran belt dated 2.7 Ga as well as Archaean rocks of basaltic compositions. The Archaean rocks were successively attached to the Tanzanian Craton with eastward accretion onto previous consolidated crust. These rocks were made up during the syn and post tectonic events, they emplaced during the eastward thrusting which resulted to the lower grade metamorphosed foreland units. During the young orogenic belts, the Tanzania Craton has been successively reworked. The project is characterized by six geological units namely: QFGn, GrSc, GSil, MGr, GGr and HP. The HP units commonly developed at Kwandege site whereas at Magambazi East from mapping and drill holes were not intersected.

Metamorphism in the Handeni project area reflects the metamorphism of the Usagaran belt. Three tectonic events were involved, namely emplacement of the Archaean Craton into the continental crust at 3 Ga, subduction of oceanic plate at 1.9 Ga, Mozambique belt at 700 to 800 Ma and the whole process of Pan African event at 650 to 500 Ma. There is an abundant occurrence of syn to post metamorphic intrusion clustering dated 1.8 Ga and eclogites formation dated 2 Ga as a magmatic postdate event. Two common metamorphic facies series have been identified at Handeni project area, namely amphibolite and granulite facies. These facies represent the prograde metamorphism events. Amphibolite facies commonly associated with garnetiferous amphibolite rocks whereas the granulite facies associated with garnetiferous granulite. Intermediate facies including quartzofeldspathic gneiss and migmatitic gneisses were also developed, especially in the country rocks.

Alteration minerals such as calcite, sericite and dolomite were developed in these rocks, commonly in HP, GGr and MGr units, which are fairly similar to those found in low grade metamorphic terranes. Sulphide minerals including gersdorffite, pentlandite, pyrrhotite and chalcopyrite were also developed in these rocks. These alteration and sulphide minerals signify the presence of hydrothermal fluid in the lithologies of Handeni project. The fluid is associated with low to medium salinity $H_2O - CO_2$. Where CO_2 was generated during the metamorphic process.

The source of metals associated with magmatic rocks are related to Archaean fragments. During the formation of the Usagaran belt and subsequently the subduction of oceanic plate,

Archaean fragments were documented in the belt with the same age (2.7 Ga) as Nyanzian, which also included other metamorphic rocks or deep crustal rocks within the belt.

It has been reported that gold mineralization is associated with the sulphide minerals including pyrrhotite, chalcopyrite and occasionally arsenopyrite. Also, based on the petrology and mineralogy as well as the bulk rock analysis from the rocks analyzed in this thesis, there is good correlation between sulphide minerals and the base metals such as nickel, cobalt, chromium and copper. Thus, it is possible that gold mineralization is associated with base metals minerals.

9.2 RECOMMENDATIONS

Gold exploration in high grade metamorphic terrane is very challenging in terms of time of deposition and the structural controls on mineralization. The highly complex effects of tectonic events resulted to multiple series of deformations which is difficult to construct the control of mineralization. Gold associated with orogenic type is structurally controlled. Thus gold deposit in the area like that of Handeni project where three or four tectonic events have been developed is very critical to explore without considering the structural features.

Geochemical analysis shows that the rocks are basaltic in composition with the added possibility of an Archaean relationship. The rocks undergo several series of tectonic events resulting to multiple phases of metamorphism and including re- metamorphosing of the low grade metamorphic rocks possible from Archaean fragments. Geochemical analysis shows the potential association of hydrothermal fluid especially at the HP, GGr and GA units, which is believed to carry gold mineralization. It is strongly recommended to conduct multi elements analysis by ICP – MS followed by AAS and be precise to each unit separately. This will help to establish the relationship between the gold mineralization and other elements associated with it. Fluid inclusions is recommended as a follow-up research in the area.

Since the area is intensively affected by deformations, detail structural mapping is essential. Geological mapping, identifying the metamorphic facies rocks, mineral alterations and quartz veins will led to the better targeting of the mineralization. Shear zones, fold troughs, faults and thrust are the important structural features to be monitored during the exploration phases. The ore shoot is normally found in the fold troughs and occasionally in the fold limbs especially within the shear zones.

REFERENCES

Archibald 2011 "Technical report on Handeni property, Handeni district Tanga region Republic of Tanzania" in *www.eastafricametals.com/i/pdf/filings/handeni-technical-report-march-2011.pdf.* Accessed on 20130722

Archibald 2012 "Technical report on Handeni property, Handeni district Tanga region Republic of Tanzania" in *www.eastafricametals.com/i/pdf/filings/Canaco_NI43-101_Report_June_28_2012.pdf.* Accessed on 20130722

Archibald 2013 "Mineral Resource Estimate and Update to s NI43-101 Technical Report for the Handeni Property" *in www.eastafricametals.com/i/pdf/filings/Handeni-Technical-Report-2013.pdf.* Accessed on 20130912.

Babievskaya. I.Z, Drobot. F.N, Fomichev. V.S. and Krenev. A.V. 2011. "Evaluation of the Mineralogical Composition of Gabbro Rocks from Chemical Analysis Data" in *Inorganic Material*, Vol. 47, no. 6 pp: 633-636.

Barnicoat. C. A. Fare. J. R, Groves. I. D. and McNaughton. J. N. 1991. "Synmetamorphic lode gold deposit in high grade Archaean settings" in *The Geological Society of America*, 19, pp: 921-924.

Beccaluva. L, Bianchini. G and Wilson. M. 2011. "Volcanism and Evolution of the African Lithosphere", in the *Geological Society of America*, special paper 478.

Borg. G. 1992. "The Archaean BIF hosted Geita gold deposit, NW Tanzania; Geology, Ore petrology, Geochemistry and Timing of events". *Federal Institute for Geoscience and Natural Resources*, Hannover. BMZ Project no. 84.2053.1, pp37.

Bohmke, F.C. and Varndell, B.J., 1986. "Gold in Granulites at Renco Mine Zimbabwe" in Anhaeusser, C.R. & Maske, S. (Eds). *Mineral Deposits of Southern Africa*. Vol. 1, pp: 221- 230 Geological Society of South Africa: Johannesburg.

Bowen. D. R. 1989. "The encyclopaedia of igneous and metamorphic petrology" *Van Nostrand Reinhold*, ISBN: 0-442-20623-2.

Brick. A.R. 2011. "Palaeoproterozoic eclogite formation in Tanzania: a structural, geochronological, thermochronological and metamorphic study of the Usagaran and

Ubende orogenic belts" *Thesis (Ph.D.) -- University of Adelaide*, School of Earth and Environmental Sciences, Pub: Adelaide Research and Scholarship.

Carr. M, 1995. "Program. Igpet" Somerset NJ: Terra Softa.

Collins. A. S, Reddy. S. M, Buchan. C and Mruma. A. 2004. "Temporal constraints on Paleoproterozoic eclogites formation and exhumation (Usagaran orogen, Tanzania)"in *Earth and Planetary Science Letters*, Vol. 224, pp; 175-192.

Colvine. A. C, Fyon. J.A, Heather. K.B, Marmont. S, Smith. P.M and Troop. D.G. 1988. "Archaean lode gold deposits in Ontario Canada; Part I. A depositional model, Part II; A genetic model" Mines and Mineral Division; *Ontario Geological Survey*; Miscellaneous paper 139, pp 108.

Cox. K. G, Bell. J. D and Pankhurst. R. J. 1979. "The interpretation of igneous Rocks". George Allen and Unwin.

Dawson. B.J. 2008. "The Gregory Rift Valley and Neogene – react Volcanoes of Northern Tanzania." Pub: *The Geological Society*, London. Memoir No 33.

Dasgupta, S. Sengupta, P. Mondal, A. & Fukuoka, M. 1993., "Mineral chemistry and reaction textures in metabasites from the Eastern Ghats belts, India and their implications" in *Mineralogical Magazine*, 57, 113-120.

Davis Jr, P. A. and Condie, K. C., 1977. "Tracce element model studies of Nyanzian greenstone belts, western Kenya" in *Geochimica et Cosmochimica Acta*, Vol. 41, 271-277.

Delvaux. D, Kervyn. F, Machayeki. A. S and Temu. E. B. 2012. "Geodynamic significance of the TRM segment in the East African Rift (W-Tanzania); Active tectonics and paleostress in the Ufipa plateau and Rukwa basin" in *Elsevier Journal of Structural Geology*, Vol. 37 pp: 161-180.

Deer. W. A, Howie. R. A and Zussman. J. 1962. "Rock Forming Minerals" Vol. 1 Ortho-and Ring Silicates, *Longmans, Green and Co. Ltd, London*, pp 77-171.

Deer. W. A, Howie. R. A and Zussman. J. 1963. "Rock Forming Minerals" Vol. 2 Chain Silicates, *Longmans, Green and Co. Ltd, London*, pp 1-166 and 203-331.

Deer. W. A, Howie. R. A and Zussman. J. 1962. "Rock Forming Minerals" Vol. 3 Sheet Silicates, *Longmans, Green and Co. Ltd, London*, pp 1-81.

Deer. W. A, Howie. R. A and Zussman. J. 1963. "Rock Forming Minerals" Vol. 4 Frame work Silicates, *Longmans, Green and Co. Ltd*, London, pp 94-153.

Deer. W. A, Howie. R. A and Zussman. J. 1962. "Rock Forming Minerals" Vol. 5 Non Silicates, *Longmans, Green and Co. Ltd, London*, pp 128-295.

Deer. W. A, Howie. R. A and Zussman. J. 1992. "An Introduction to the Rock Forming Minerals" (2nd Ed). *London; Pearson Prentice Hall*.

Dirks. P.H.G.M, Blenkinsop. T.G. and Jelsma. H. A. 2002. "The Geological evolution of Africa" in *Encyclopaedia of Life Support System (EOLSS), Geology*, Vol. IV, pp; 1-15.

Eskola. E. P. 1993. "Die Entstehung der Gesteine". Julius Springer. Berlin.

Fritz. H, Tenczer. V, Hauzenberger. C, Wallbrecher. E, Hoinkes. G. and Muhongo. S. 2005. "Central Tanzanian tectonic map a step forward to decipher Proterozoic structural events in the East African Orogen" in *Tectonics*, Vol. 24, TC6013, 26p.

Fritz. H, Tenczer. V, Hauzenberger. C, Wallbrencher. E and Muhongo. S. 2009. "Hot granulite nappes – Tectonic styles and thermal evolution of the Proterozic granulite belts in East Africa" in *Elsevier Tectonophysics* Vol. 477 pp: 160-173.

Frost. R. B, Mavrogenes. A. J and Tomkins. G. A. 2002. "Partial melting of sulphide ore deposits during medium – and high grade metamorphism." in *The Canadian Mineralogist,* Vol. 40. Pp; 1-18.

Fyfe. W.S, Price. N. J and Thompson. A. B. 1978. "Fluids in the Earth's Crust developments" in *Geochemistry, Elsevier Amsterdam*, Vol. 1, 383p.

Ganguly, J. 1979. "Garnet and clinopyroxene solid solutions, and geothermometry based on Fe-Mg distribution coefficient" in *Geochim. Cosmochim Acta*, Vol. 43, pp: 102l-1029.

Goldfarb R. J. Baker. T, Dube. B, Groves. D. I, Hart. R.J.C and Gosselin. P. 2005. "Distribution, Character and Genesis of Gold Deposit in Metamorphic Terranes" in *Economic Geology* 100th Anniversary, pp; 407-450.

Gottfried. M. 2012. “Geologists correct a rift in Africa” in *Michigan State University Today, http://www.msutoday.msu.edu/news/2012/geologists-correct-a-rift-in-africa/.* Accessed on 20121102.

Groves, D. I, Ridley. J.R, Bloem. E.M.J, Gebre-Mariam. M., Hagemann, S.G, Hronsky. J.M.A, Knight. J.T, McNaughton. N.J, Ojala. J, Vielreicher. R.M, McCauaig. T.C and Holyland. P. W. 1995. “Lode-gold deposits of the Yilgarn block; products of Late Archaean crustal scale over pressured hydrothermal system in Early Precambrian Processes” Coward M. P and Ries A.C (Eds), in *Geological Society of London*, Special Publ, 95, pp; 155 – 172.

Groves, D. I, Goldfarb, R. J, Gebre-Mariam, M, Hagemann, S. G, Robert, F. 1998. “Orogenic gold deposits: A proposed classification in the context of their crustal distribution and relationship to other gold deposit types” in *Ore Geology Reviews,* Vol. 13, pp: 7 - 27.

Groves, D. I, Goldfarb, R. J, Knox-Robinson. M.C, Ojala. G.S, Yun. Y.G and Holyland. P. 2000. “Late – kinematic timing of orogenic gold deposits and significance for computer based – based exploration techniques with emphasis on the Yilgarn Block, Western Australia” in Elsevier *Ore Geology Reviews*, Vol. 17, pp: 1-38.

Groves, D. I, Goldfarb. R. J, Robert. F, Hart. C.J.R. 2003. “Gold Deposits in Metamorphic Belts: Overview of Current Understanding, Outstanding Problems, Future Research, and Exploration Significance” in *Economic Geology,* Vol. 98, pp. 1–29.

Groves, D.I. 2010. “Discovery of the Magambazi Gold Deposit in a Previously Unrecognised Gold Province in NE Tanzania: Role of the Univ. West. Austr. Economic Geology Centres Exploring in a New Paradigm” in *Centre for Exploration Targeting*, Quarterly News 11, pp: 10-18.

Harpum, J.R. 1970. “Summary of the geology of Tanzania: Structure and geotectonics of the Precambrian”. Tanzania Geological Survey, *Ministry of Energy and Minerals*. 1 Part V, pp58.

Harris, J.F., 1981. “Summary of the geology of Tanzania, economic geology”. In *Tanganyika Geological Survey, Ministry of energy and minerals*. 1 Part IV, pp: 143.

Hodgson. C. J. 1993. “Mesothermal lode gold deposit” in Mineral Deposit Modelling (Eds). Kirkham. R. V, Sinclair. W. D, Thorpe. R. I and Duke. J. M, *Geological Association of Canada*, Special Paper No. 40, pp 635 – 678.

Howard, E.A. 2011. “Technical report on Handeni property, Handeni district Tanga region Republic of Tanzania” *in http://www.handenigold.com/report*. Accessed on 20130829.

http://www.mem.go.tz/. Tanzania Ministry of Energy and Minerals (MEM) web site Accessed on 20130513.

http://www.shantagold.com/projects/chunya. Accessed on 20130519.

http://www.gst.go.tz/ © 2007-2011. Accessed on 20130918.

Irvine. T. N and Baragar. W. R. A. 1971. “A guide to the chemical classification of the common volcanic rocks” in *Canadian Journal of Earth Sciences*. Vol. 8, pp: 523-548.

Jiang, D., 1997. “Brevia fracturing of garnet crystals in anisotropic metamorphic rocks during uplift: Discussion” in *Journal of Structural Geology*, 19, 1429-1431.

Kabete, J.M., Groves, D.I., McNaughton, N.J., Mruma, A.M., and Maboko, M.A.H., 2008 “A new tectonic subdivision of the Archaean Tanzania Craton and its significance to gold metallogeny” in *Extended Abstract Volume*, SEG-GSSA 2008.

Kabete, J.M, Groves, D.I, McNaughton, N.J and Mruma, A.H 2012 a. “A new tectonic and temporal framework for the Tanzanian Shield: Implications for gold metallogeny and undiscovered endowment” in *Elsevier Ore Geology Review,* Vol. 48, pp 88-124.

Kabete, J.M, Groves, D.I, McNaughton, N.J and Mruma, A.H 2012 b. “Reconnaissance SHRIMP U–Pb zircon geochronology of the Tanzania Craton, Evidence for Neoarchean granitoid–greenstone belts in the Central Tanzania Region and the Southern East African Orogen” in *Elsevier Precambrian Research,* 216-219 pp 232-266.

Kuehn, S. Ogola, J. & Kuehn, S., 1990. “Regional Setting and Nature of gold Mineralization in Tanzania and Southwest Kenya” in *Precambrian Research*, Vol.46, pp; 71-82.

Kröner. A and Stern. R.J. 2004. “Pan-African Orogeny North African Phanerozoic Rift Valley” in *Encyclopedia of Geology, Pub: Elsevier, Amsterdam*, vol. 1, pp: 1-12.

Kruhl. J. H. 1996. “Prism-and basal-plane parallel subgrain boundaries in quartz: a microstructural geothermobarometer” in *Journal of Metamorphic Geology*, Vol. 14, pp: 581 – 589.

Lau. W. K. 2009. “Geochemistry and Sm-Nd isotropic composition of eclogite and associated rocks in the Usagaran belt, Tanzania”, Adelaide, University Adelaide, Pub. *Research and Scholarship.*

Le Bas. M. J, Le Maitre. R.W, Streckeisen. A and Zanettin. B. 1986. “A chemical classification of volcanic rock based on the Total Alkali-Silica diagram” in *Journal of Petrology*, Vol. 27, pp; 745- 750.

Leake. B. E. 1978. “Nomenclature of amphiboles”. *Mineralogical Magazine*, 42, pp; 533-563.

Levinson. A. A. 1974. “Introduction to Exploration Geochemistry” 2nd Ed, *Applied Publishing Ltd, Illinois*, 924p.

Link. K, Koehn. D, Barth. G.M, Tiberindwa. V.J, Barifaijo. E, Aanyu. K and Foley. F. S. 2010. “Continuous cratonic crust between the Congo and Tanzania blocks in western Uganda.” in *Int. J Earth Sci. (Geol Rundsch*) Vol. 99 pp: 1559-1573.

Maboko. M.A.H. 2000. “Nd and Sr isotopic investigation of the Archaean Proterozoic boundary in north eastern Tanzania; constraints on the nature of Neoproterozoic tectonics in the Mozambique belt “in *Precambrian Research*, Vol. 102, pp; 87-98.

Maboko. M.A.H. and Nakamura. E. 2002. “Isotopic dating of Neoproterozoic crustal growth in the Usambara Mountain of northeast Tanzania evidence for coeval crust formation in the Mozambique belt and the Arabian – Nubian shield” in *Precambrian Research*, Vol. 113, pp; 227-242.

Malisa. E and Muhongo. S. 1990. “Tectonic Settings of the Gemstone Mineralisation in the Proterozoic Metamorphic Terrane of Mozambique Belt in Tanzania” in *Precambrian Research, Elsevier Science Publishers B. V*, Vol. 46 pp: 167 – 176.

Mallet. C and Bretar. F. 2009. “Full- wave form topographic lidar; State of the art in ISPRS” in *Journal of Photogrammetry and Remote Sensing*, Pub; Elsevier, Vol. 64, pp; 1-16.

Microsoft Corporation. 2012. “Microsoft office” home and student. One Microsoft way Redmond, WA 98052-6399, USA.

Mikucki. E. J and Ridley. R.J. 1993. "The hydrothermal fluid of Archaean lode-gold deposits at different metamorphic grades: compositional constraints from ore and wallrock alteration assemblages" in *Mineral Deposit.* Vol. 28, pp: 469 – 481.

Moller, A. Appel, P. Mezger, K. & Schenk, V., 1995. "Evidence for a 2 Ga subduction zone: Eclogites in the Usagaran belt of Tanzania" in *the Geological Society of America-Geology,* Vol. 23, 1067-1070.

Moller. A, Mezger. K and Schenk. V. 1998. "Crustal age domains and the evolution of the continental crust in the Mozambique Belt f Tanzania. Combine Sm-Nd, Rb-Sr and Pb-Pb isotopic evidence" in *Journal of Petrology,* Vol. 39 no. 4 pp: 749 – 783.

Moller. A, Mezger. K and Schenk. V. 2000. "U-Pb dating of metamorphic minerals, Pan African metamorphism and prolonged slow cooling of granulites in Tanzania, East Africa, *Precambrian Research,* Vol. 104, pp: 123-146.

Mruma. A.H. 1989. "Stratigraphy, metamorphism and tectonic evolution of the early Proterozic Usagaran belt, Tanzania", Res Terrae, V, Ser. A. p.193.

Morimoto. N, Fabries. J. Ferguson. A. K, Ginzburg. I. V, Ross. M, Seifert. F. A, Zussman. J, Aoki. K and Gottardi. G. 1988. "Nomenclature of pyroxenes" in *American Mineralogist,* 73, 1123-1133.

Phillips. G. N and Powell. R. 2009. "The Formation of gold deposits; Review and Evolution of the continuum model" in *Earth Science Review,* Elsevier, Vol. 94, pp; 1-21.

Quennell, A.M., McKinley, A.C.M., Aiken, W.G., 1956. "Summary of the geology of Tanganyika: introduction and stratigraphy" in *Tanganyika Geological Survey* (Eds.), Memoir 1, pp: 1-264.

Rammlmair. D, Horndorf. A, Borg. G and Hiza. G. N 1990. "Nouvelles datations isotropique de granites et des gabbros de l region greenstone – granitique due Sukumaland, NW Tanzania" in *the 15th Colloq African Geology,* Nancy. Abstract, Vol.43.

Reddy, Steven and Collins, A.S. and Mruma, A. 2003. "Complex high strain deformation in the Usagaran Orogen, Tanzania: structural setting of Palaeoproterozoic eclogites" in *Tectonophysics* 375 (1-4): 101-123.

Reddy. S.M, Collins. A.S, Buchan. C and Mruma. A.H. 2004. "Heterogeneous excess argon and Neoproterozoic heating in the Usagaran Orogen, Tanzania, revealed by single grain 40Ar/39Ar thermochronology" in *Journal of African Earth Sciences.* Vol. 39 pp: 165–176.

Richard. L.R. 1995. "Minpet: Mineralogical and Petrological Data Processing System ".*Minpet Geological Software.* Ver. 2.02. Quebec

Ridley. J. Mikucki. E.J. and Groves. D. I. 1995. "Archaean lode gold deposits; Fluid flow and chemical evolution in vertically extensive hydrothermal systems." in *Ore Geology Reviews,* Vol. 10, p279 – 293.

Robles-Cruz, S.E. Watangua, M. Isodoro, L. Melgarejo, J.C. Gali, S. and Olimpio, A., 2009. "Contrasting compositions and textures of ilmenite in the Catoca kimberlite, Angola, and implications in exploration for diamond" in *Lithos,* P*ubl. Elsevier,* Vol. 112, pp: 966-975.

Rollinson. H. R. 1982. "PT-conditions in coeval greenstone belts and granulite from the Archaean of Sierra Leone" in *Earth Planet. Science letter,* Vol. 59 pp: 177 – 191.

Rollinson. H. R. 1993. "Using geochemical data: evaluation, presentation, interpretation" in *Longman Group. UK.* 352p.

Rose. A. W and Burt. D. M. 1979. "Hydrothermal alteration" in Barnes. H.L. (ed) Geochemistry of hydrothermal ore deposits", *Pub: John Wiley and Sons, New York,* pp; 173-235.

Saager. R and Meyer. M. 1984. "Gold distribution in Archaean granitoid and supercrustal rocks from Southern Africa – a comparison (55-70)" in Foster. R. P (Ed), Gold '82 *The geology, geochemistry and genesis of gold deposits, Balkema,* 490p.

Sabins. F.F. 1999. "Remote Sensing for mineral exploration" in *Ore Geology Reviews,* Pub; Elsevier, Vol. 14, pp; 157-183.

Scheepers. R. 2010. "Technical Report NI43 – 101 on the Handeni property for Douglas Lake Minerals Inc." in *www.handenigold.com/handeni-gold reports,* Accessed on 20130901.

Scheepers. R. 2011. "Technical Report NI43 – 101 on the Handeni property for Douglas Lake Minerals Inc." in *www.handenigold.com/handeni-gold reports,* Accessed on 20130901.

Semkiwa. P.M, Kafumu, P.D, Ayubu, S.Y, Petro, F.N, Kalemani, M.C, Nyelo, G.M, Rutaihwa, P.B, Ndonde. P.B, Mcharo. B.A, Ntulanalwo. V.B, Temu. E.B, Minde. A.B. and Salum. S.S. 2005. "United Republic of Tanzania. Opportunities for mineral resource development" in *Ministry of Energy and Minerals* (Eds.), Fourth Edition, Tanzania Printers. 128 pp.

Sommer, H. Kroner, A. Hauzenberger, C. Muhongo, S. & Wingate, T.D., 2003. "Metamorphic petrology and zircon geochronology of high-grade rocks from the central Mozambique Belt of Tanzania: crustal recycling of Archaean and Palaeoproterozoic material during the Pan-African orogeny" in *Journal of Metamorphic Geolog*, 21, 915-934.

Sommer. H, Hauzenberger. C, Kroner. A and Muhongo. S. 2005. "SHRIMP zircon ages for post-Usagaran granitoid and rhyolitic rocks from the Palaeoproterozoic terrain of southwestern Tanzania" in *South Africa Journal of Geology* Vol. 108 no 2, pp247-256.

Sommer. H, Kroner. A, Hauzenberger. C and Muhongo. S. 2005. "Reworking of Archaean and Palaeoproterozoic crust in the Mozambique belt of central Tanzania as documented by SHRIMP zircon geochronology" in *Science direct Journal of African Earth Science*, Vol. 43 pp: 447 - 463.

Sommer. H, Hauzenberger. C, Kroner. A and Muhongo. S. 2008. "Isothermal decompression history in the ''Western Granulite" terrain, central Tanzania: Evidence from reaction textures and trapped fluids in metapelites" in *Science direct Journal of African Earth Sciences* Vol. 51 pp: 123–144.

Spear. S. F. 1993. "Metamorphic Phase Equilibria and Pressure- temperature – time paths" in *Mineralogical Society of America*, 799p.

Stern. R. J. 1994. "Arc Assembly and continental collision in the Neoproterozoic East Africa Orogeny implications for the consolidation of Gondwana", *Annual Review of Earth and Planetary Science*, vol. 22, pp: 319-351.

Thomas. R. J, Roberts. N.M.W, Jacobs. J, Bushi. A.M, Horstwood. M.S.A and Mruma. A. 2013. "Structural and geochronological constraints on the evolution of the eastern margin of the Tanzania Craton in Mpwapwa area, central Tanzania" in *Precambrian Research*, Vol. 224, pp; 671-689.

Thompson. R.N. 1982 “Magmatism of the British tertiary province” in *Scottish Journal of Geology*, Vol. 18 pp; 49-107.

Vogt. M, Kroner. A, Poller. U, Sommer, H, Muhongo. S and Wingate. M.T.D. 2006. “Archaean and Palaeoproterozoic gneisses reworked during a Neoproterozoic (Pan-African) high-grade event in the Mozambique belt of East Africa: Structural relationships and zircon ages from the Kidatu area, central Tanzania” in *Journal of African Earth Sciences*. Vol. 45 pp: 139–155.

Vyhnal, C.R. McSween, H.Y. and Speer, J. A., 1991. “Hornblende chemistry in southern Appalachian granitoids: Implications for aluminium hornblende thermobarometry and magmatic epidote stability” in *American Mineralogist*, 76, 176-188.

Windley. B. F. 1995. “The Evolving Continents” Pub; *John Wiley and Sons*. Chichesster, 3rd edition 526 pp.

Winter. D. J. 2001. “Principles of Igneous and Metamorphic Petrology” Pub: Pearson Education, Inc. Pearson Prentice Hall, New Jersey, U.S.A.

Yoshida. M, Windley. B.F and Dasgupta. S. 2002. “Proterozoic East Gondwana, Super continent Assembly and Breakup” Pub; *Geological Society, London*. Paper no 206.

APPENDICES

Appendix A. Composition of pentlandite from the representative samples.

Lithology	Hornblende Pyroxenite									
Sample	H81A			H83A			H113			
Analytical number	1	2	3	4	5	6	7	8	9	10
wt %-Comment	Core	Core	Core	Core	Rim	Core	Rim	Core	Rim	Core
S	35.85	15.97	14.20	15.67	15.72	16.19	14.82	14.96	15.30	14.91
Fe	32.49	6.69	6.44	7.31	7.63	7.89	2.82	2.68	2.63	2.63
Ni	31.67	29.11	29.30	28.16	27.80	28.00	30.30	30.15	29.18	30.11
Cu	0.00	0.00	0.00	0.01	0.00	0.00	0.00	0.06	0.09	0.06
Co	0.22	1.06	1.00	1.09	1.12	1.14	1.30	1.32	1.38	1.34
Total	**100.22**	**52.83**	**50.93**	**52.24**	**52.27**	**53.23**	**49.24**	**49.18**	**48.58**	**49.04**

Appendix B. Composition of pyrrhotite from the representative samples

Lithology	GGr				Gsil	GA		HP		
Sample	H7A1		H54A		H7A2	H01A	H78A	H81A	H83A	
Analytical number	2	3	5	6	4	1	7	8	9	10
wt %-Comment	Core	Rim	Core	Core	Core	Core	Core	Core	Core	Core
S	43.02	42.45	43.48	43.63	41.64	43.06	43.35	39.31	41.83	42.02
Fe	60.05	60.11	59.41	57.70	61.21	60.08	60.17	61.27	60.02	60.23
Ni	0.24	0.45	0.28	0.08	0.07	0.15	0.60	0.12	0.21	0.25
Cu	0.03	0.03	0.04	0.06	0.00	0.01	0.10	0.05	0.00	0.02
Co	0.14	0.10	0.18	0.18	0.06	0.11	0.16	0.06	0.05	0.06
Total	**103.47**	**103.13**	**103.39**	**101.64**	**102.97**	**103.41**	**104.37**	**100.81**	**102.11**	**102.59**

Appendix C. Chalcopyrite composition from the representative samples

Lithology	Garnetiferous Amphibolite							HP	Garnetiferous Granulite					
Sample	H01A		H79A		H13A			H81A	H7A1		H44A		H54A	
Analytical number	3	5	6	7	11	12	13	8	1	2	9	10	15	16
wt %-Comment	Core	Core	Core	Rim	Core	Rim	Core	Core	Rim	Core	Core	Core	Core	Core
S	38.04	37.83	38.24	38.07	38.56	37.79	38.38	38.89	37.80	37.82	37.31	37.51	38.23	38.08
Fe	30.14	30.52	30.47	30.77	29.77	29.72	30.01	42.08	30.94	31.38	29.95	30.51	29.14	30.65
Ni	0.12	0.00	0.00	0.00	0.00	0.00	0.00	1.74	0.00	0.00	0.00	0.06	0.12	0.20
Cu	33.85	33.42	33.43	33.73	33.91	33.98	33.46	15.87	33.60	33.82	33.54	33.48	33.26	32.28
Co	0.00	0.03	0.03	0.02	0.04	0.02	0.04	0.04	0.06	0.03	0.02	0.07	0.05	0.00
Total	**102.15**	**101.80**	**102.17**	**102.58**	**102.28**	**101.51**	**101.89**	**98.62**	**102.40**	**103.04**	**100.82**	**101.63**	**100.79**	**101.20**

Garnetiferous Amphibolite = GA, Hornblende pyroxenite = HP, GSil = Garnet Silica and GGr = Garnetiferous granulite

Appendix D. Composition of gersdorffite from the representative samples

Lithology	Hornblende Pyroxenite											
Sample	H81A					H113						
Analytical number	1	2	3	10	16	2	4	10	13	14	15	17
wt %-Comment	Core	Core	Core	Core	Core	Core	Core	Core	Core	Core	Core	Core
S	10.02	10.54	10.44	11.10	16.46	15.53	16.70	15.30	14.53	15.98	17.21	15.46
Fe	3.06	3.11	2.90	3.49	7.01	3.82	5.50	4.11	2.99	4.13	5.84	3.17
Ni	28.30	27.58	27.74	28.23	25.88	26.89	26.65	27.34	28.36	27.45	25.87	27.66
Co	0.80	0.98	0.76	0.83	0.91	1.13	1.12	1.29	1.04	1.23	1.11	1.30
As	57.71	57.59	58.37	56.72	49.66	52.25	50.07	52.73	52.97	51.29	50.18	52.66
Total	99.89	99.79	100.21	100.37	99.91	99.62	100.03	100.77	99.88	100.08	100.21	100.26

Appendix E. Composition of Ilmenite of the representative samples.

Lithology	Garnet Silica		GGr			Garnetiferous Amphibolite					
Sample number	H39A		H97A			H124					
Analytical number	1	2	3	4	5	6	7	8	9	10	11
Wt% - Comment	Core	Core	Core	Core	Core	Core	Core	Core	Core	Core	Core
SiO2	0.02	0.02	0.03	0.04	0.00	0.03	0.02	0.03	0.65	0.03	8.41
TiO2	55.59	55.59	53.22	51.73	53.19	53.30	53.69	53.43	52.44	53.30	49.53
Al2O3	0.00	0.00	0.03	0.00	0.03	0.02	0.00	0.00	0.03	0.02	0.03
FeO	44.54	44.54	45.41	43.31	45.46	46.79	45.16	45.11	45.30	46.79	43.28
MnO	0.28	0.28	0.21	0.17	0.12	0.15	0.16	0.14	0.00	0.15	0.21
MgO	0.71	0.71	0.30	0.35	0.36	0.25	0.27	0.26	0.06	0.25	0.22
CaO	0.03	0.03	0.00	0.01	0.00	0.19	0.31	0.12	0.01	0.19	0.07
Na2O	0.00	0.00	0.02	0.01	0.00	0.00	0.00	0.00	0.01	0.00	0.00
K2O	0.00	0.00	0.00	0.00	0.01	0.00	0.01	0.01	0.00	0.00	0.01
Cr2O3	0.04	0.04	0.07	0.03	0.02	0.00	0.11	0.07	0.10	0.00	0.11
NiO	0.00	0.00	0.00	0.00	0.00	0.02	0.02	0.00	0.00	0.02	0.00
Total	**101.21**	**101.21**	**99.28**	**95.65**	**99.19**	**100.74**	**99.75**	**99.17**	**98.60**	**100.74**	**101.85**
Ideal number of Oxygen anions	3	3	3	3	3	3	3	3	3	3	3
Ti	1.03	1.03	1.01	1.02	1.01	1.00	1.01	1.01	1.00	1.00	0.87
Al	0.00	0.00	0.00	0.00	0.00	0.00	0.00	0.00	0.00	0.00	0.00
Fe	0.91	0.91	0.96	0.95	0.96	0.98	0.95	0.95	0.96	0.98	0.85
Mn	0.01	0.01	0.00	0.00	0.00	0.00	0.00	0.00	0.00	0.00	0.00
Mg	0.03	0.03	0.01	0.01	0.01	0.01	0.01	0.01	0.00	0.01	0.01
Ca	0.00	0.00	0.00	0.00	0.00	0.01	0.01	0.00	0.00	0.01	0.00
Na	0.00	0.00	0.00	0.00	0.00	0.00	0.00	0.00	0.00	0.00	0.00
Si	0.00	0.00	0.00	0.00	0.00	0.00	0.00	0.00	0.02	0.00	0.20
K	0.00	0.00	0.00	0.00	0.00	0.00	0.00	0.00	0.00	0.00	0.00
Cr	0.00	0.00	0.00	0.00	0.00	0.00	0.00	0.00	0.00	0.00	0.00
Ni	0.00	0.00	0.00	0.00	0.00	0.00	0.00	0.00	0.00	0.00	0.00
Total	**1.97**	**1.97**	**1.99**	**1.98**	**1.99**	**2.00**	**1.99**	**1.98**	**1.98**	**2.00**	**1.93**
Ideal number of cations	2	2	2	2	2	2	2	2	2	2	2
F	0.000	0.000	0.000	0.000	0.000	0.000	0.000	0.000	0.000	0.000	0.000
Cl	0.000	0.000	0.000	0.000	0.000	0.000	0.000	0.000	0.000	0.000	0.000

Sample H39A from garnet silica, H97A from garnetiferous granulite and H124 from mafic granulite rocks.

Appendix F. Composition of Calcite

Lithology	GGr					Garnetiferous Amphibolite				Garnet Silica				
Sample number	H79B		H124			H01A	H7A1			H7A2				
Analytical number	13	14	15	16	17	1	2	3	4	5	6	7	9	12
Wt% - Comment	Core	Rim	Core	Core	Rim	Rim	Rim	Rim	Core	Core	Core	Core	Rim	Core
SiO2	0.00	0.00	0.00	0.00	0.00	0.00	0.00	0.00	0.00	0.00	0.00	0.00	0.00	0.00
TiO2	0.00	0.01	0.00	0.00	0.03	0.05	0.00	0.00	0.00	0.00	0.00	0.00	0.00	0.00
Al2O3	0.00	0.02	0.02	0.02	0.00	0.00	0.02	0.01	0.02	0.00	0.01	0.01	0.00	0.00
FeO	0.10	0.03	3.63	3.88	4.22	1.11	0.09	0.01	0.06	0.10	0.08	1.09	0.00	0.51
MnO	0.03	0.00	0.27	0.34	0.35	0.30	0.00	0.07	0.02	0.15	0.84	4.17	0.14	0.66
MgO	0.02	0.02	1.13	2.31	1.66	0.25	0.02	0.03	0.02	0.00	0.02	0.07	0.03	0.05
CaO	53.90	53.81	50.24	52.51	51.45	55.97	54.24	53.75	50.10	58.41	59.37	57.95	59.88	60.33
Na2O	0.03	0.08	0.01	0.00	0.00	0.01	0.02	0.00	0.00	0.00	0.00	0.01	0.00	0.01
K2O	0.01	0.01	0.00	0.02	0.00	0.01	0.00	0.00	0.00	0.00	0.00	0.00	0.01	0.00
Cr2O3	0.06	0.00	0.03	0.00	0.00	0.00	0.00	0.00	0.00	0.00	0.00	0.00	0.09	0.00
NiO	0.01	0.00	0.01	0.00	0.02	0.00	0.00	0.01	0.00	0.00	0.00	0.00	0.00	0.00
BaO	0.00	0.00	0.00	0.00	0.00	0.00	0.00	0.00	0.01	0.00	0.00	0.00	0.00	0.00
SrO	0.00	0.00	0.00	0.00	0.00	0.00	0.00	0.00	0.16	0.00	0.00	0.00	0.00	0.00
Total	54.14	53.98	55.35	59.06	57.73	57.70	54.40	53.87	50.38	58.66	60.31	63.29	60.14	61.56

Appendix G. Composition of Magnesite

Lithology	Hornblende pyroxenite			
Sample number	H113			
Analytical number	18	19	20	21
Wt% - Comment	Rim	Rim	Rim	Core
SiO2	0.04	0.02	0.04	0.04
TiO2	0.00	0.02	0.00	0.00
Al2O3	0.00	0.01	0.01	0.00
FeO	5.92	5.75	5.59	5.99
MnO	0.20	0.21	0.19	0.18
MgO	40.16	40.13	39.75	40.58
CaO	0.76	0.63	0.69	0.57
Na2O	0.01	0.00	0.00	0.02
K2O	0.01	0.00	0.01	0.00
Cr2O3	0.00	0.04	0.00	0.01
NiO	0.03	0.01	0.01	0.09
BaO	0.00	0.00	0.00	0.00
SrO	0.00	0.00	0.00	0.00
Total	47.11	46.81	46.28	47.46

Appendix H. Composition of Dolomite

Lithology	Hornblende pyroxenite			
Sample number	H83A			
Analytical number	22	23	24	25
Wt% - Comment	Rim	Rim	Core	Core
SiO2	0.00	0.00	0.00	0.00
TiO2	0.01	0.02	0.04	0.00
Al2O3	0.04	0.00	0.02	0.00
FeO	2.78	2.46	2.52	2.90
MnO	0.09	0.12	0.14	0.12
MgO	22.54	22.55	22.48	22.60
CaO	32.77	33.29	31.95	32.47
Na2O	0.02	0.01	0.00	0.02
K2O	0.01	0.01	0.01	0.01
Cr2O3	0.02	0.00	0.00	0.00
NiO	0.01	0.01	0.01	0.00
BaO	0.00	0.00	0.00	0.00
SrO	0.00	0.00	0.00	0.00
Total	58.28	58.47	57.16	58.12

Appendix I. Microprobe standard

Elemnt	X-r	ay Crystal	CH	Acc.v	Peak Pos.	(nm)	BG_L	BG_U (mm)
Si	Ka	TAP	-1	15	77.927	0.71254	5	5
Ca	Ka	PETJ	-1	15	107.835	0.33584	5	5
Al	Ka	TAP	-2	15	91.078	0.83393	5	5
Mg	Ka	TAP	-2	15	107.898	0.989	5	5
Fe	Ka	LIF	-2	15	134.66	0.1936	5	5
K	Ka	PETL	-3	15	119.825	0.37414	5	5
Mn	Ka	LIFL	-3	15	146.207	0.21018	5	5
Ni	Ka	LIFL	-3	15	115.351	0.16579	5	5
Na	Ka	TAPL	-4	15	129.699	1.19101	5	5
Ti	Ka	PETL	-4	15	88.25	0.27485	5	5
Cr	Ka	PETL	-4	15	73.607	0.22897	3	5

Elemnt	Pe	ak Back	Pksk	Ga in	High.V	Base.L	Wind	ow.W	Mo	de
Si	10	.0 5.0	1	32	1638	-1	(V)	I		nt
Ca	10	.0 5.1	1	16	1638	-1	(V)	I		nt
Al	10	.0 5.2	1	32	1642	-1	(V)	I		nt
Mg	10	.0 5.3	1	32	1642	-1	(V)	I		nt
Fe	10	.0 5.4	1	16	1636	-1	(V)	I		nt
K	10	.0 5.5	1	64	1664	-1	(V)	I		nt
Mn	10	.0 5.6	1	32	1666	-1	(V)	I		nt
Ni	30	.0 5.7	1	32	1666	-1	(V)	I		nt
Na	10	.0 5.8	1	32	1648	-1	(V)	I		nt
Ti	10	.0 5.9	1	16	1646	-1	(V)	I		nt
Cr	10	.0 5.10	1	16	1646	-1	(V)	I		nt

Appendix J. Composition of Titanite

Sample number	**H7A1**		**H01A**	**H44A**
Analytical number	**1**	**2**	**3**	**4**
Wt% - Comment	**Core**	**Core**	**Core**	**Core**
SiO2	30.55	30.52	30.45	31.02
TiO2	39.04	40.04	40.15	39.06
Al2O3	1.61	1.27	1.15	1.41
FeO	0.94	0.13	0.29	0.23
MnO	0.02	0.02	0.02	0.00
MgO	0.03	0.01	0.00	0.03
CaO	28.22	28.23	28.63	28.26
Na2O	0.00	0.00	0.01	0.00
K2O	0.01	0.00	0.01	0.02
Cr2O3	0.02	0.00	0.07	0.05
NiO	0.03	0.00	0.00	0.00
Total	100.45	100.22	100.76	100.07

H01A from GA unit whereas H7A1 and H44A from GG unit.

Appendix K. List of. Addendum

AS-Arabian Shield

BR-Brasilino

DA-Damara

DM-Dom Feliciano

DR-Denman Darling

EW-Eliswirth Whitmore Mountains

EARS – East Africa Rift valley System

Ga – Billion years in geology time

GP-Gariep

GA –Garnetiferous Amphibolite

GSil- Garnet Silica

GrSc- Graphitic Schist

GGr – Garnetiferous Granulite

HP – Hornblende Pyroxenite

ICP-AES- Inductively Coupled Plasma-Atomic Emission Spectrometry

IR = Infra-Red

ICP-MS-Inductively Coupled Plasma-Mass Spectrometry

KHS- Kilindi Handeni Superterrane

KB-Kako

LVGF – Lake Victoria Gold Field

MA-Mauretanides,

MB-Mozambique Belt

Ma – Million years in geology time

MMI- Mobile Metal Ion

MGr= GA

NS-Nubian Shield

PM-Peterman Ranges

PB-Pryolz Bay

PR-Pampean Ranges

PS-Peterson

QFGn- Quartzofeldspathic Gneiss

QM-Queen Maud Land

RB-Rokelides

SD-Saldania

SG-Southern Granulite Terrane

TM- Thematic Mapper

TTG = Tonalite-trondhjemite-granodiorite

TS-Trans Sahara Belt

WB-West Congo

ZB-Zambezi